Intraseasonal Variability in the Tropics

The Madden-Julian Oscillation (MJO)

Discovered by Rol Madden and Paul Julian at NCAR in 1971

Characterized by an envelope of convection ~10,000 km wide moving eastward at around 5 m/s

Most active over regions of high sea surface temperature (> 27°C)

Can have a profound impact on the extratropical circulation

Is poorly represented in general circulation models, if at all

Composed of a variety of higher frequency, smaller scale disturbances

Madden and Julian, 1972

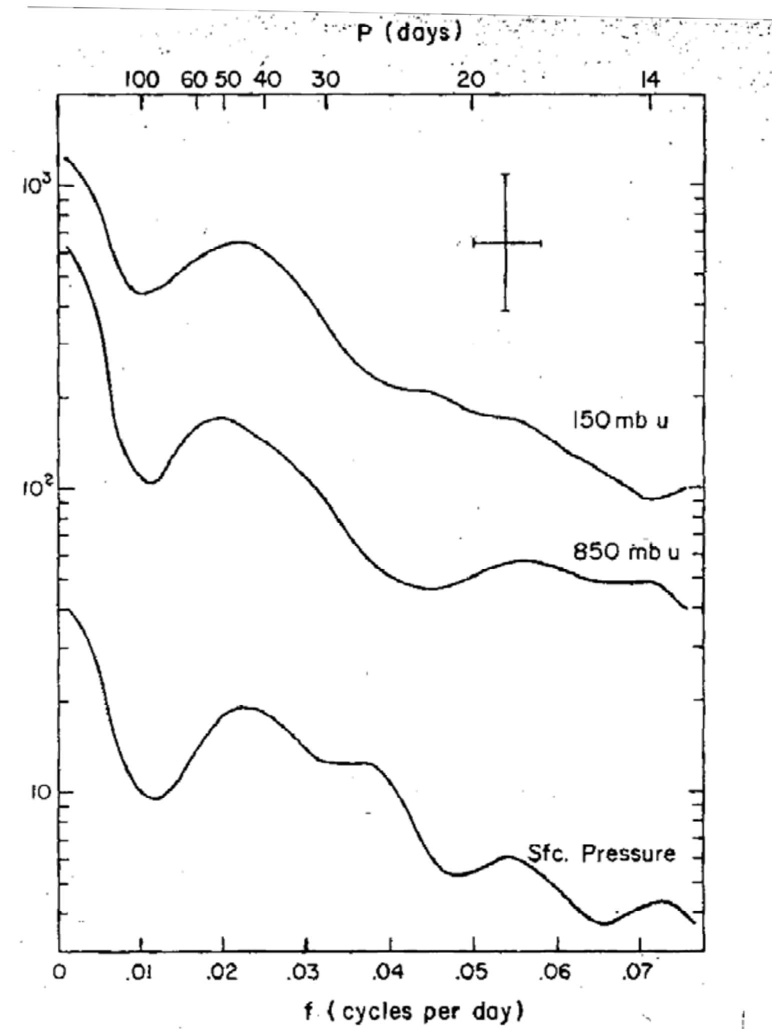

FIG. 2. Individual variance spectra for the 850- and 150-mb zonal wind component and station (sfc) pressure for the Canton Island record. The use of a logarithmic ordinate permits a constant scaling to be used for the chi-square degrees of freedom sampling analysis. This scaling [$\chi^2(0.1\%)/51$] and the bandwidth of the analysis, $\Delta f=0.0081$ day^{-1}, are shown by the cross. Spectral densities are normalized to unit bandwidth (m^2 sec^{-2} day^{-1}).

Madden and Julian, 1972

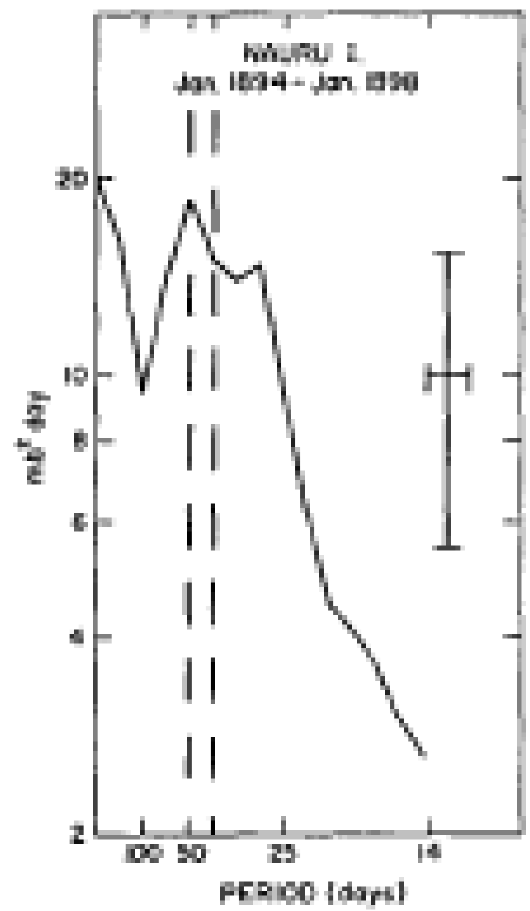

FIG. 2. Variance spectrum for station pressures at Nauru I. (0°24′S, 161°0′E). Ordinate is logarithmic and abscissa (frequency) is linear. The 40–50 day period range is indicated by the dashed vertical lines. Prior 95% confidence limits and the bandwidth of of the analysis (0.008 day⁻¹) are indicated by the cross.

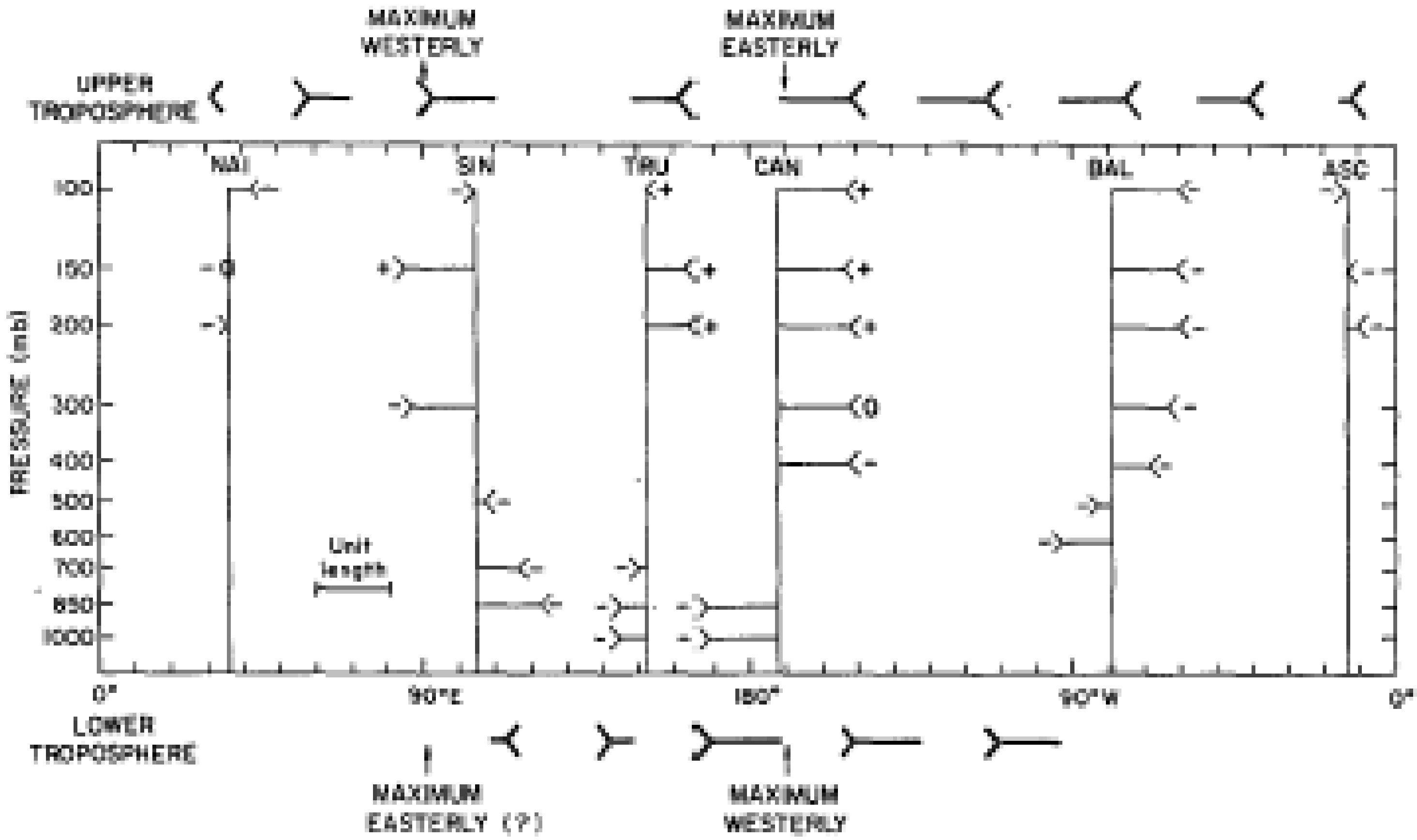

FIG. 6. Zonal wind oscillation in the equatorial plane at the time when the station pressure is a maximum at Canton based on the phase angles of Table 4. The unit length represents the maximum excursion at each location. The +, −, or 0 at the tail of each wind arrow represents the sign of the instantaneous local change of the zonal wind. Arrows are plotted only at levels whose coherence squares from Table 4 are above their background coherence square, and whose spectra, as tabulated in Table 3, indicate a peak. Heavy arrows at the top and bottom represent a schematic of the upper and lower tropospheric wind disturbance that is consistent with the plotted wind arrows and that will satisfy the local changes if it propagates eastward.

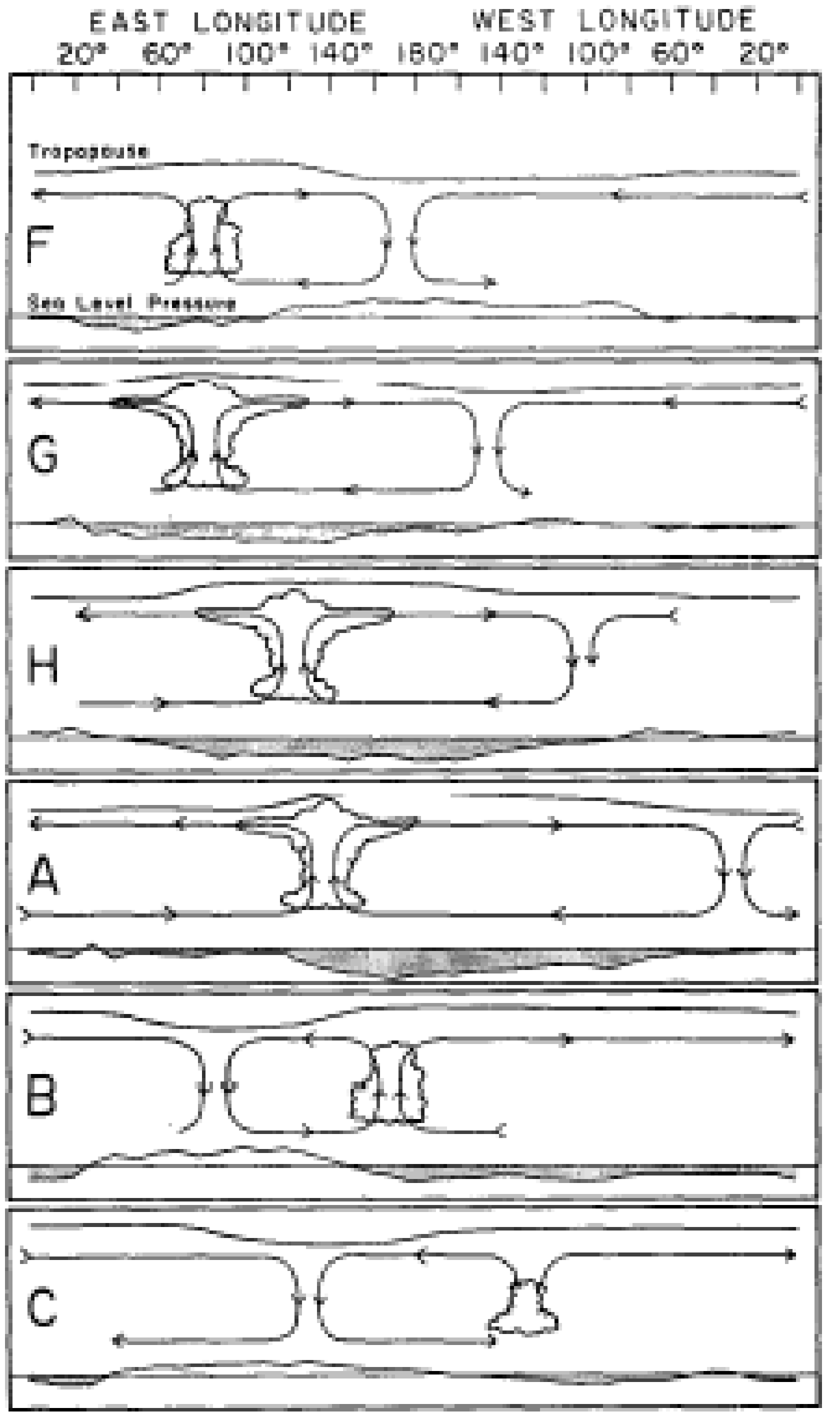

EAST LONGITUDE
WEST LONGITUDE
20° 60° 100° 140° 180° 140° 100° 60° 20°
Tropopause
F
Sea Level Pressure
G
H
A
B
C

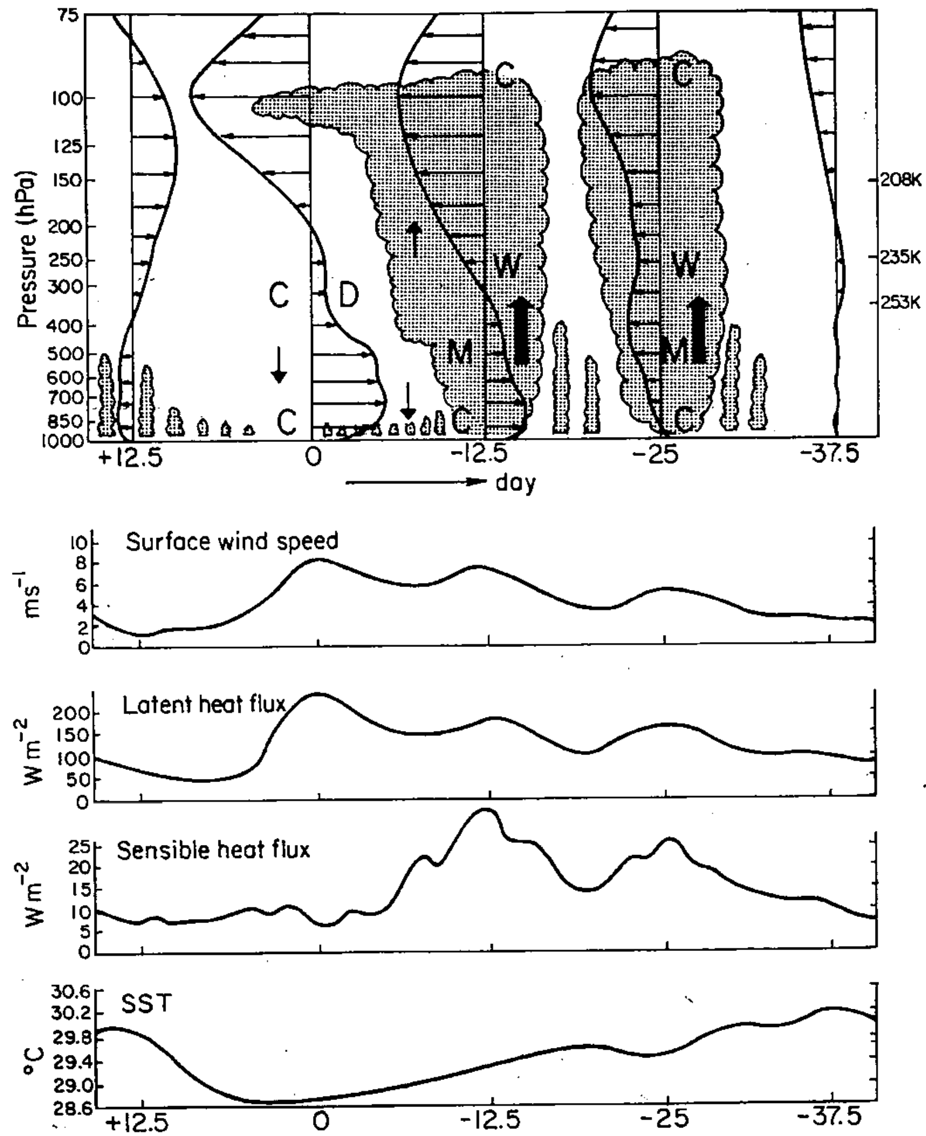

FIG. 16. A descriptive model of the kinematic, thermodynamic, and surface properties of the December to early January westerly wind burst as it passed the IFA. Day 0 is time of maximum low-level westerlies, with earlier times indicated by negative days (placed to the right so that the left portion of the diagram is to the west: see caution in text, however, about fully interpreting diagram as west–east section). Letters in figure refer to anomalies W: warm, C: cool, M: moist, and D: dry. Heavy arrows indicate strong vertical motion; light arrows weak vertical motion. Clouds are schematic, horizontal scales exaggerated. Temperatures corresponding to pressure levels are indicated on right.

Lin and Johnson, JAS, 1996

Perturbations in surface properties and OLR/precip confined to Indian Ocean and western Pacific, but upper tropospheric wind signals are global

European Center forecast 200 hPa velocity potential, 4 January to 13 February, 2005

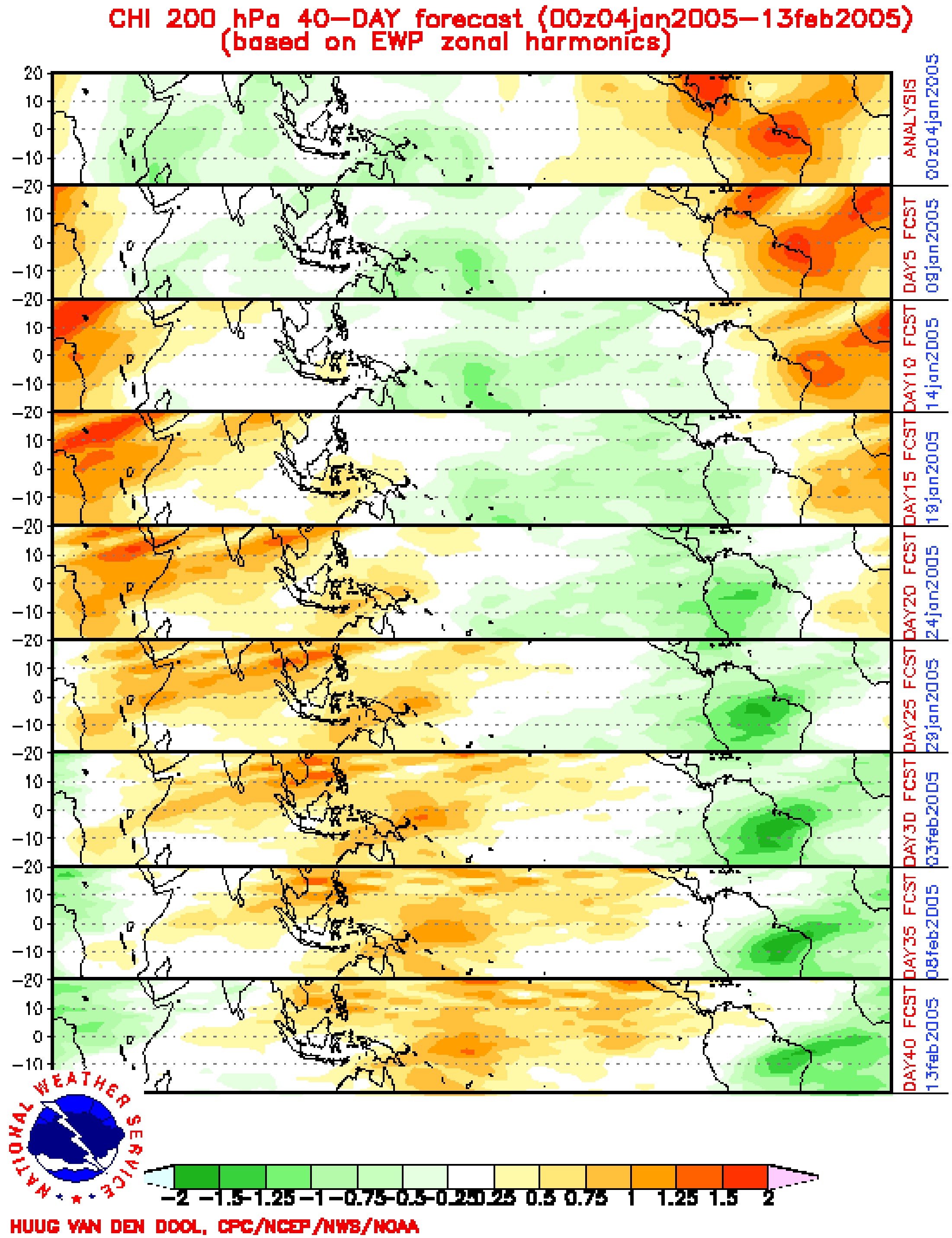

Observational analyses courtesy of:

George N. Kiladis
NOAA Aeronomy Laboratory, Boulder, Colorado

Katherine H. Straub
Susquehanna University

Patrick T. Haertel
University of North Dakota

OLR power spectrum, 15ºS-15ºN, 1979–2001 (Symmetric)

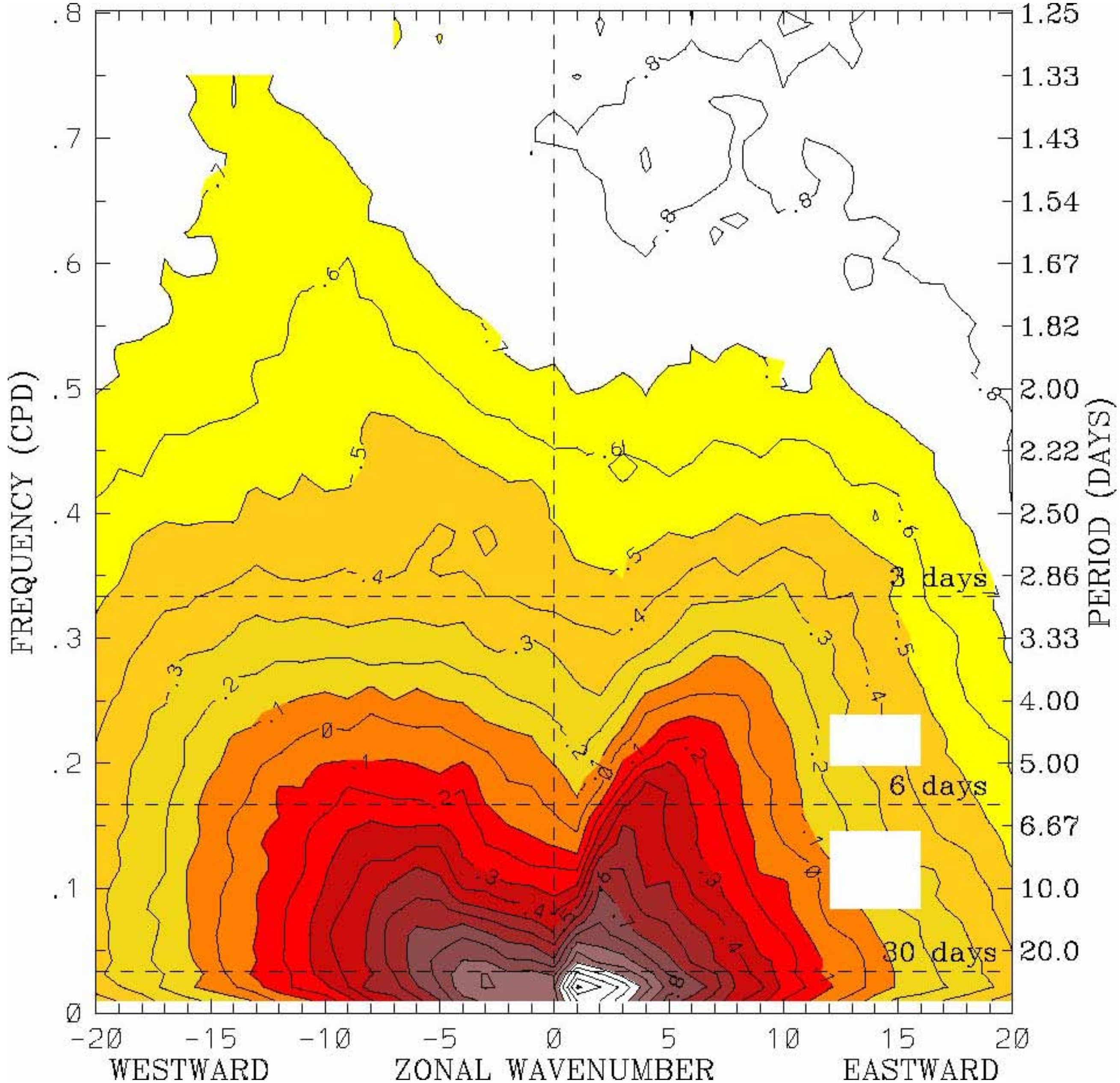

from Wheeler and Kiladis, 1999

OLR power spectrum, 15ºS-15ºN, 1979–2001 (Antisymmetric)

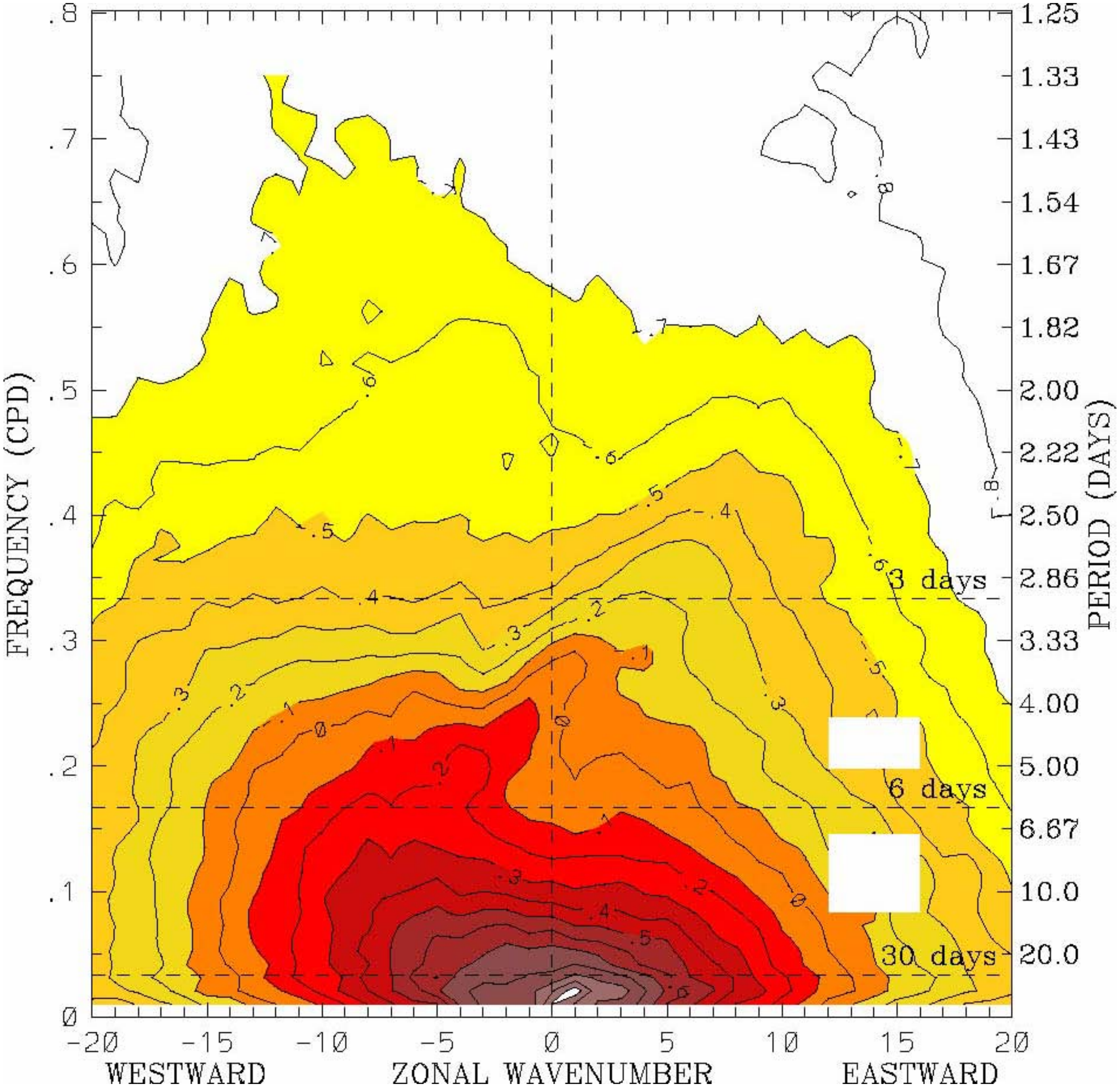

from Wheeler and Kiladis, 1999

OLR background spectrum, 15ºS-15ºN, 1979–2001

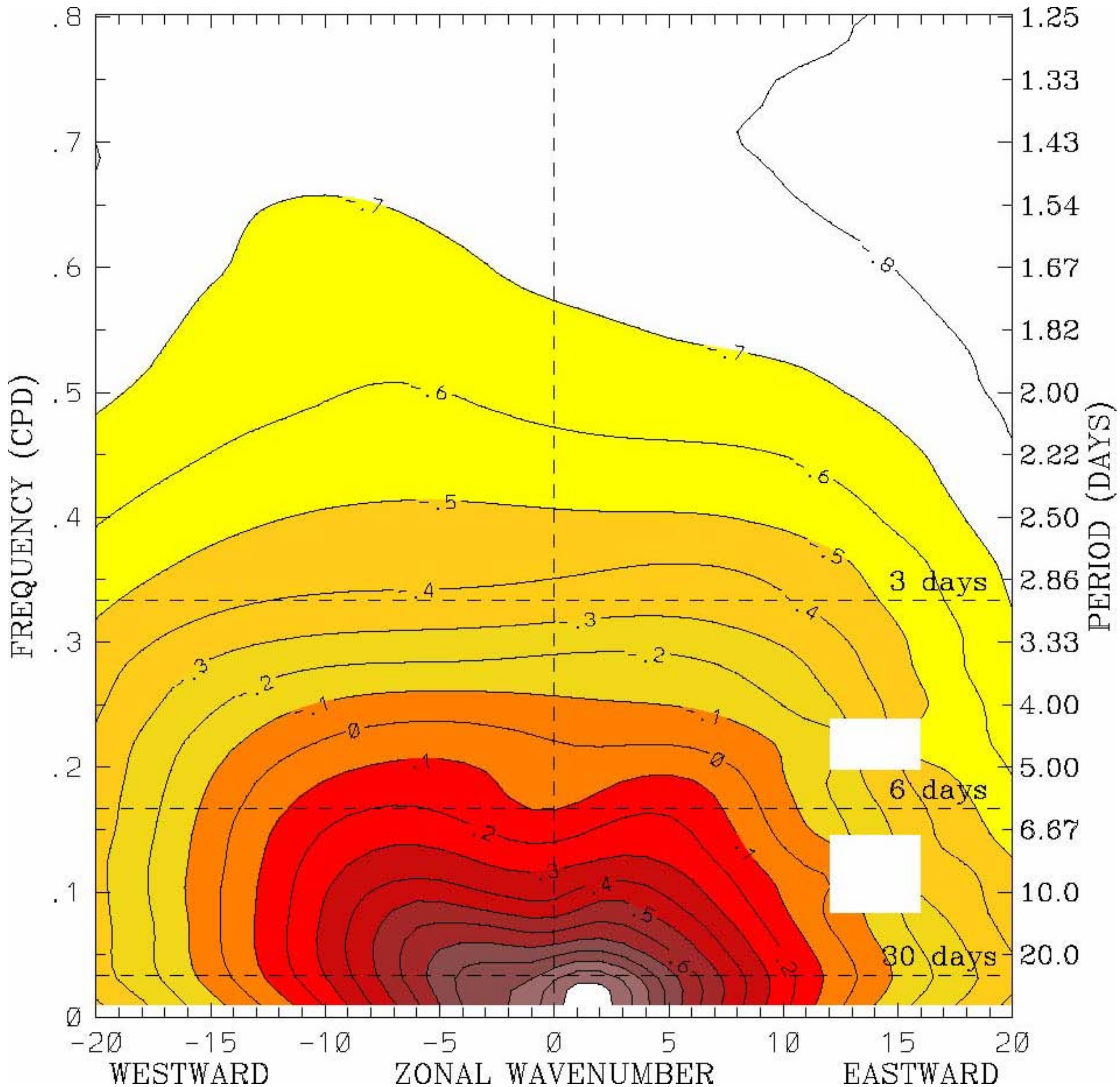

from Wheeler and Kiladis, 1999

OLR power spectrum, 1979–2001 (Symmetric)

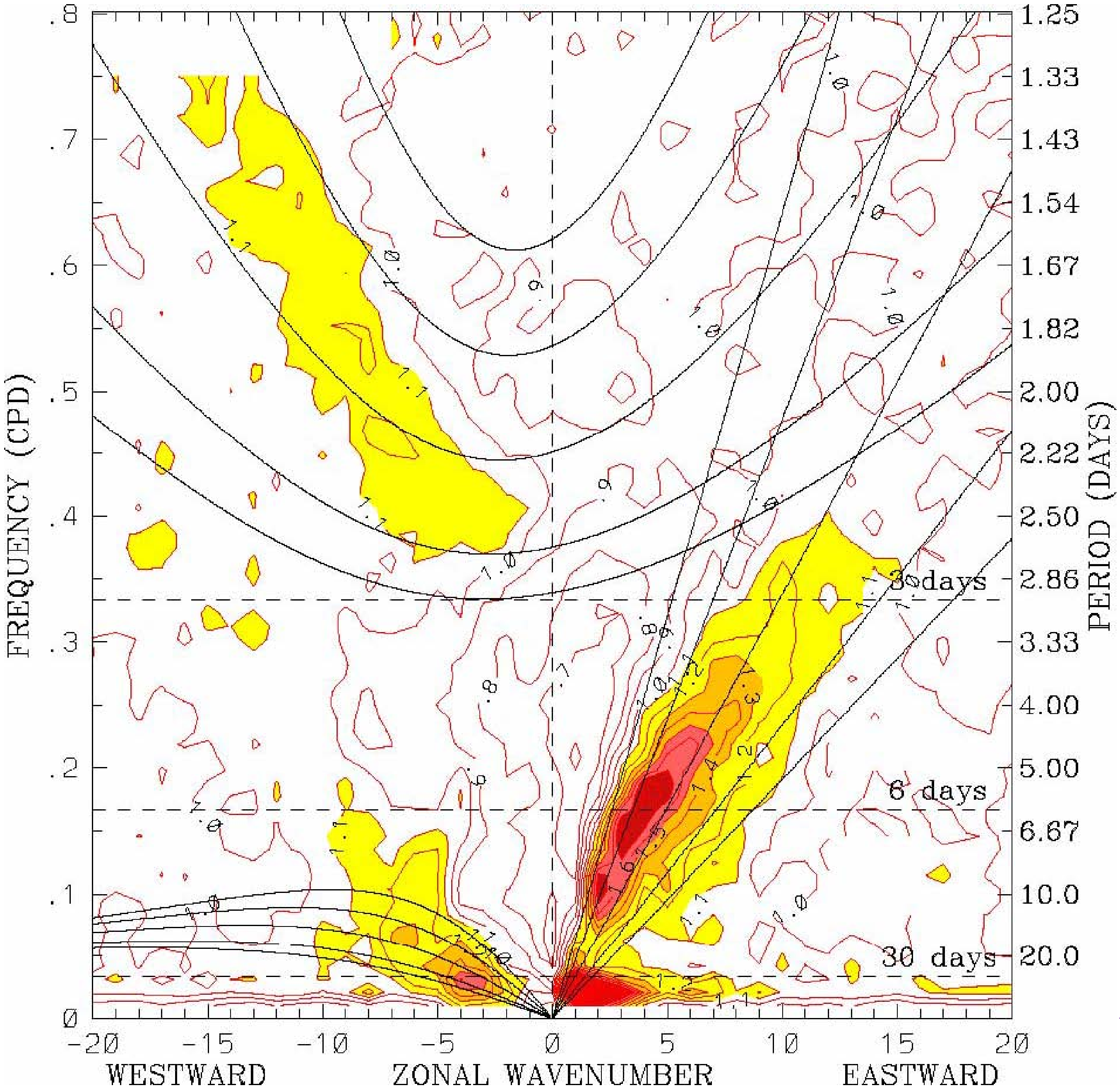

from
Wheeler and Kiladis, 1999

OLR power spectrum, 1979–2001 (Symmetric)

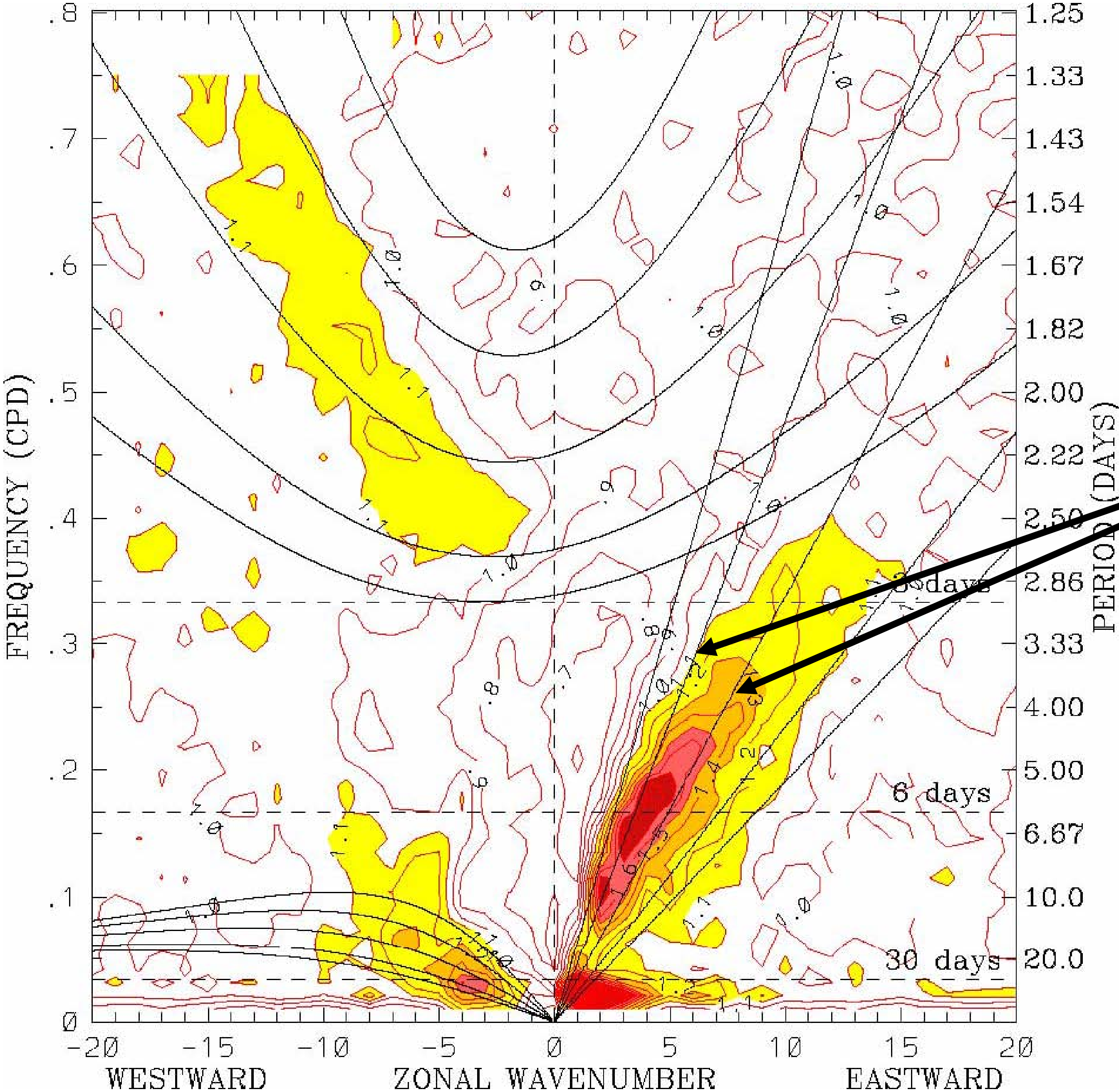

Kelvin wave dispersion curves for equivalent depths of 25 and 50 m

Kelvin wave Phase Speed: 15 m s^{-1}

from
Wheeler and Kiladis, 1999

OLR power spectrum, 1979–2001 (Symmetric)

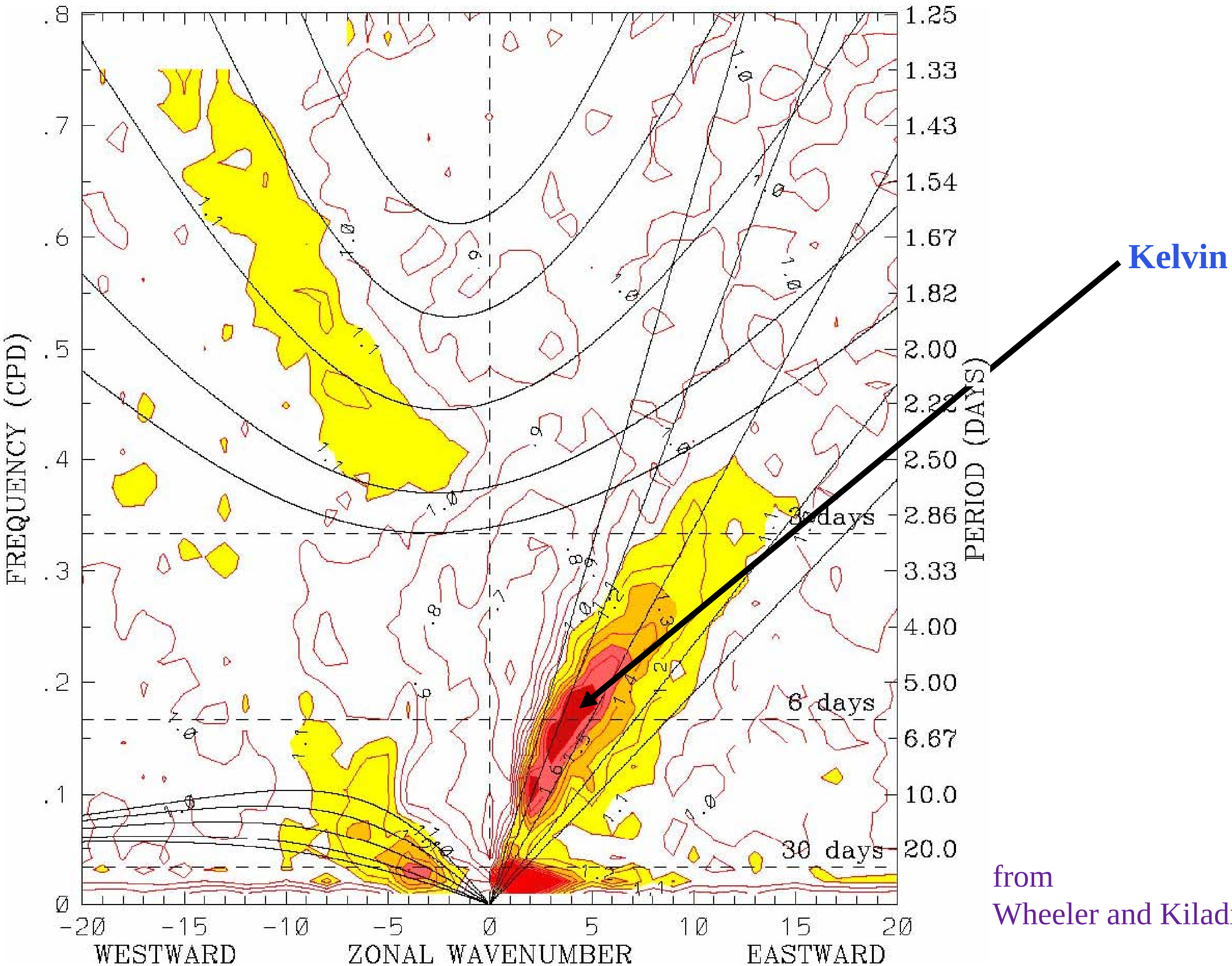

from
Wheeler and Kiladis, 1999

OLR power spectrum, 1979–2001 (Symmetric)

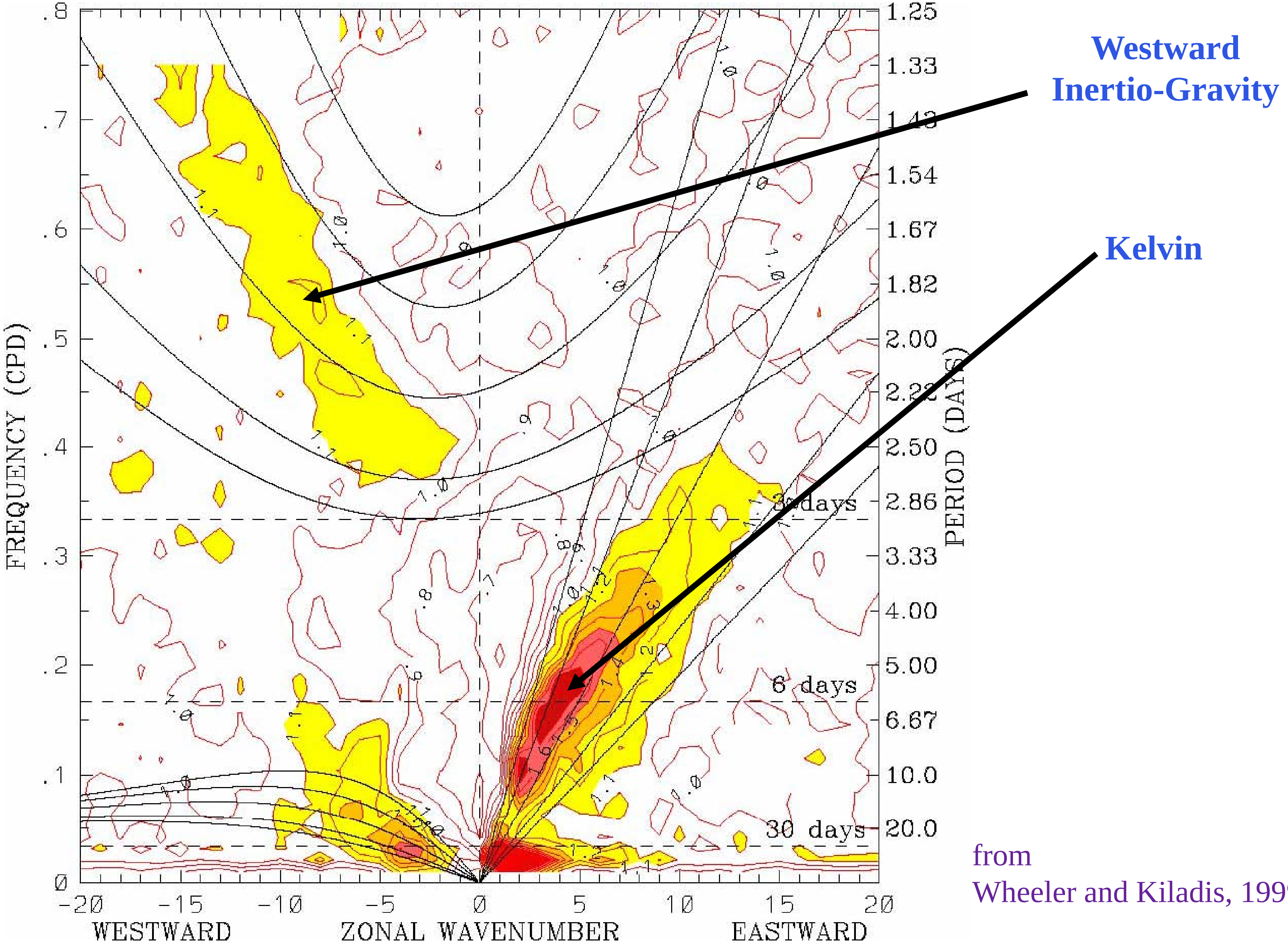

from
Wheeler and Kiladis, 1999

OLR power spectrum, 1979–2001 (Symmetric)

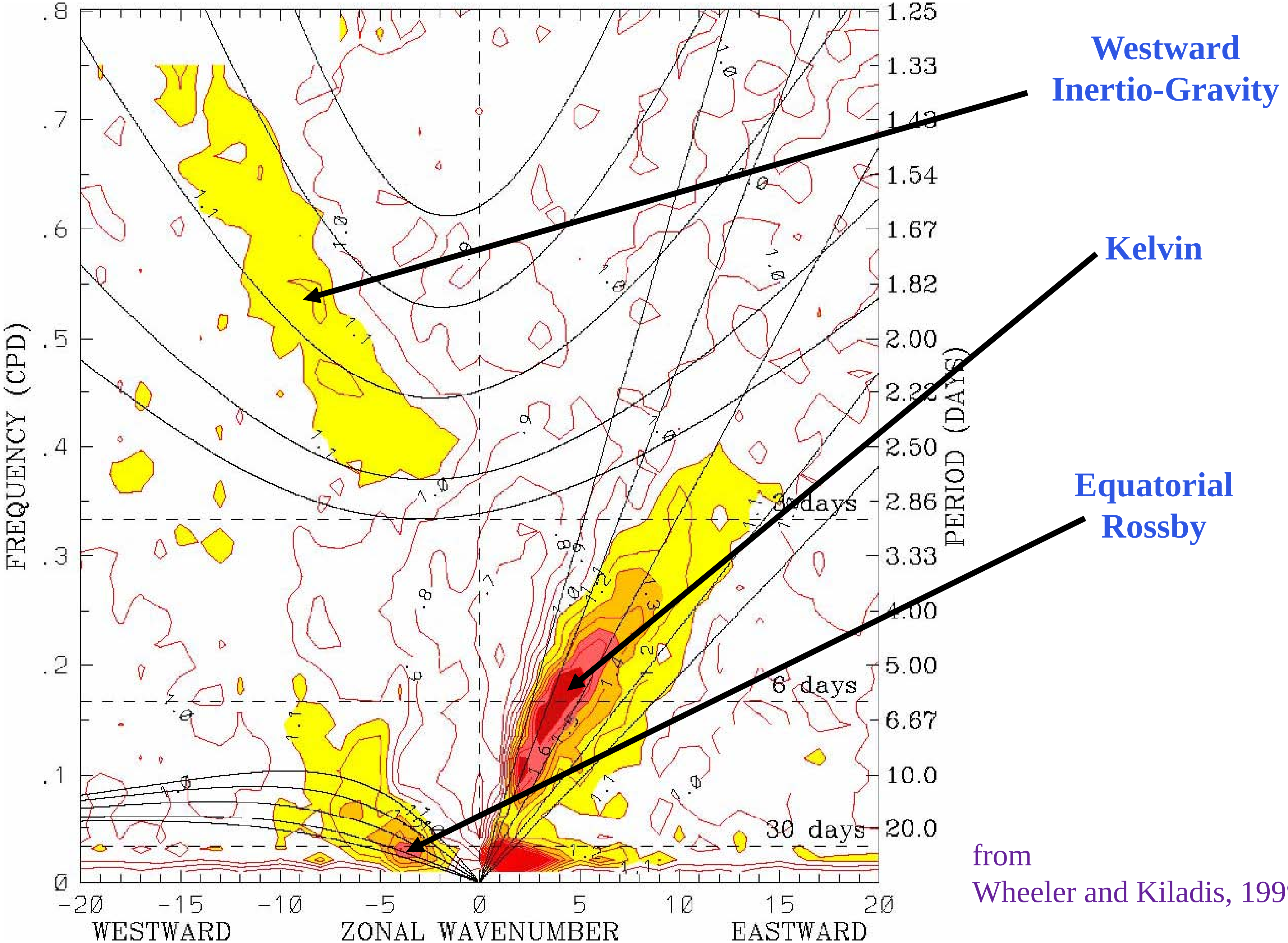

from
Wheeler and Kiladis, 1999

OLR power spectrum, 1979–2001 (Symmetric)

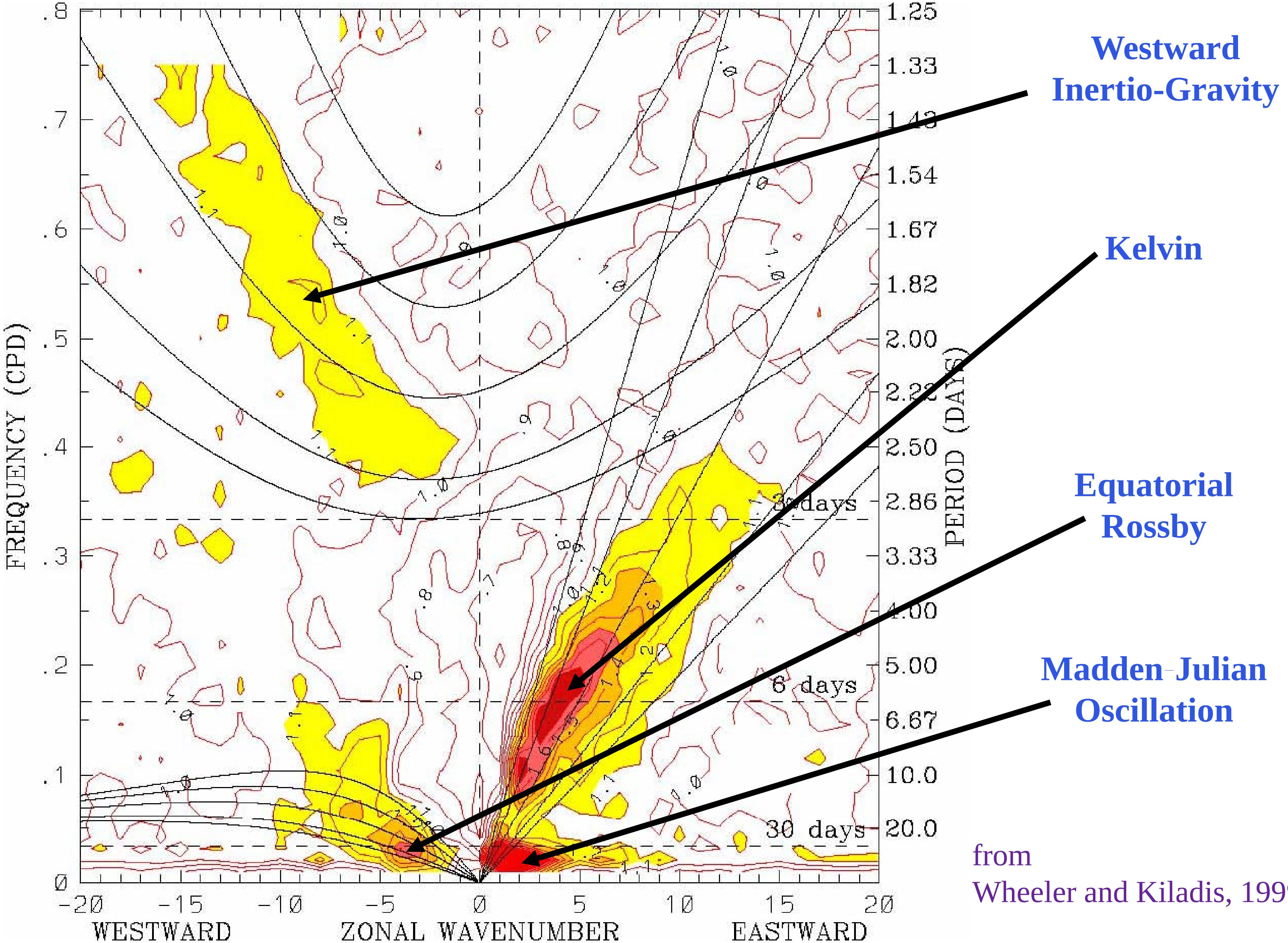

from
Wheeler and Kiladis, 1999

OLR power spectrum, 1979–2001 (Antisymmetric)

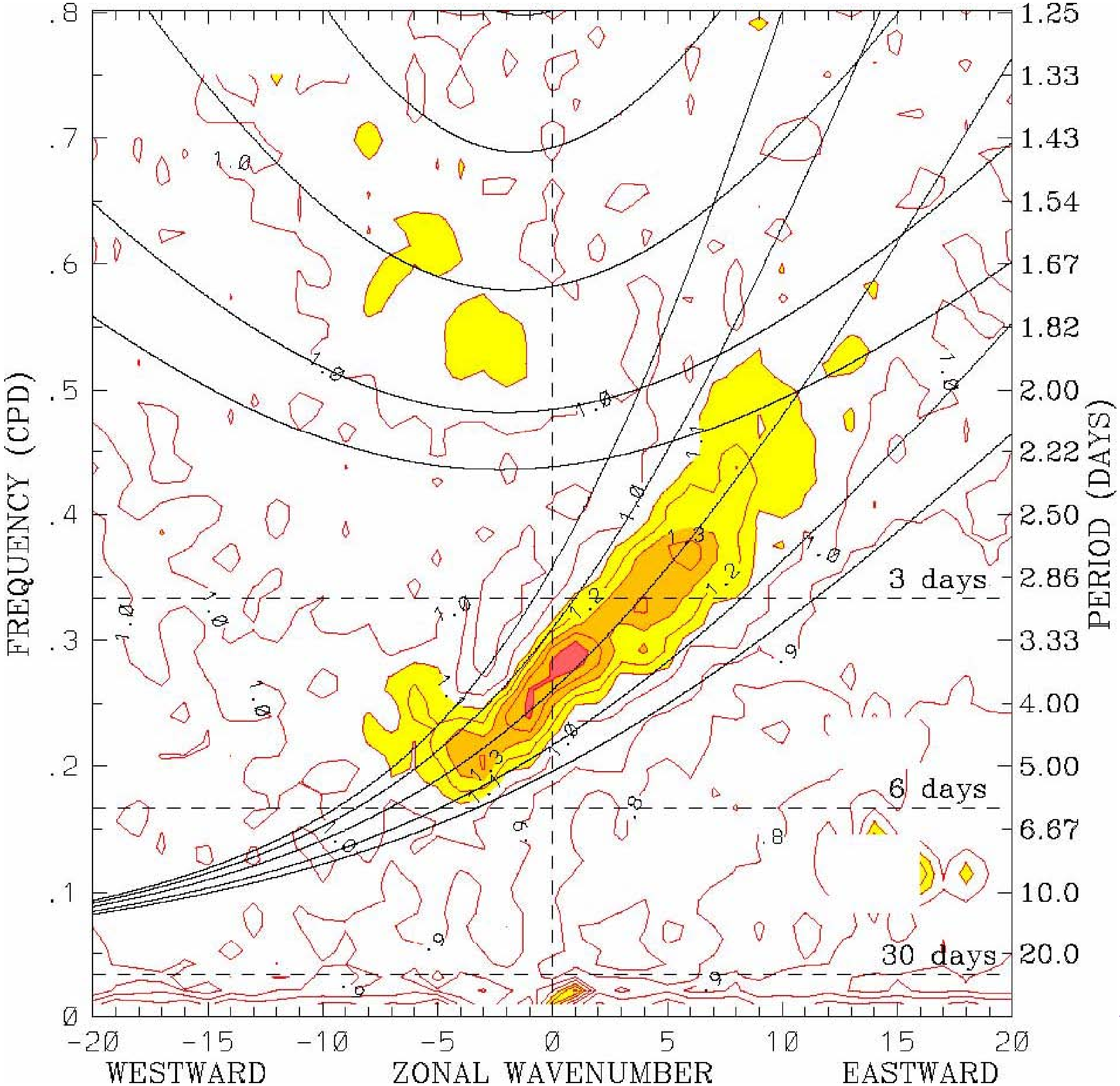

from
Wheeler and Kiladis, 1999

OLR power spectrum, 1979–2001 (Antisymmetric)

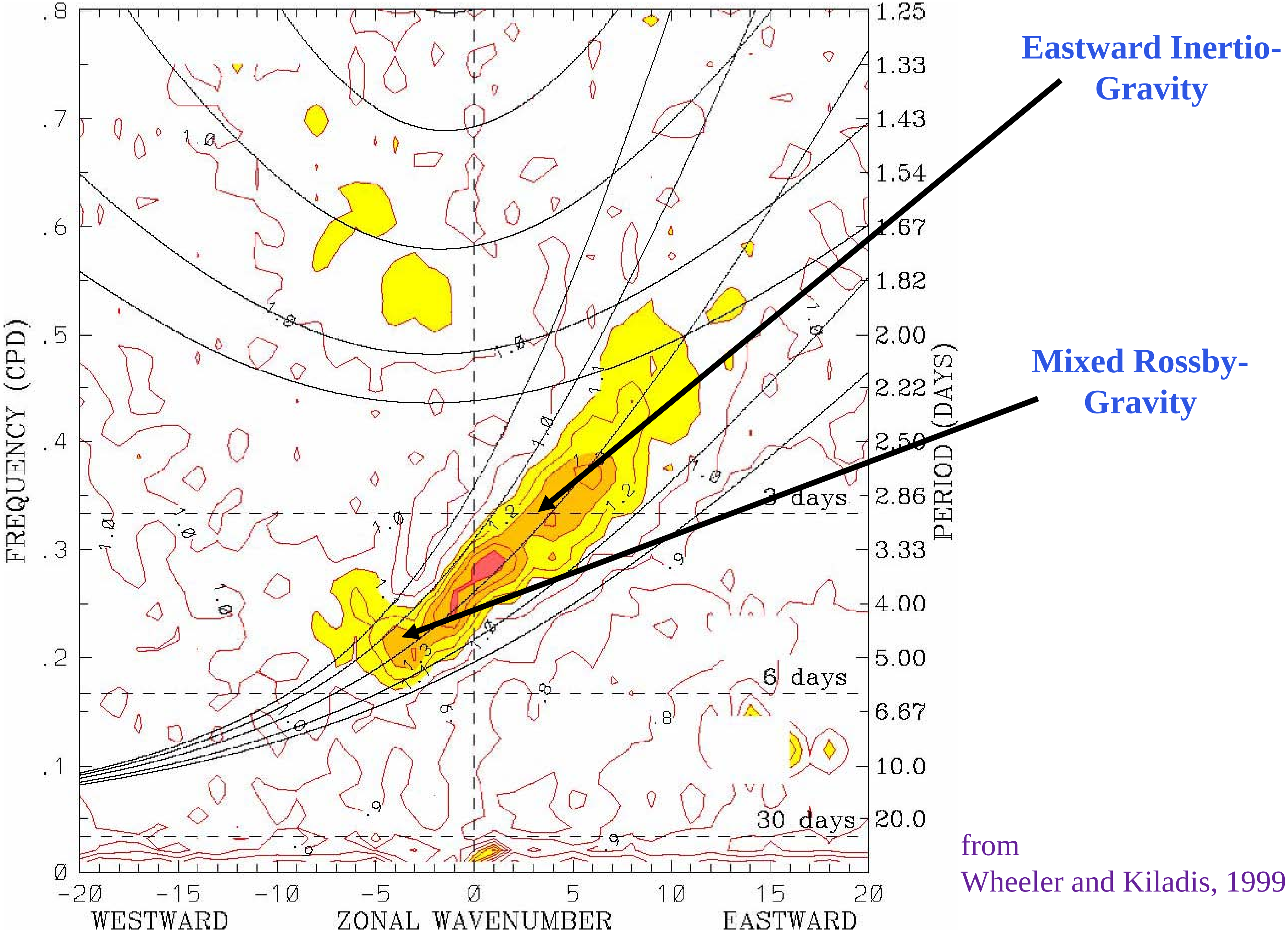

from
Wheeler and Kiladis, 1999

OLR power spectrum, 1979–2001 (Symmetric)

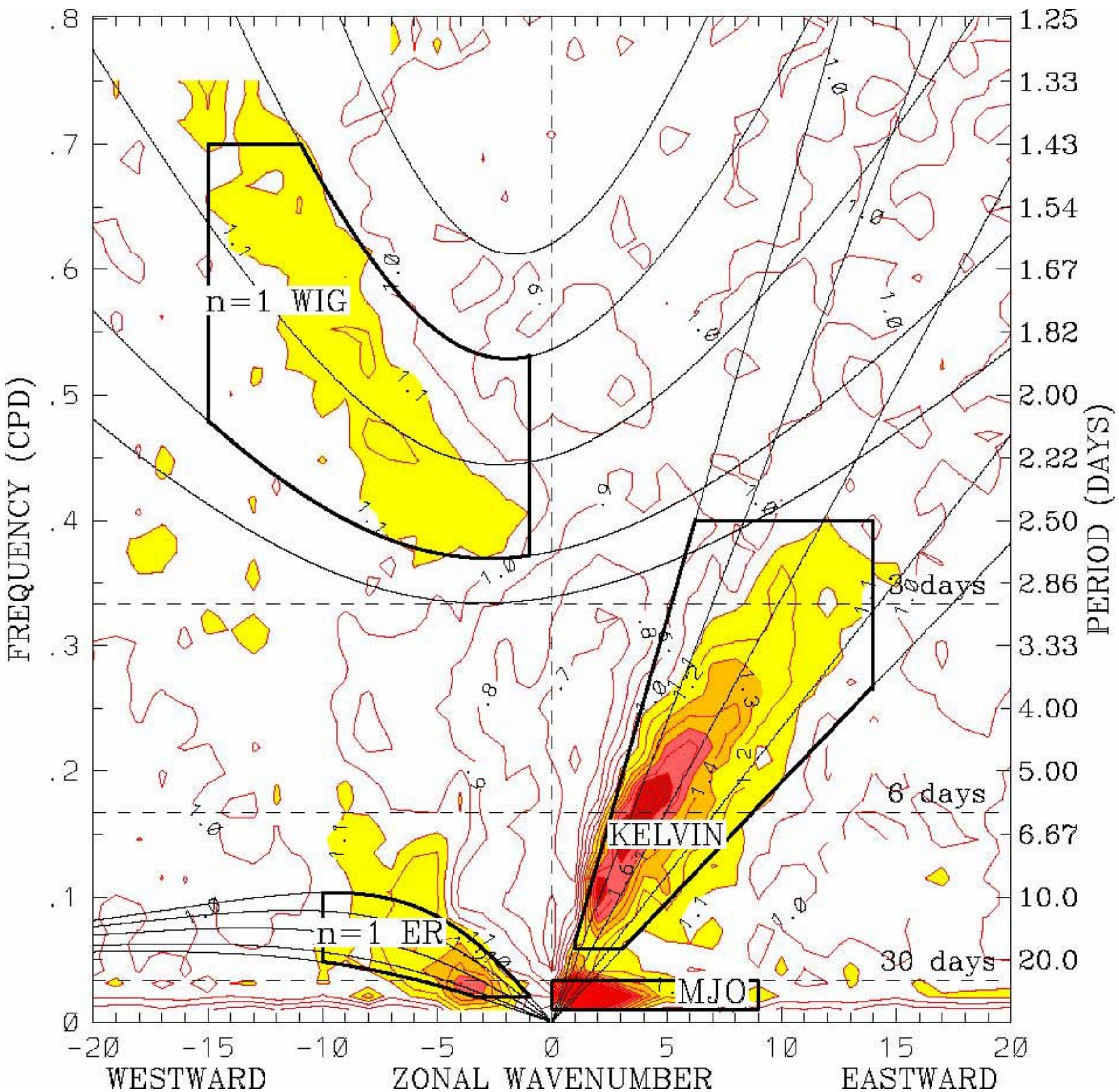

OBSERVATIONS OF KELVIN WAVES AND THE MJO

Time–longitude diagram of CLAUS Tb (2.5S–7.5N), January–April 1987

Cloud Archive User Service (CLAUS)

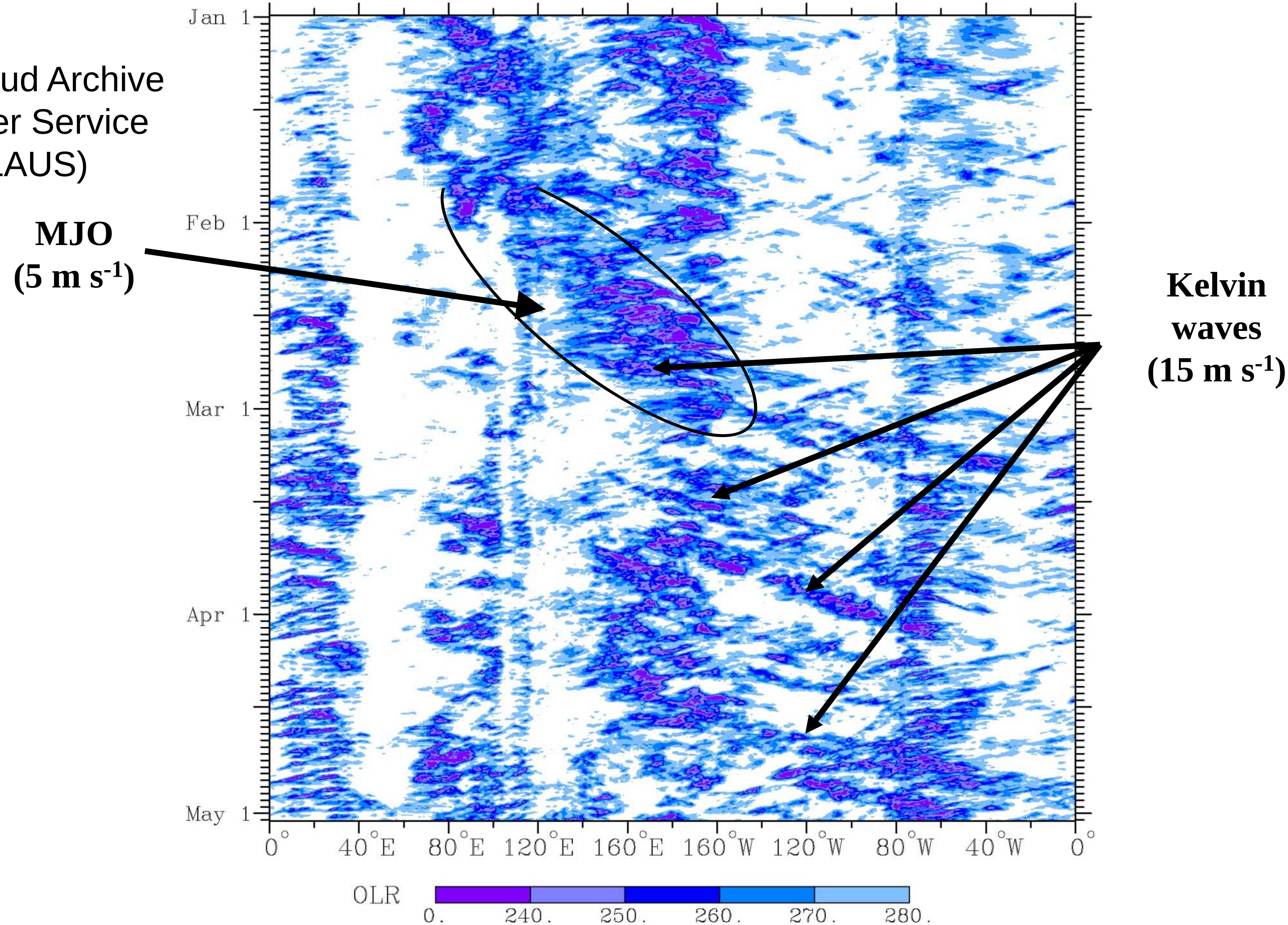

OBSERVATIONS OF KELVIN WAVES AND THE MJO

Time–longitude diagram of CLAUS Tb (5S–equator), February 1987

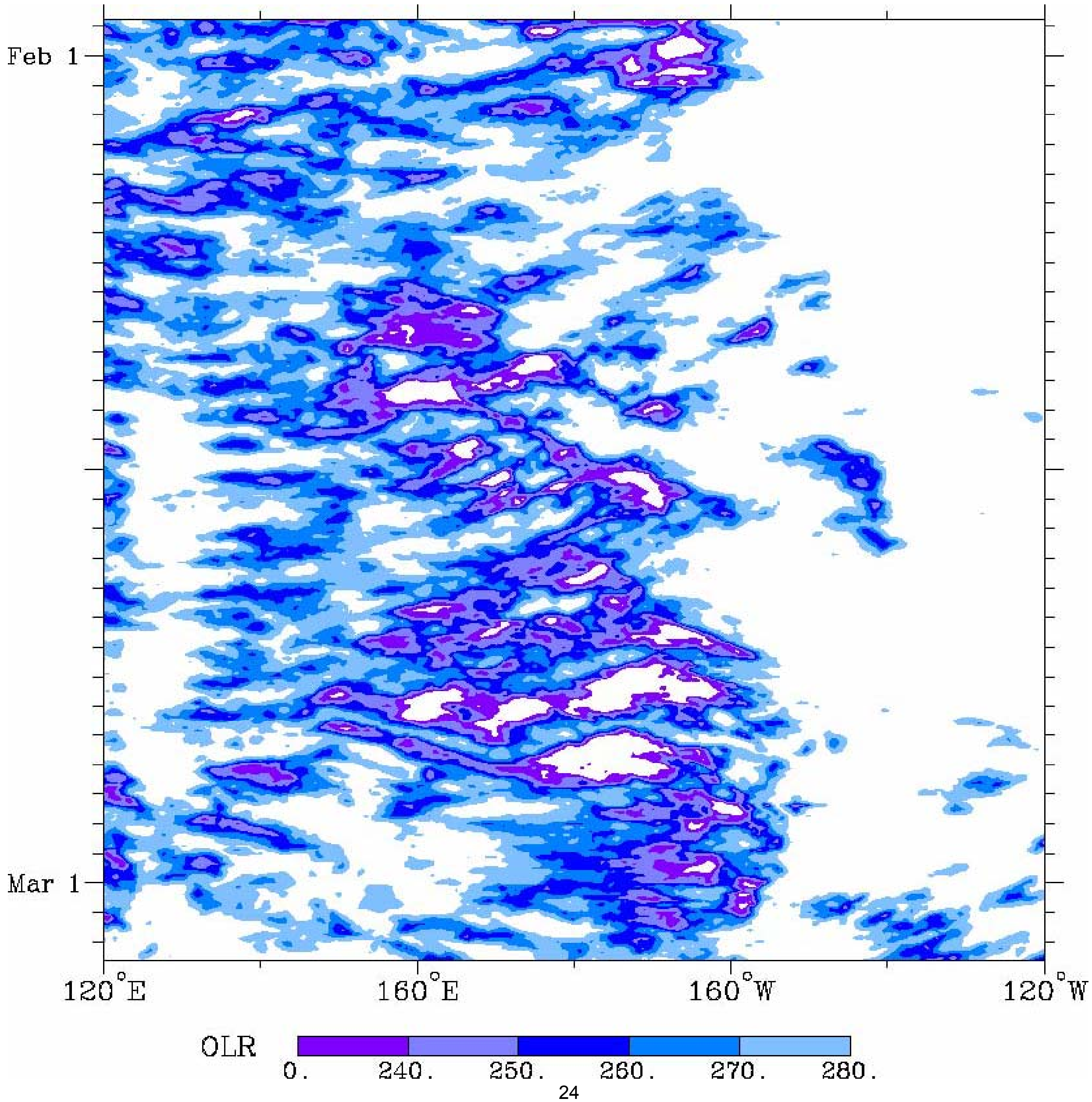

OBSERVATIONS OF TWO DAY (WIG), KELVIN WAVES AND THE MJO

Time–longitude diagram of CLAUS Tb (2.5S–2.5N), October–December 1992

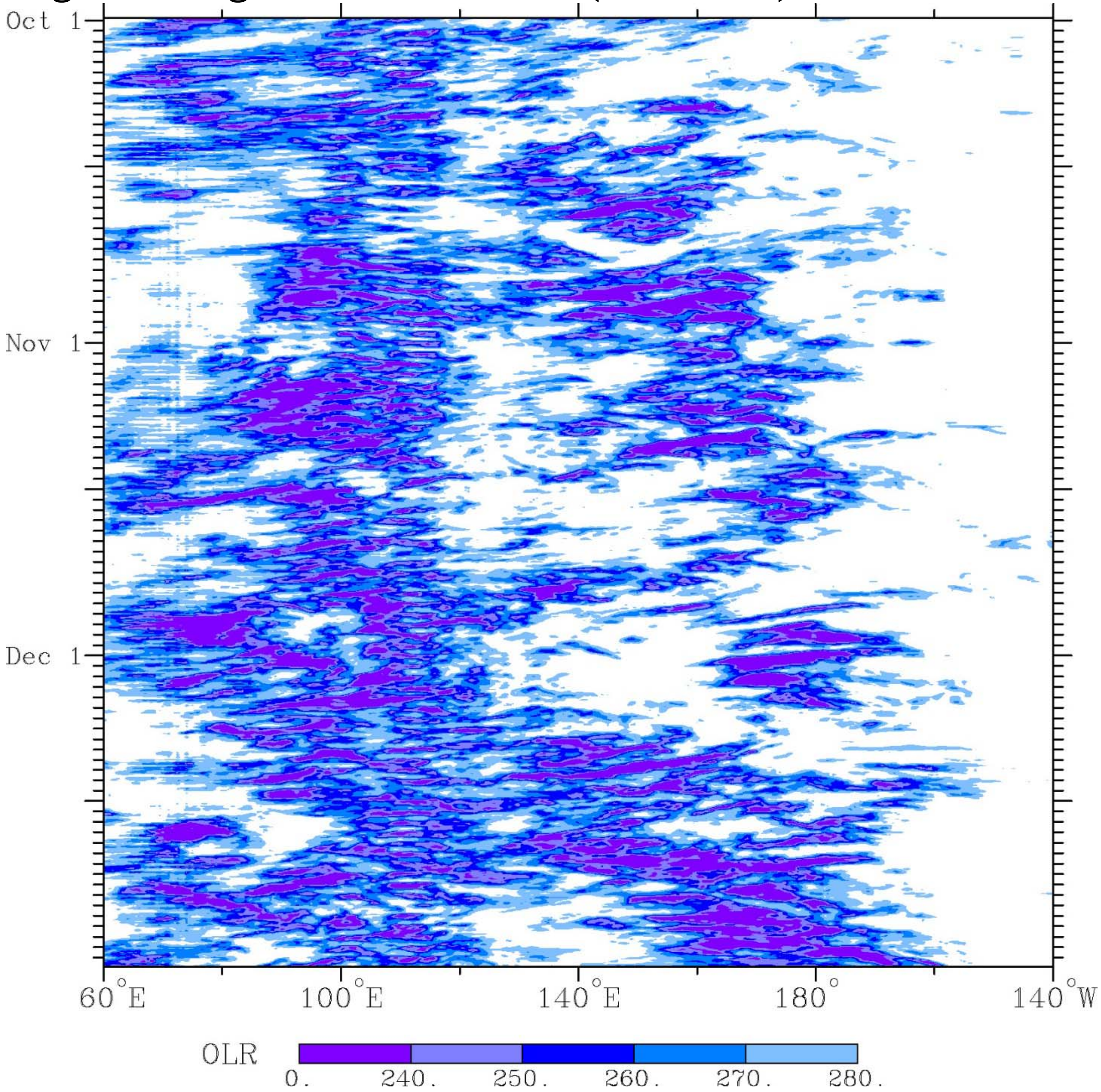

OBSERVATIONS OF TWO DAY (WIG), KELVIN WAVES AND THE MJO

Time–longitude diagram of CLAUS Tb (2.5S–2.5N), October–December 1992

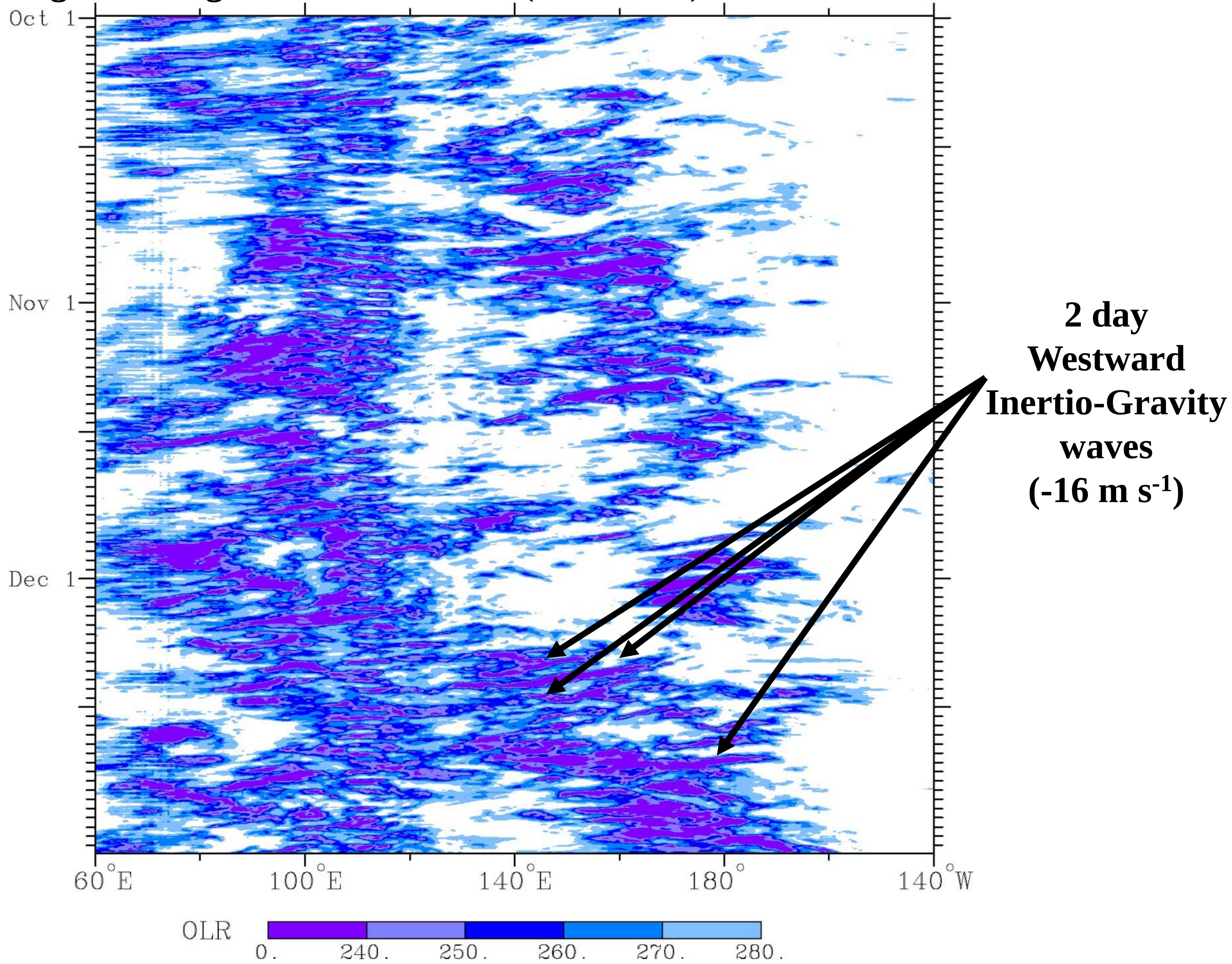

OBSERVATIONS OF TWO DAY (WIG), KELVIN WAVES AND THE MJO

Time–longitude diagram of CLAUS Tb (2.5S–2.5N), October–December 1992

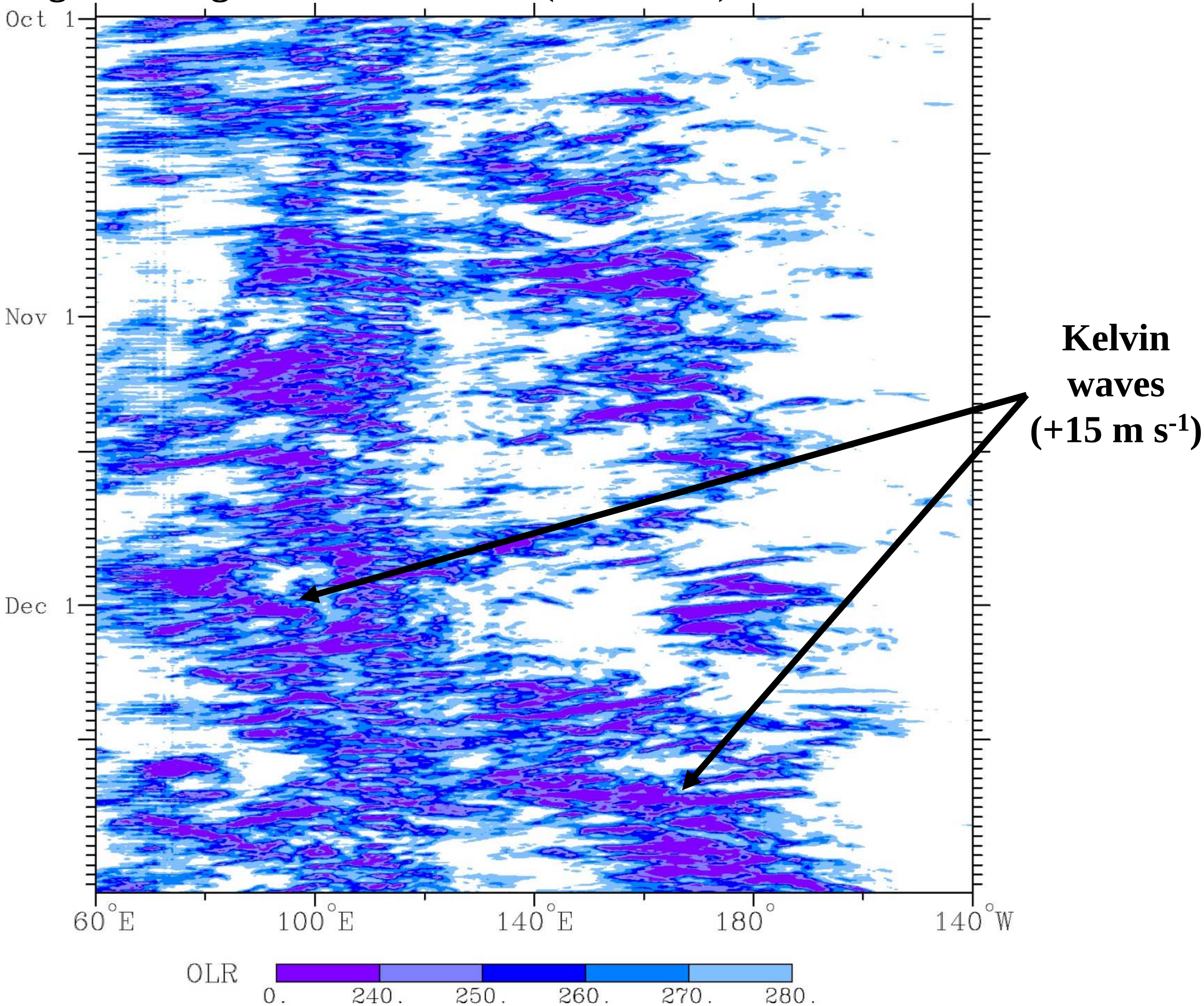

OBSERVATIONS OF KELVIN WAVES AND THE MJO

Time–longitude diagram of CLAUS Tb (2.5S–7.5N), January–April 1987

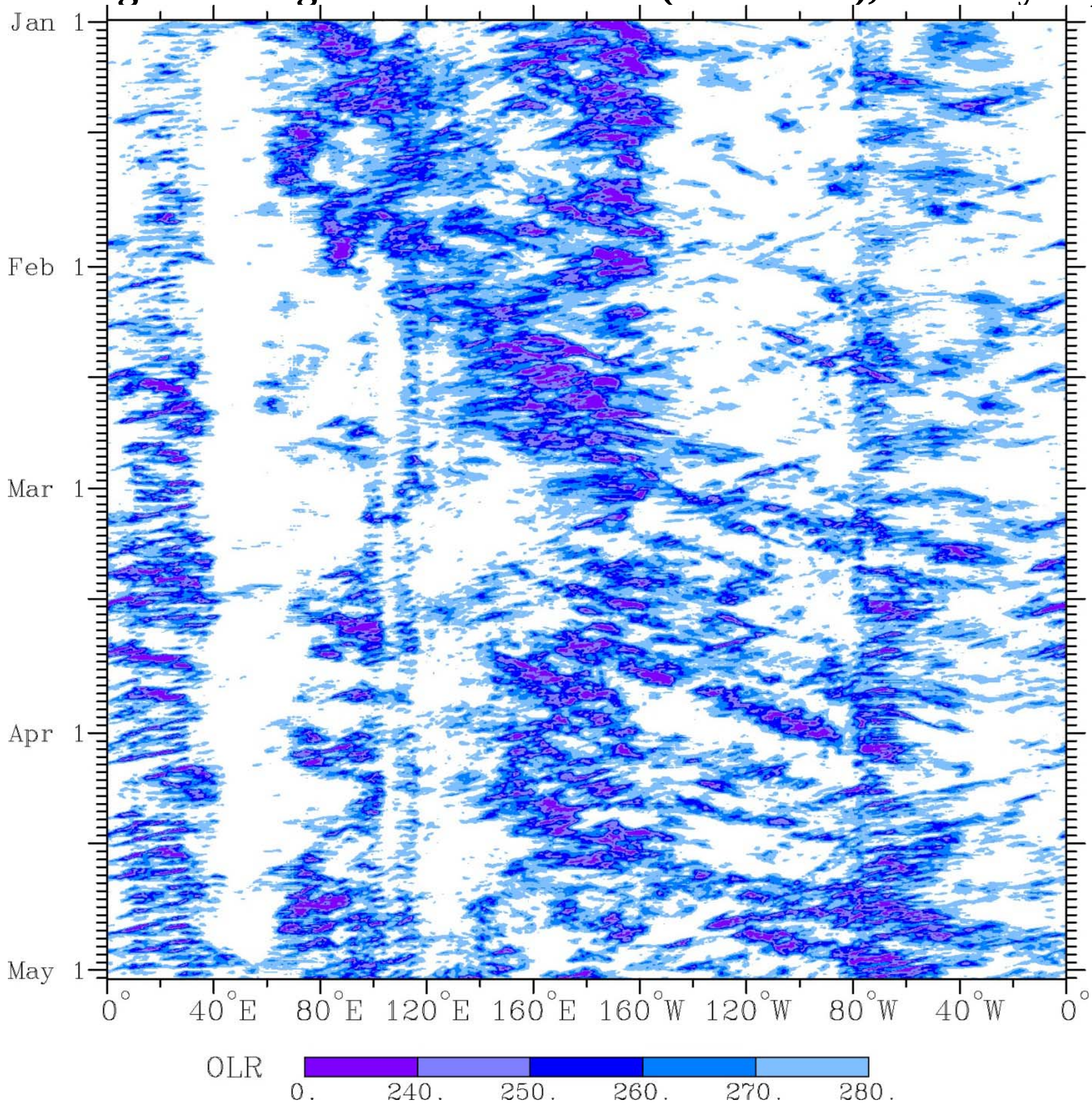

OBSERVATIONS OF KELVIN WAVES AND THE MJO

Time–longitude diagram of CLAUS Tb (2.5S–7.5N), January–April 1987

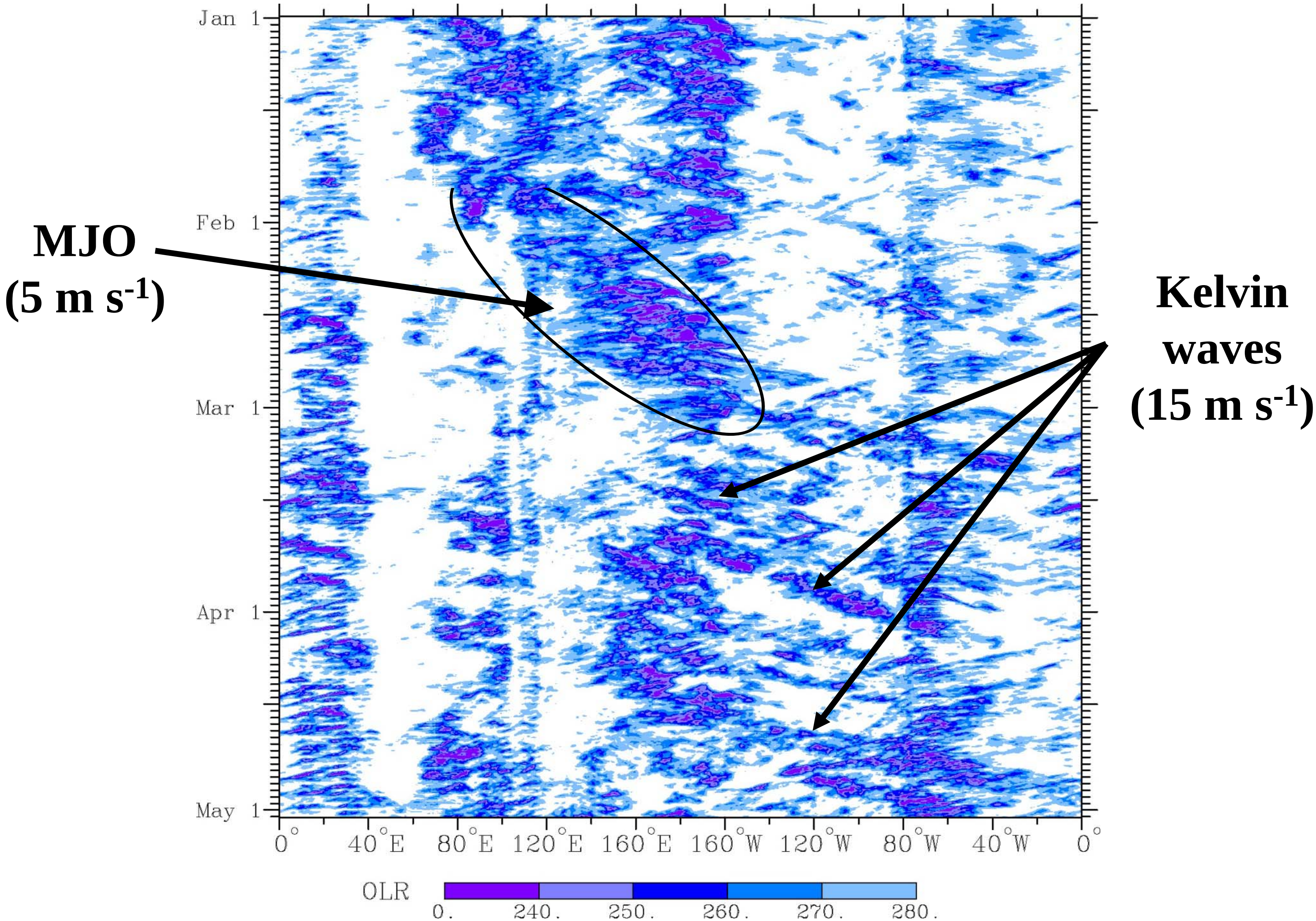

OBSERVATIONS OF KELVIN AND MRG WAVES

Time–longitude diagram of CLAUS Tb (2.5S–7.5N), May 1987

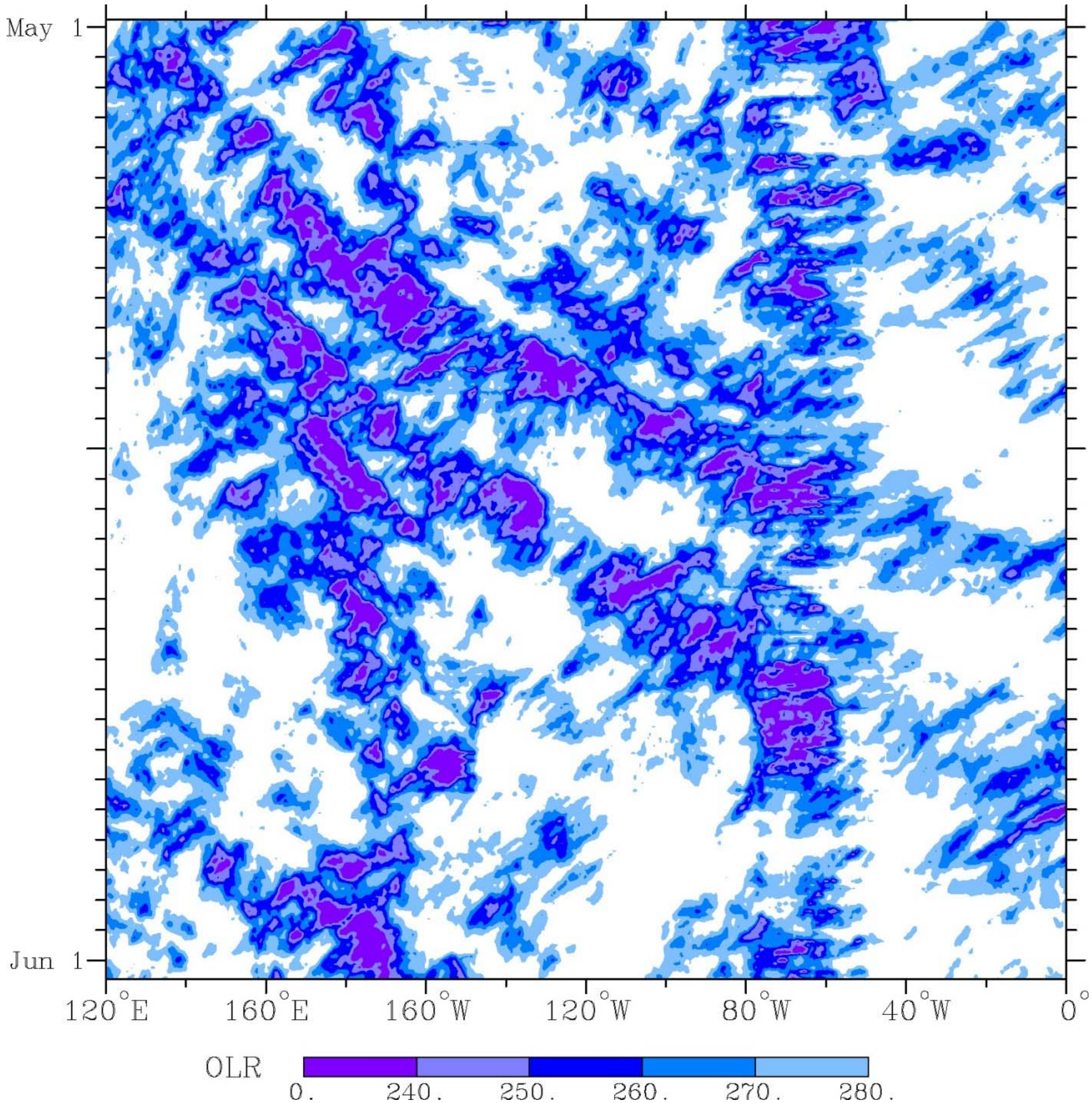

1998 OLR   2.5ºS-2.5º N

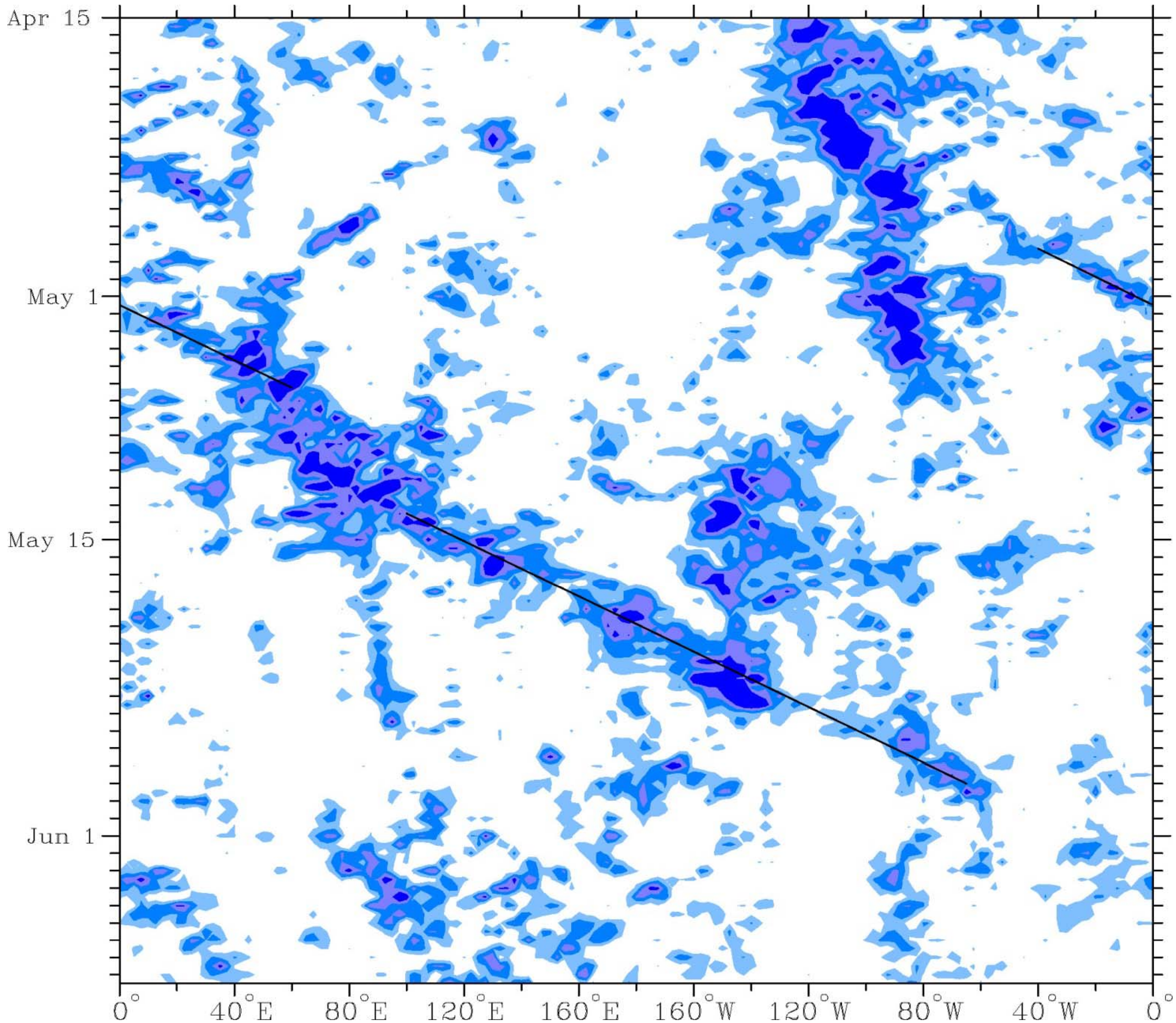

OLR shading starts at - 10 W m^{-2} at 20 W m^{-2} intervals, negative only

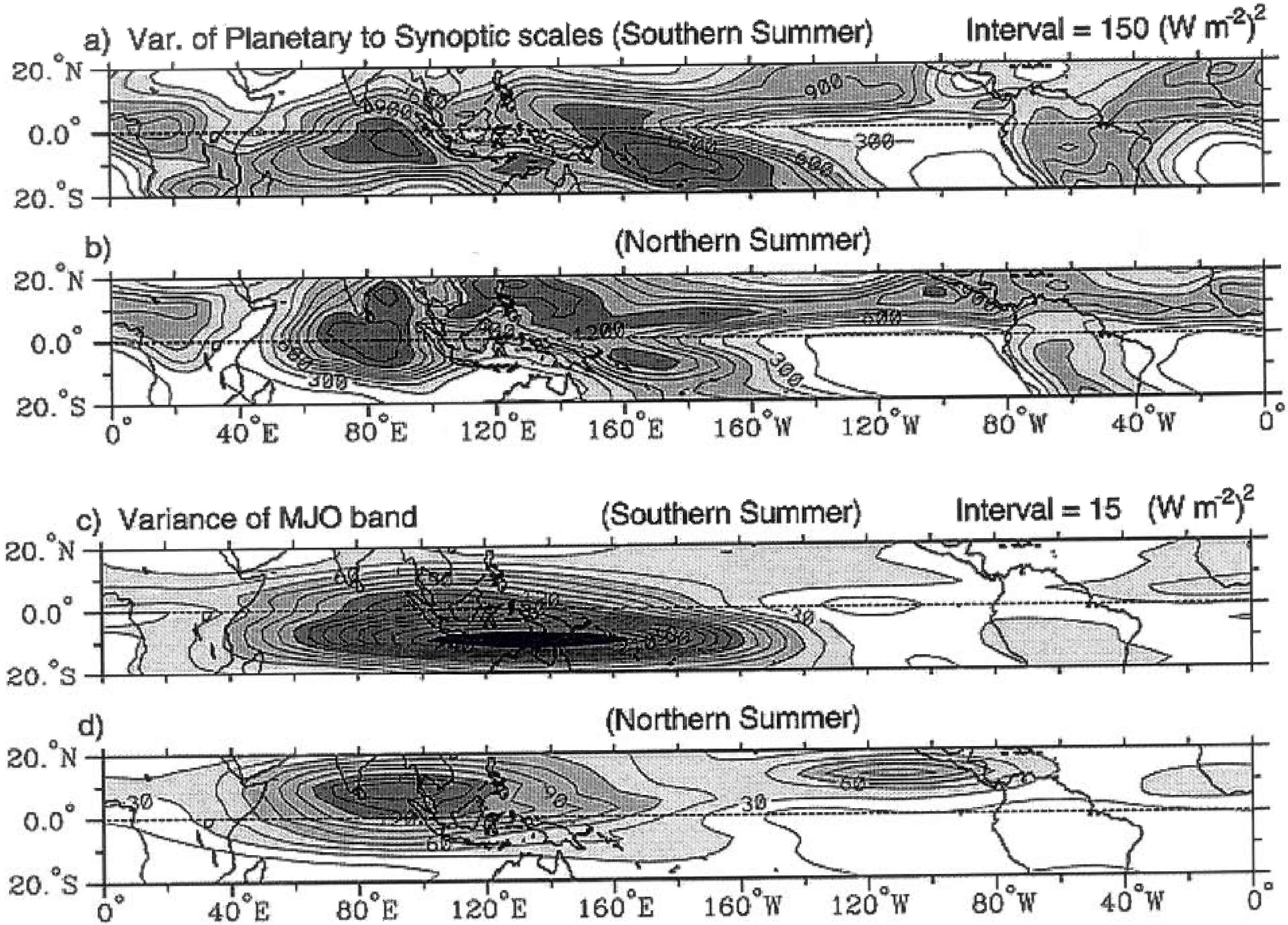
a) Var. of Planetary to Synoptic scales (Southern Summer)
Interval = 150 (W m^{-2})^2
b)
(Northern Summer)
c) Variance of MJO band
(Southern Summer)
Interval = 15 (W m^{-2})^2
d)
(Northern Summer)
20.°N
0.0°
20.°S
0°
40°E
80°E
120°E
160°E
160°W
120°W
80°W
40°W
0°
900
300
600
1200
30
60
90

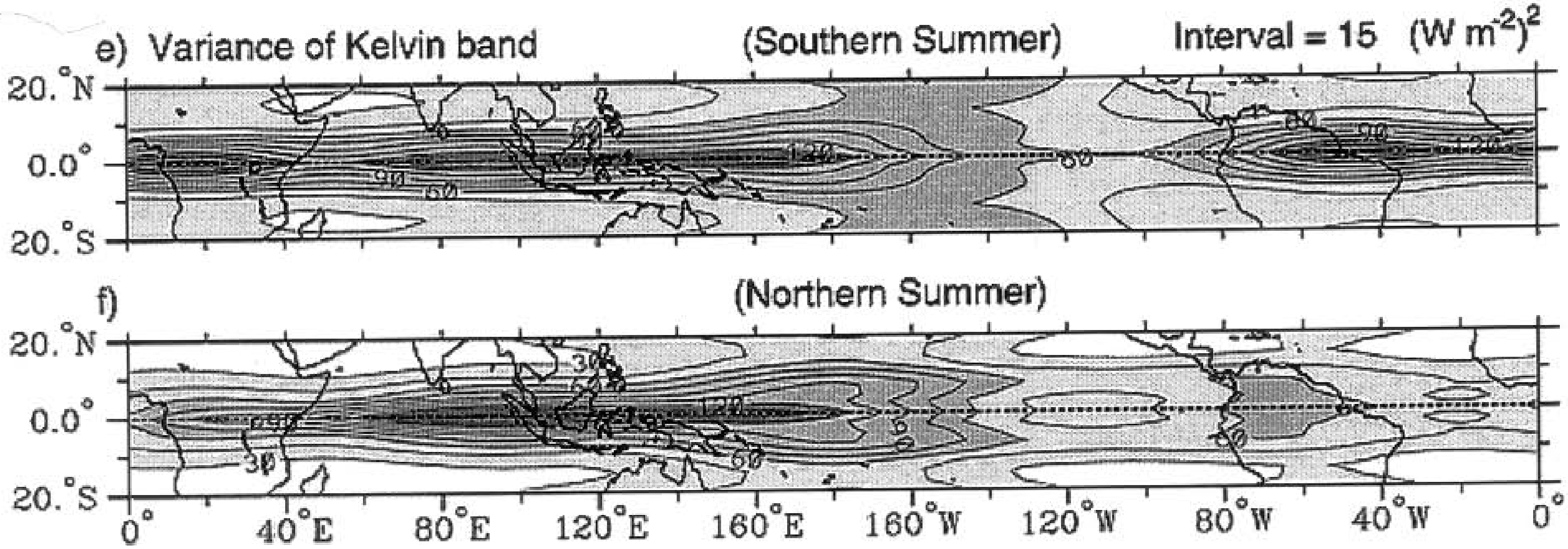
e) Variance of Kelvin band
(Southern Summer)
Interval = 15 (W m-2)2
f)
(Northern Summer)
20.°N
0.0°
20.°S
0°
40°E
80°E
120°E
160°E
160°W
120°W
80°W
40°W
0°

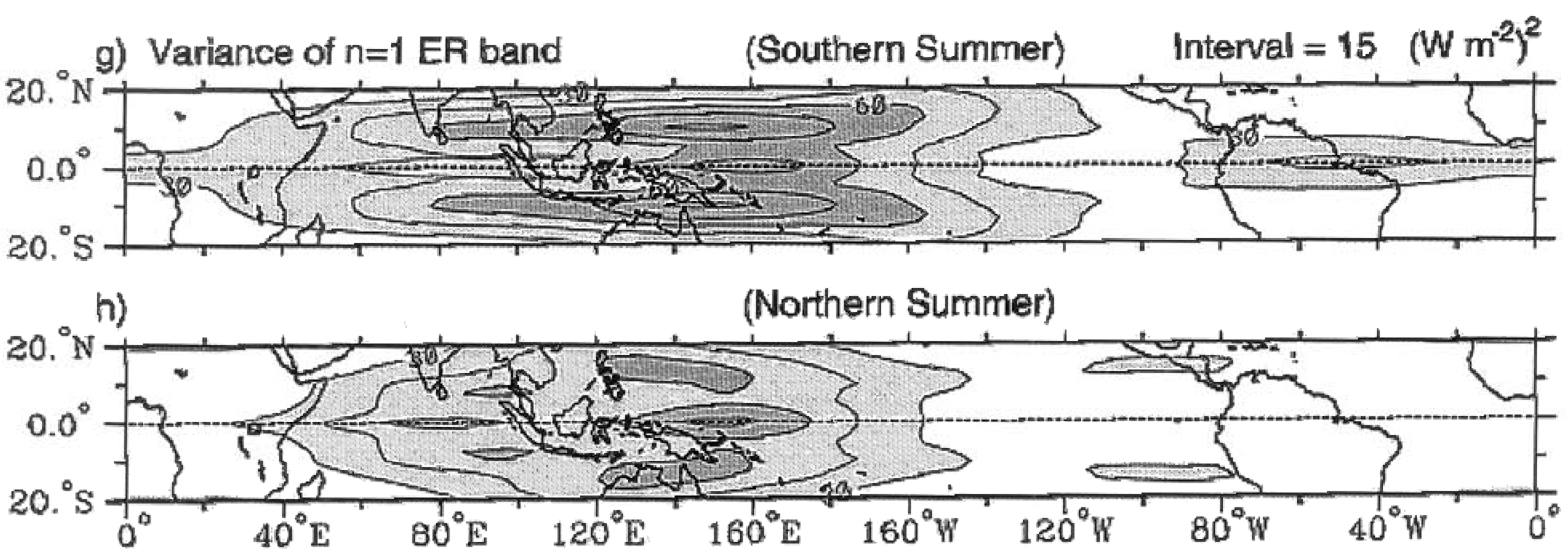
g) Variance of n=1 ER band
(Southern Summer)
Interval = 15 (W m-2)2
h)
(Northern Summer)
20.°N
0.0°
20.°S
0°
40°E
80°E
120°E
160°E
160°W
120°W
80°W
40°W
0°

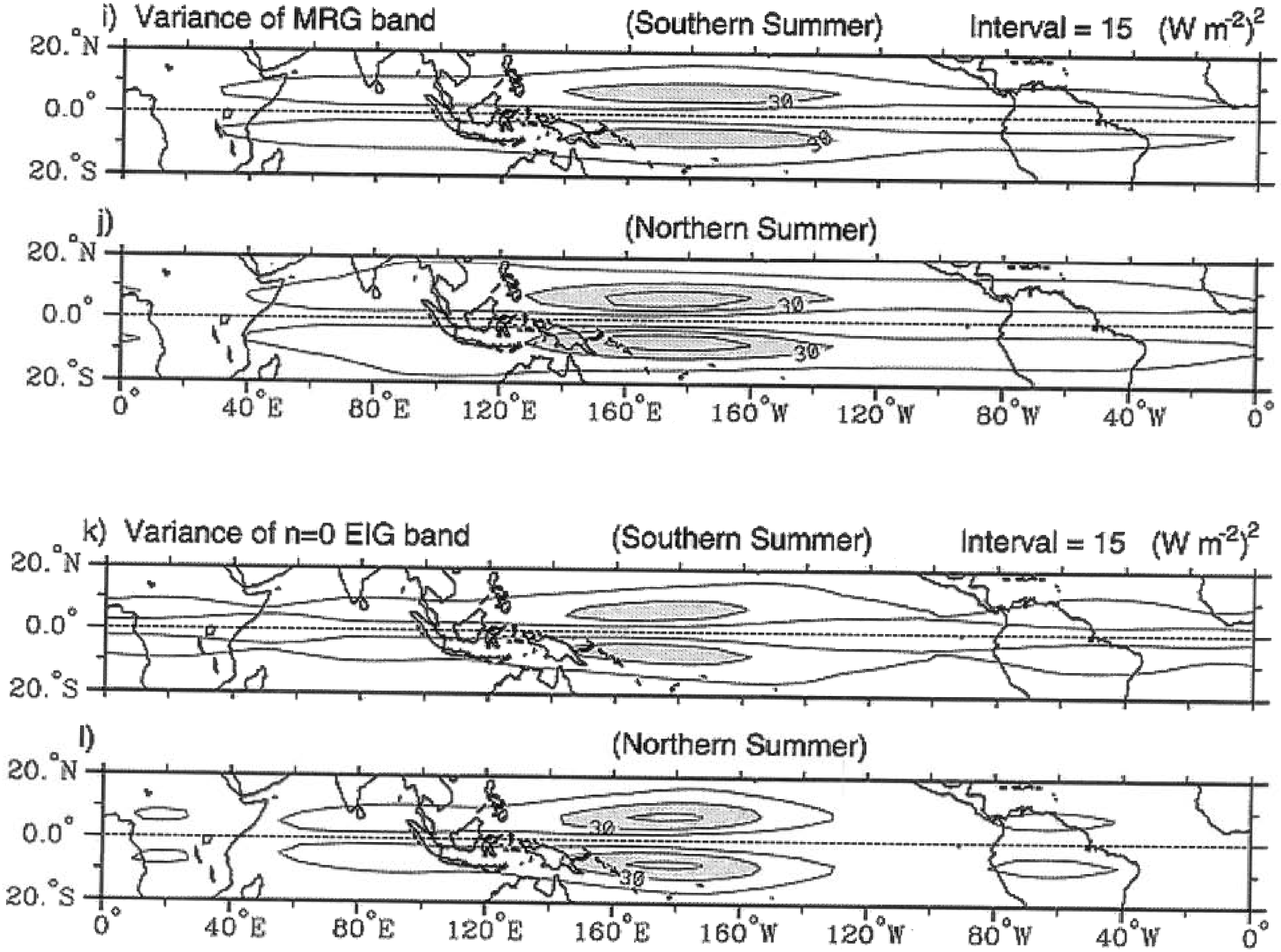

i) Variance of MRG band
(Southern Summer)
Interval = 15 (W m-2)2
j)
(Northern Summer)
20.°N
0.0°
20.°S
30
0° 40°E 80°E 120°E 160°E 160°W 120°W 80°W 40°W 0°
k) Variance of n=0 EIG band
(Southern Summer)
Interval = 15 (W m-2)2
l)
(Northern Summer)

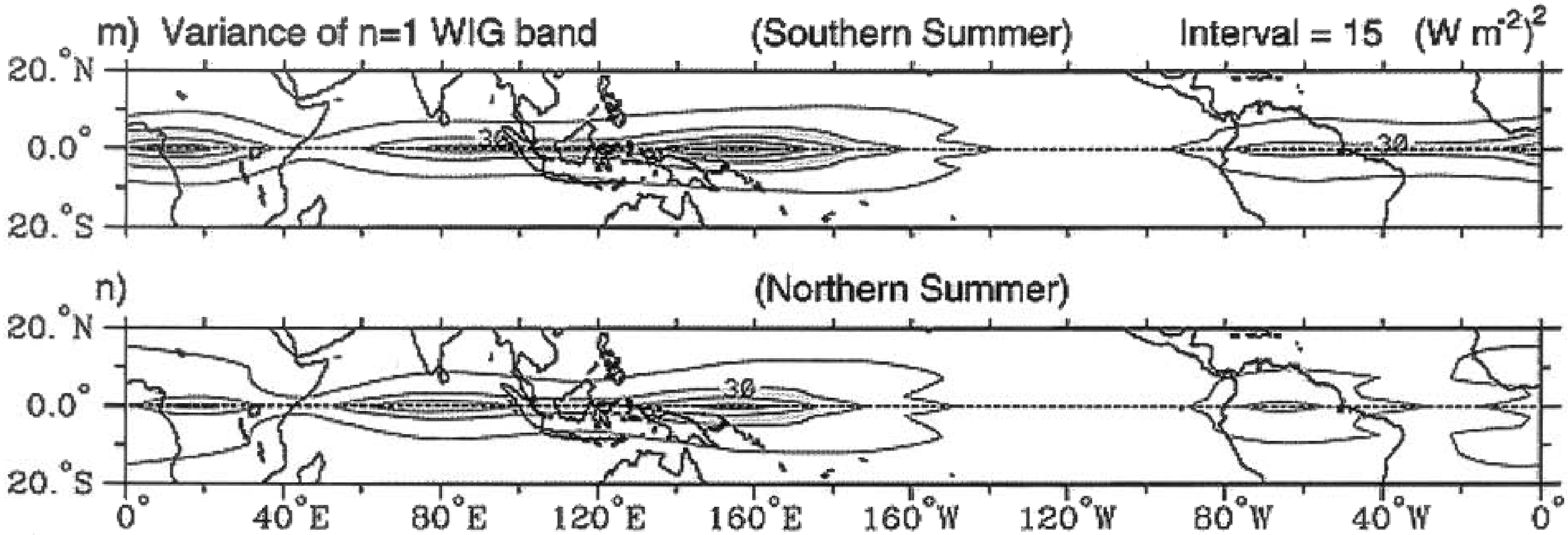
m) Variance of n=1 WIG band
(Southern Summer)
Interval = 15 (W m-2)2
n)
(Northern Summer)
20.°N
0.0°
20.°S
30
0°
40°E
80°E
120°E
160°E
160°W
120°W
80°W
40°W
0°

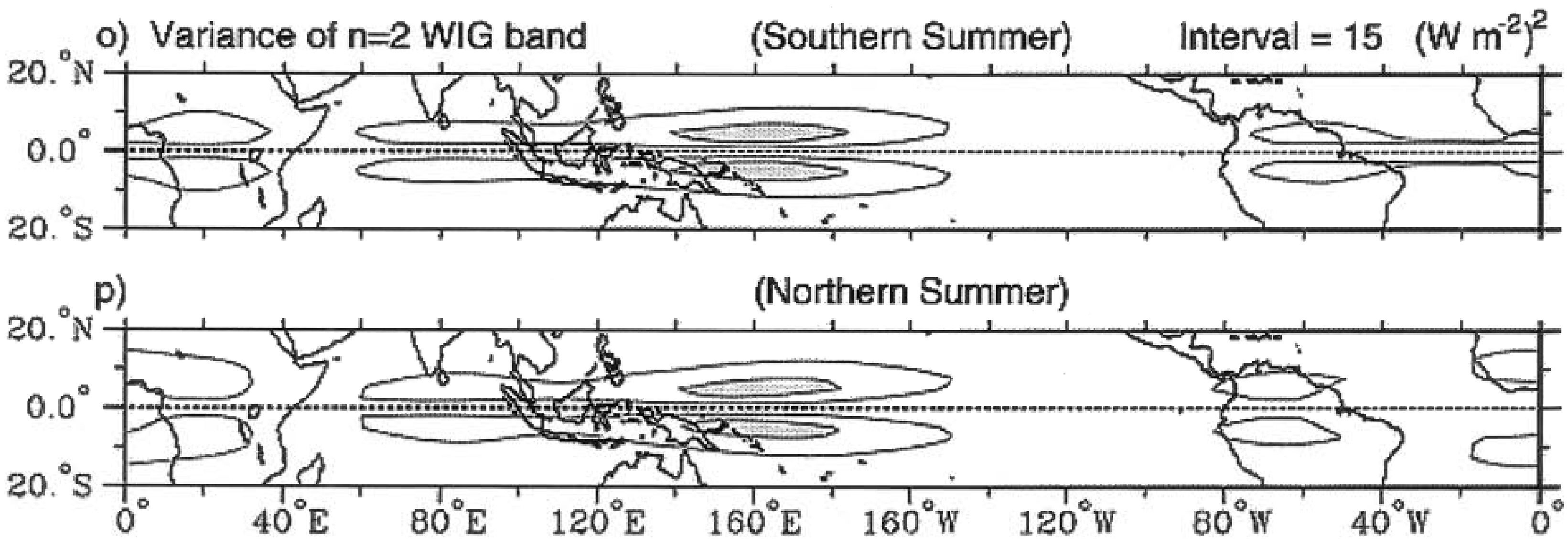
o) Variance of n=2 WIG band
(Southern Summer)
Interval = 15 (W m-2)2
p)
(Northern Summer)
20.°N
0.0°
20.°S
0°
40°E
80°E
120°E
160°E
160°W
120°W
80°W
40°W
0°

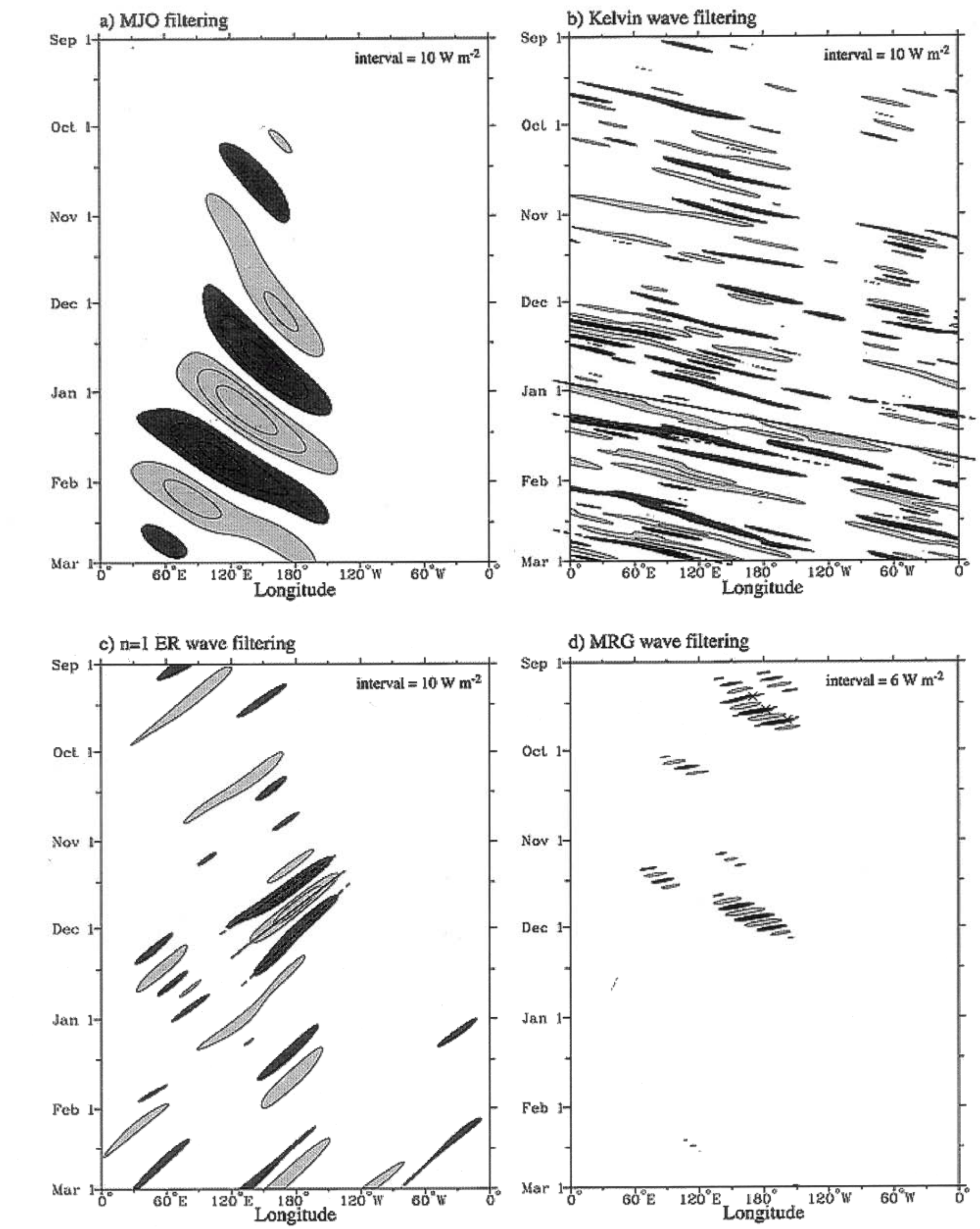

Fig. 9. (a) Time-longitude section of the OLR anomalies for the MJO-filtered band for the same 6-month sample period as Fig. 8, averaged for the latitudes from 10°S to 2.5°N. The zero contour

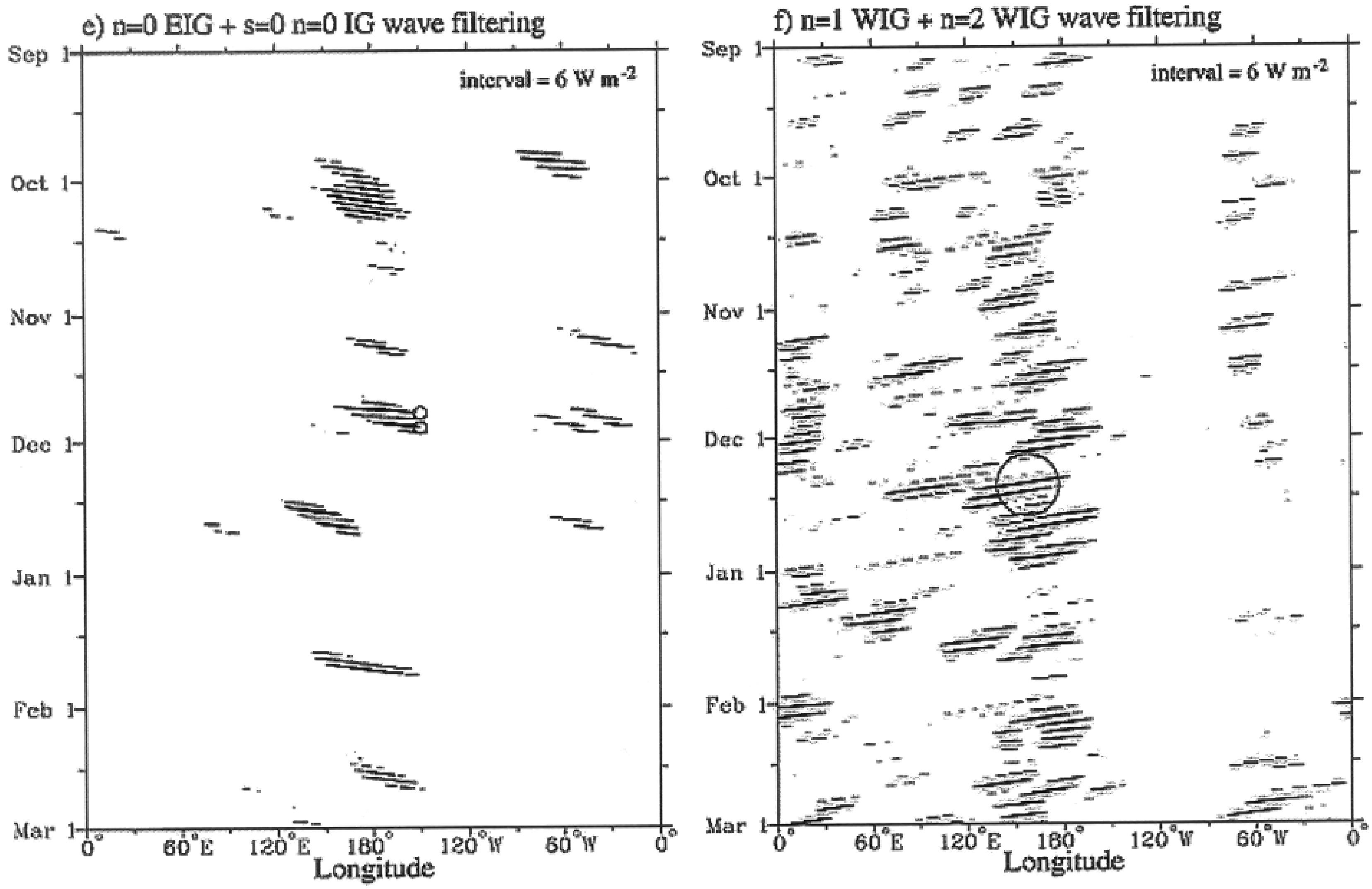

Fig. 9 (*Continued*) (e) The $n = 0$ EIG wave-filtered plus the $s = 0$, $n = 0$ IG wave-filtered band. (f) The $n = 1$ WIG wave-filtered plus the $n = 2$ WIG wave-filtered bands.

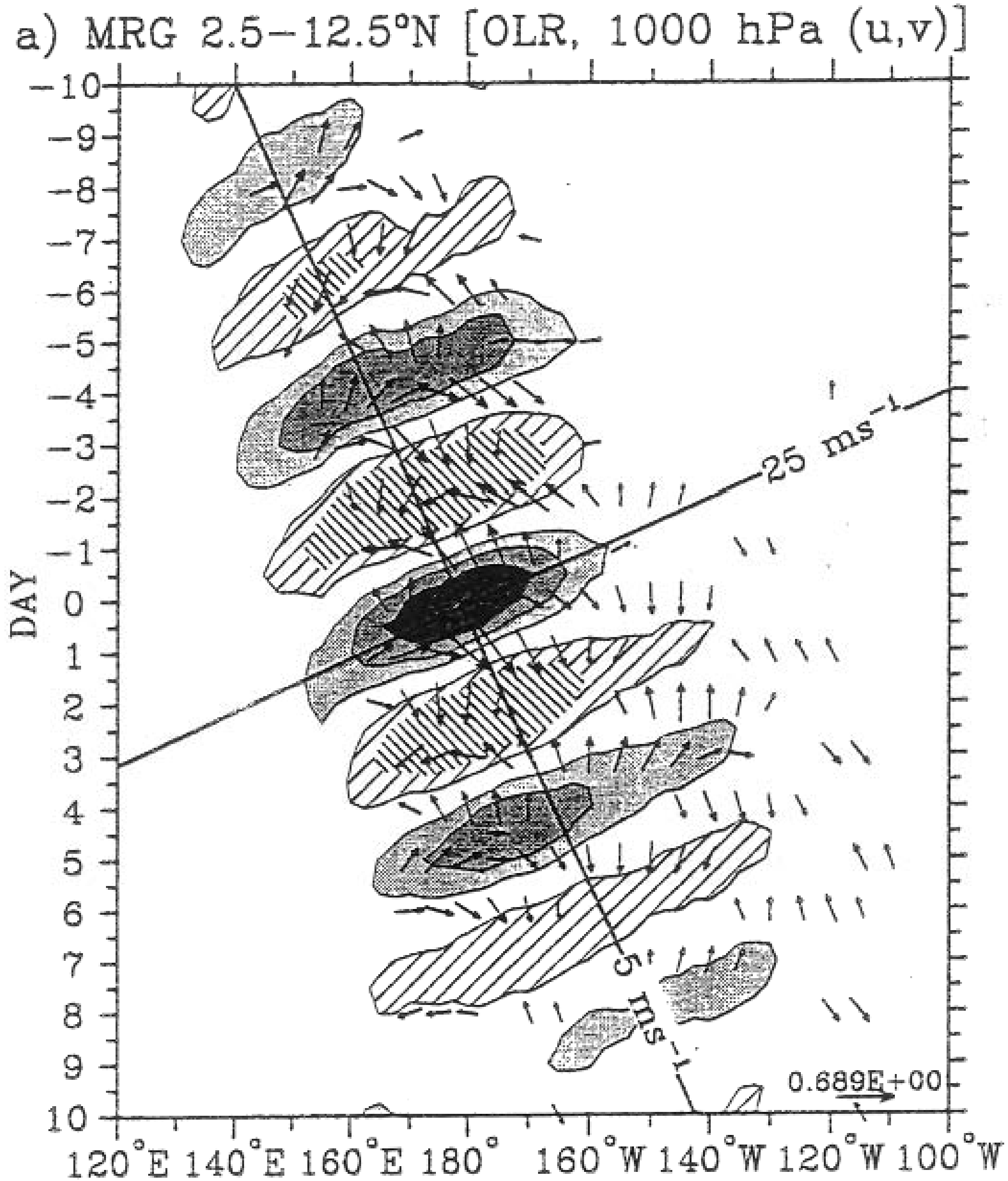
a) MRG 2.5–12.5°N [OLR, 1000 hPa (u,v)]
DAY
−10
−9
−8
−7
−6
−5
−4
−3
−2
−1
0
1
2
3
4
5
6
7
8
9
10
120°E 140°E 160°E 180° 160°W 140°W 120°W 100°W
25 ms−1
5 ms−1
0.689E+00

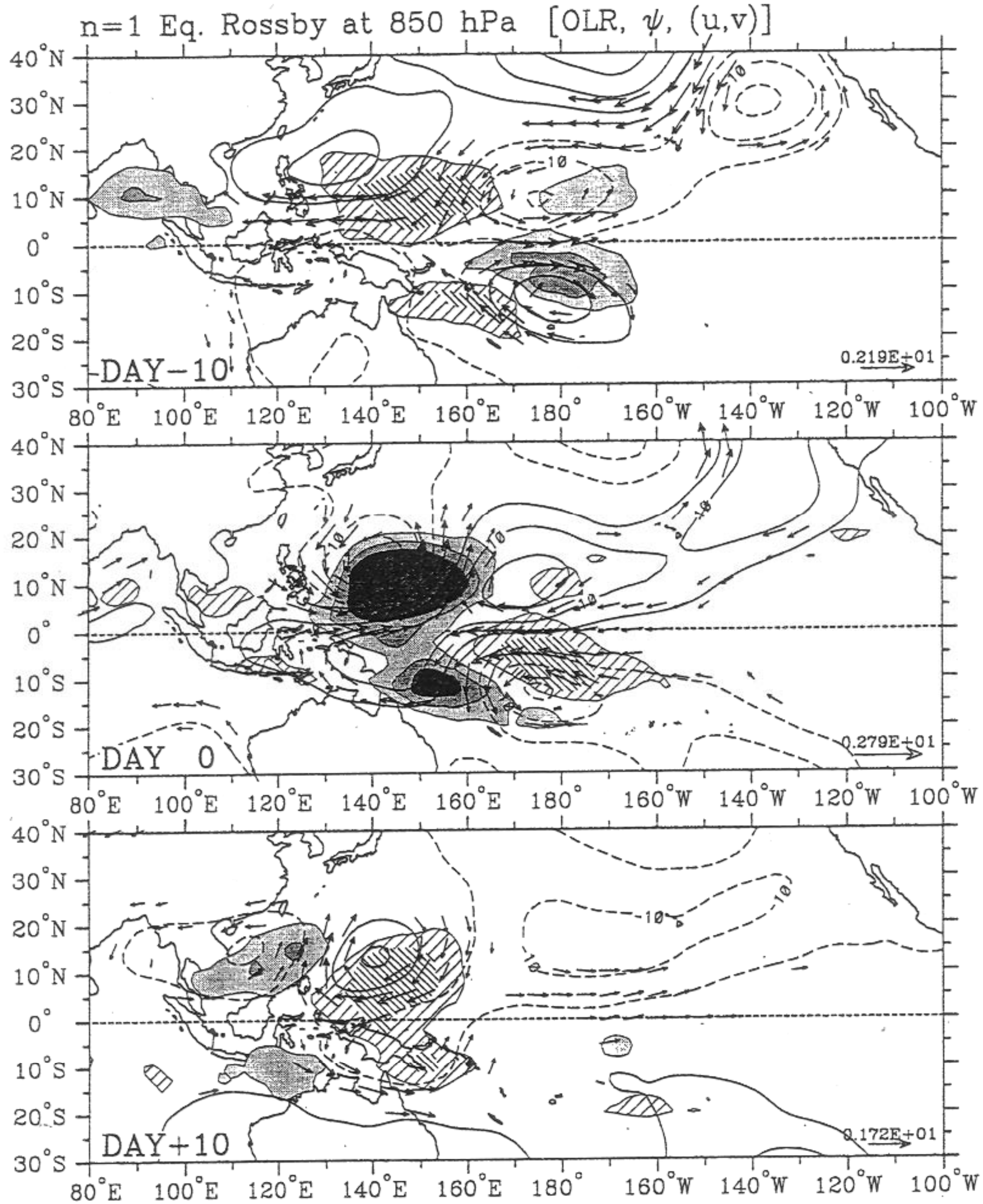

n=1 Eq. Rossby at 850 hPa [OLR, ψ, (u,v)]
DAY-10
DAY 0
DAY+10
0.219E+01
0.279E+01
0.172E+01
40°N
30°N
20°N
10°N
0°
10°S
20°S
30°S
80°E 100°E 120°E 140°E 160°E 180° 160°W 140°W 120°W 100°W

a) n=1 ER section at 150°E [T, (v,w)]

b) n=1 ER section at 140°E [u]

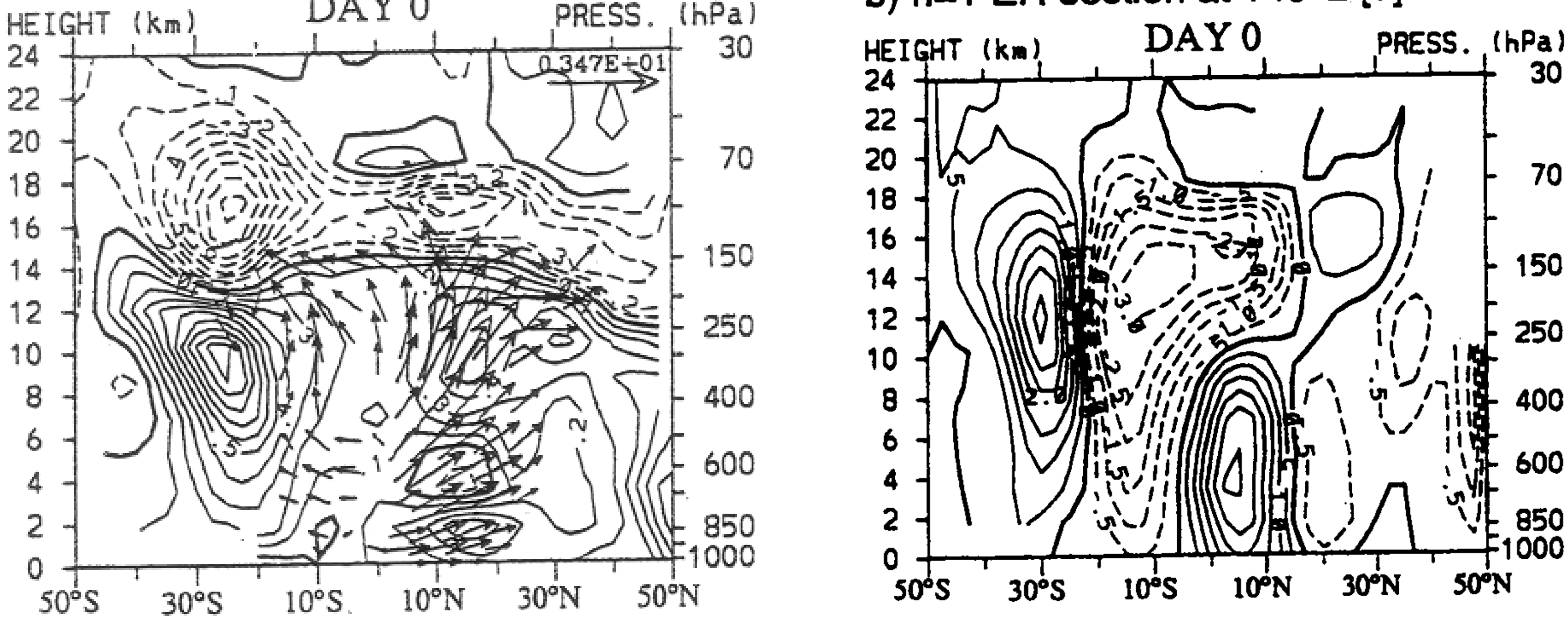

c) n=1 ER section along Eq. [u, (u,w)]

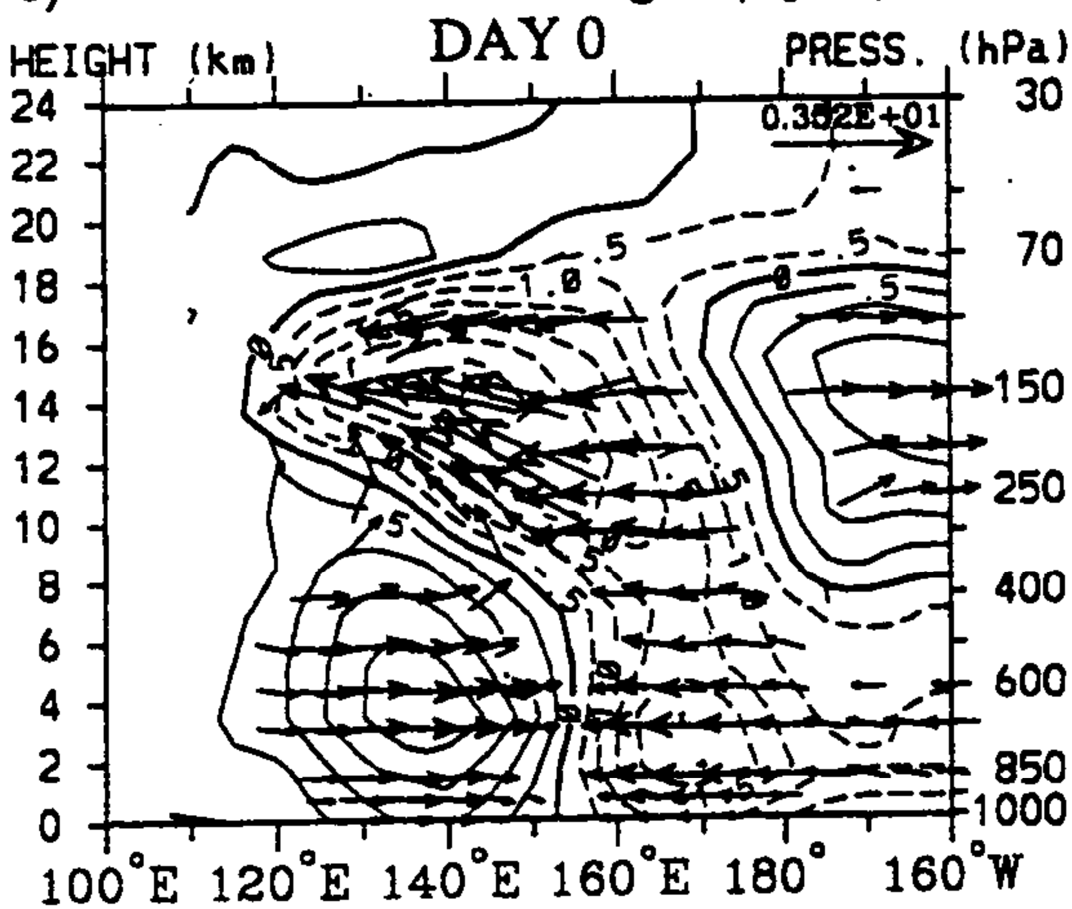

Regression Model

Simple Linear Model:

$$y = ax + b$$

where: x= predictor (filtered OLR)
y= predictand (OLR, circulation)

OLR and 850 hPa Flow Regressed against MJO-filtered OLR (scaled -40 W m^2) at eq, 155°E, 1979-1993

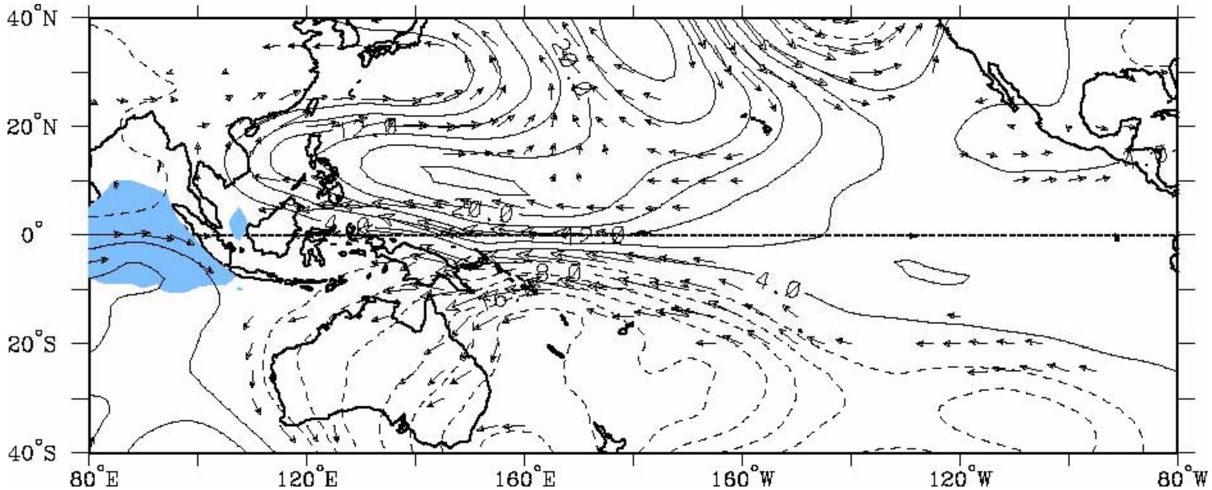

Day-16

Streamfunction (contours 4 X 10^5 m^2 s^{-1})

Wind (vectors, largest around 2 m s^{-1})

OLR (shading starts at +/- 6 W s^{-2}), negative blue

OLR and 850 hPa Flow Regressed against MJO-filtered OLR (scaled -40 W m^2) at eq, 155°E, 1979-1993

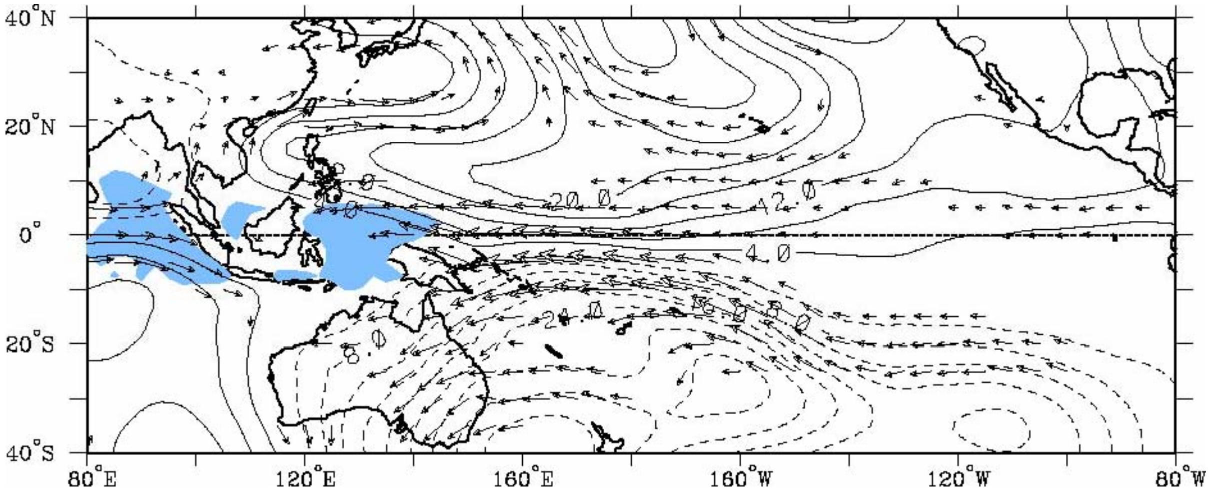

Day-12

Streamfunction (contours 4 X 10^5 m^2 s^{-1})

Wind (vectors, largest around 2 m s^{-1})

OLR (shading starts at +/- 6 W s^{-2}), negative blue

OLR and 850 hPa Flow Regressed against MJO-filtered OLR (scaled -40 W m^2) at eq, 155°E, 1979-1993

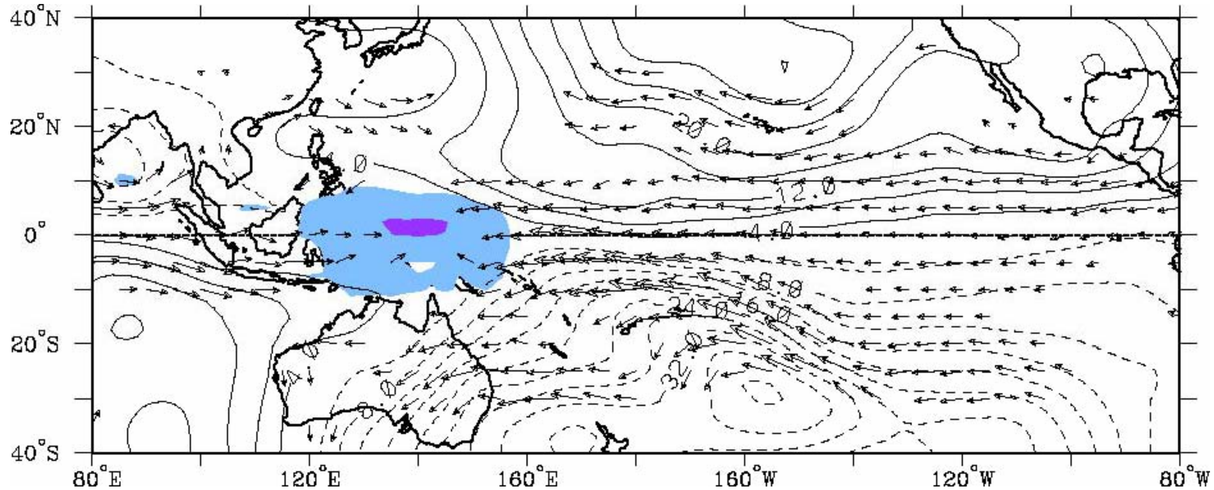

Day-8

Streamfunction (contours 4 X 10^5 m^2 s^{-1})

Wind (vectors, largest around 2 m s^{-1})

OLR (shading starts at +/- 6 W s^{-2}), negative blue

OLR and 850 hPa Flow Regressed against MJO-filtered OLR (scaled -40 W m^2) at eq, 155°E, 1979-1993

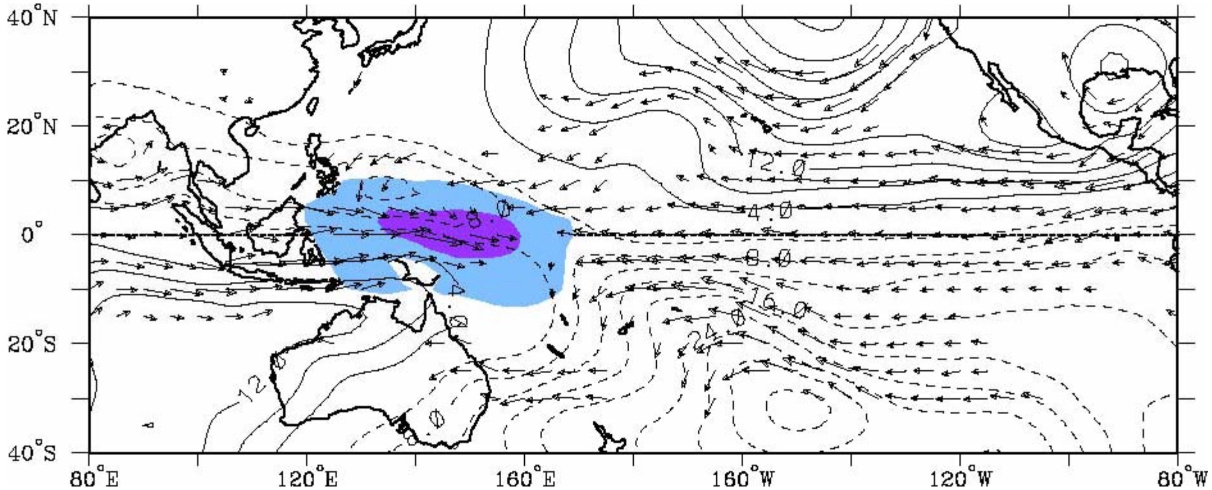

Day-4

Streamfunction (contours 4 X 10^5 m^2 s^{-1})

Wind (vectors, largest around 2 m s^{-1})

OLR (shading starts at +/- 6 W s^{-2}), negative blue

OLR and 850 hPa Flow Regressed against MJO-filtered OLR (scaled -40 W m^2) at eq, 155°E, 1979-1993

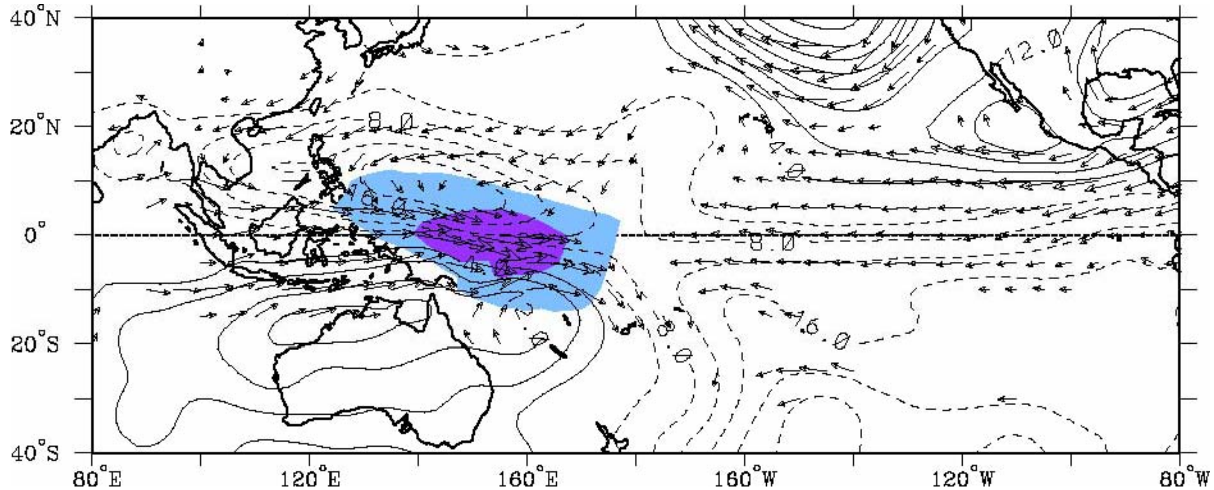

Day 0

Streamfunction (contours 4 X 10^5 m^2 s^{-1})

Wind (vectors, largest around 2 m s^{-1})

OLR (shading starts at +/- 6 W s^{-2}), negative blue

OLR and 850 hPa Flow Regressed against MJO-filtered OLR (scaled -40 W m^2) at eq, 155°E, 1979-1993

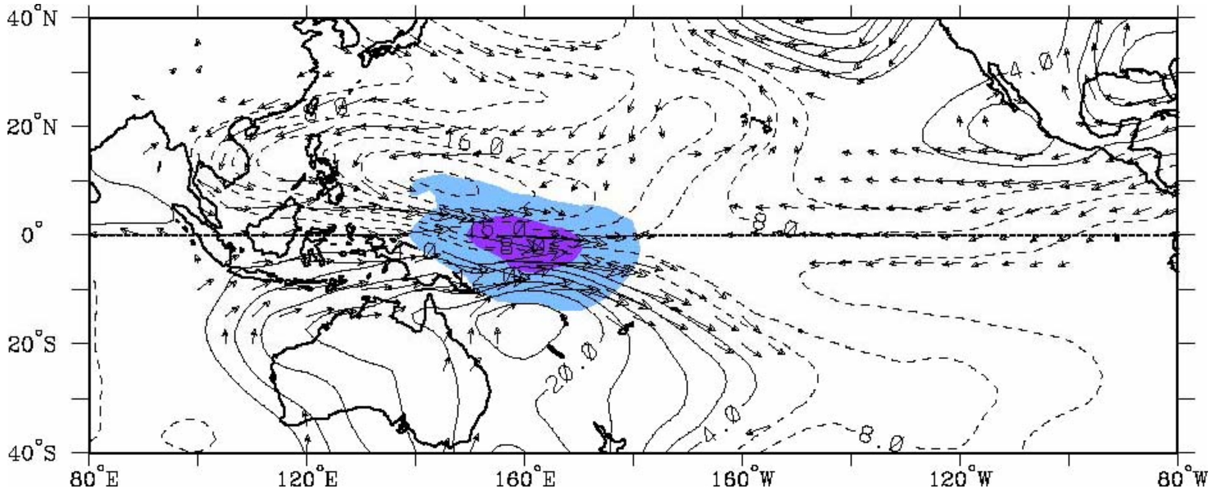

Day+4

Streamfunction (contours 4 X 10^5 m^2 s^{-1})

Wind (vectors, largest around 2 m s^{-1})

OLR (shading starts at +/- 6 W s^{-2}), negative blue

OLR and 850 hPa Flow Regressed against MJO-filtered OLR (scaled -40 W m^2) at eq, 155°E, 1979-1993

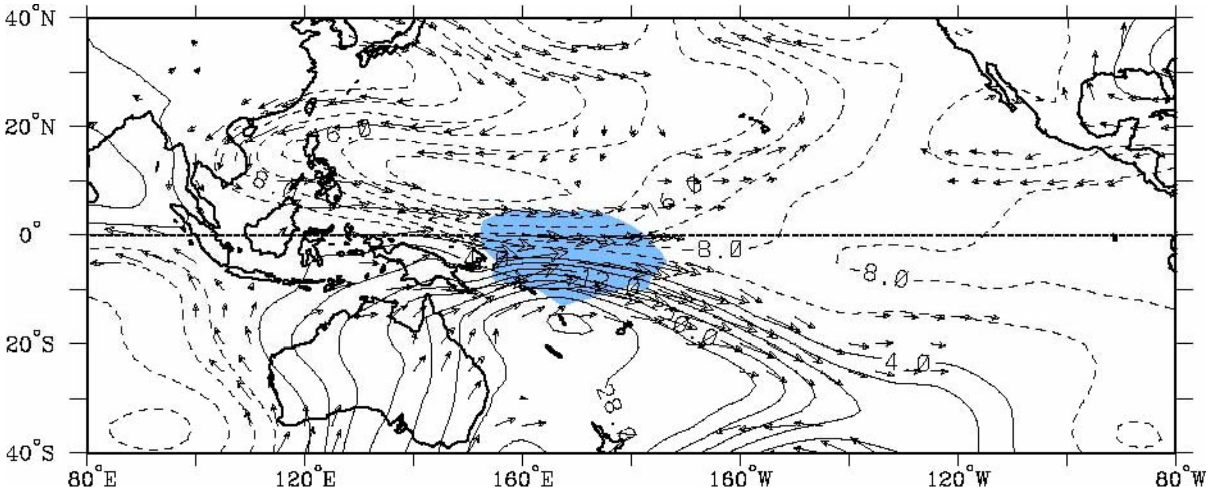

Day+8

Streamfunction (contours 4 X 10^5 m^2 s^{-1})

Wind (vectors, largest around 2 m s^{-1})

OLR (shading starts at +/- 6 W s^{-2}), negative blue

OLR and 850 hPa Flow Regressed against MJO-filtered OLR (scaled -40 W m^2) at eq, 155°E, 1979-1993

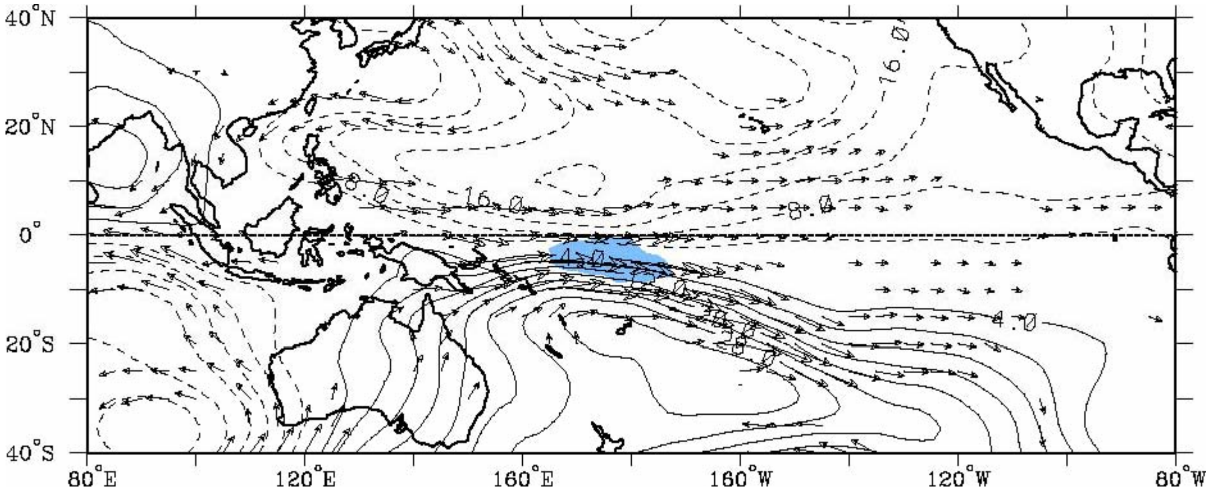

Day+12

Streamfunction (contours 4 X 10^5 m^2 s^{-1})

Wind (vectors, largest around 2 m s^{-1})

OLR (shading starts at +/- 6 W s^{-2}), negative blue

Convective Fraction from TRMM TMI Regressed against MJO-filtered OLR at Eq, 80°E (scaled -40 W m²) for 1998-2003

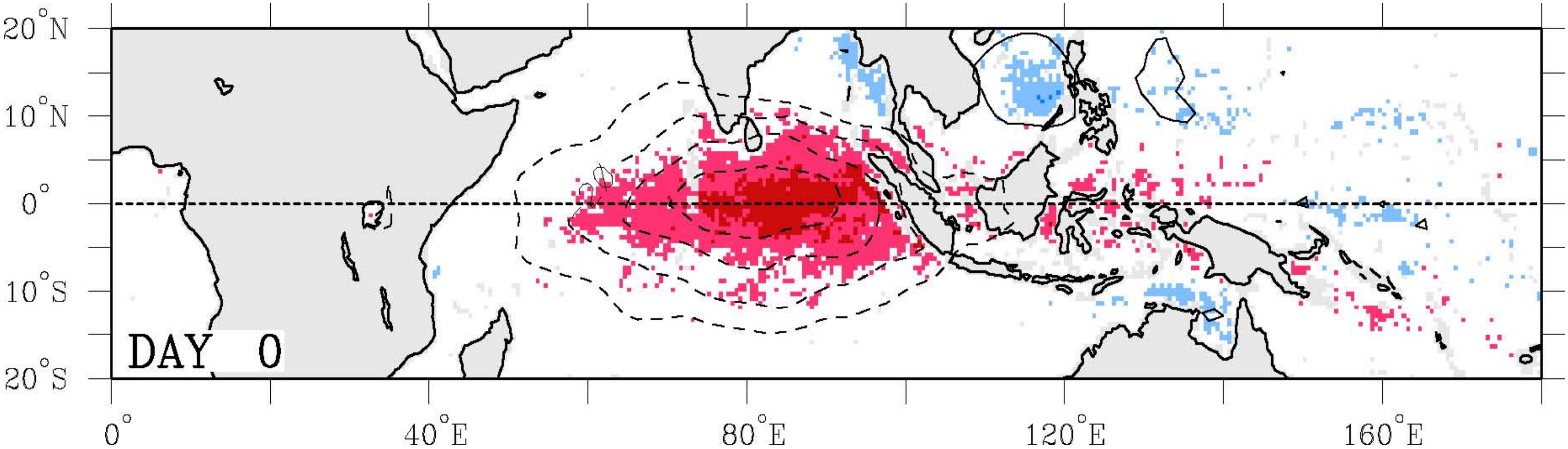

OLR (contours, 10 W m^{-2})

Convective Fraction (shading, ± 2 and 5%), red positive

Convective Fraction from TRMM TMI Regressed against MRG-filtered OLR at 7.5°N, 172.5°W (scaled -40 W m^2) for 1998-2003

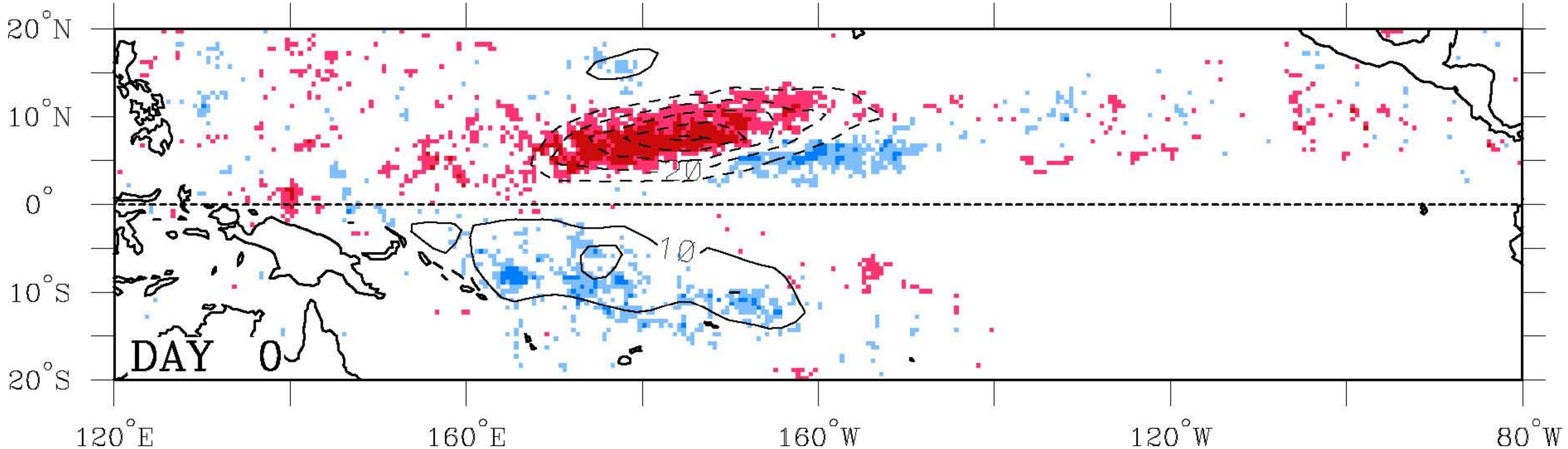

OLR (contours, 10 W m^{-2})
Convective Fraction (shading, ± 2 and 5%), red positive

Convective Fraction from TRMM TMI Regressed against Kelvin-filtered OLR at 7.5°N, 172.5°W (scaled -40 W m^2) for 1998-2003

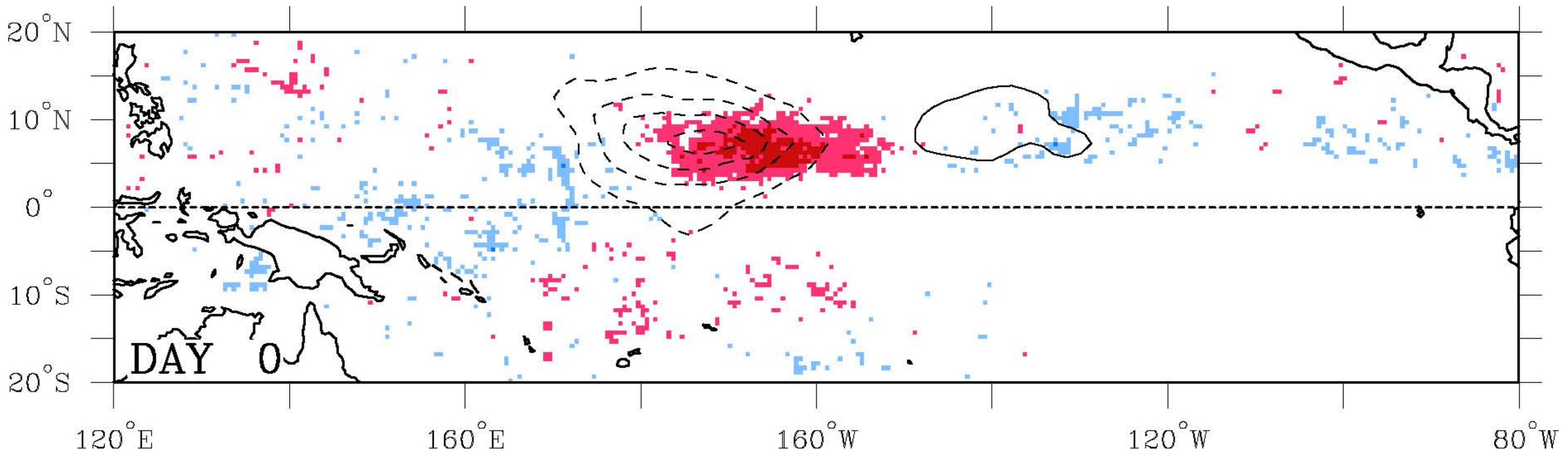

OLR (contours, 10 W m^{-2})
Convective Fraction (shading, ± 2 and 5%), red positive

Morphology of a Tropical Mesoscale Convective Complex in the eastern Atlantic during GATE (from Zipser et al. 1981)

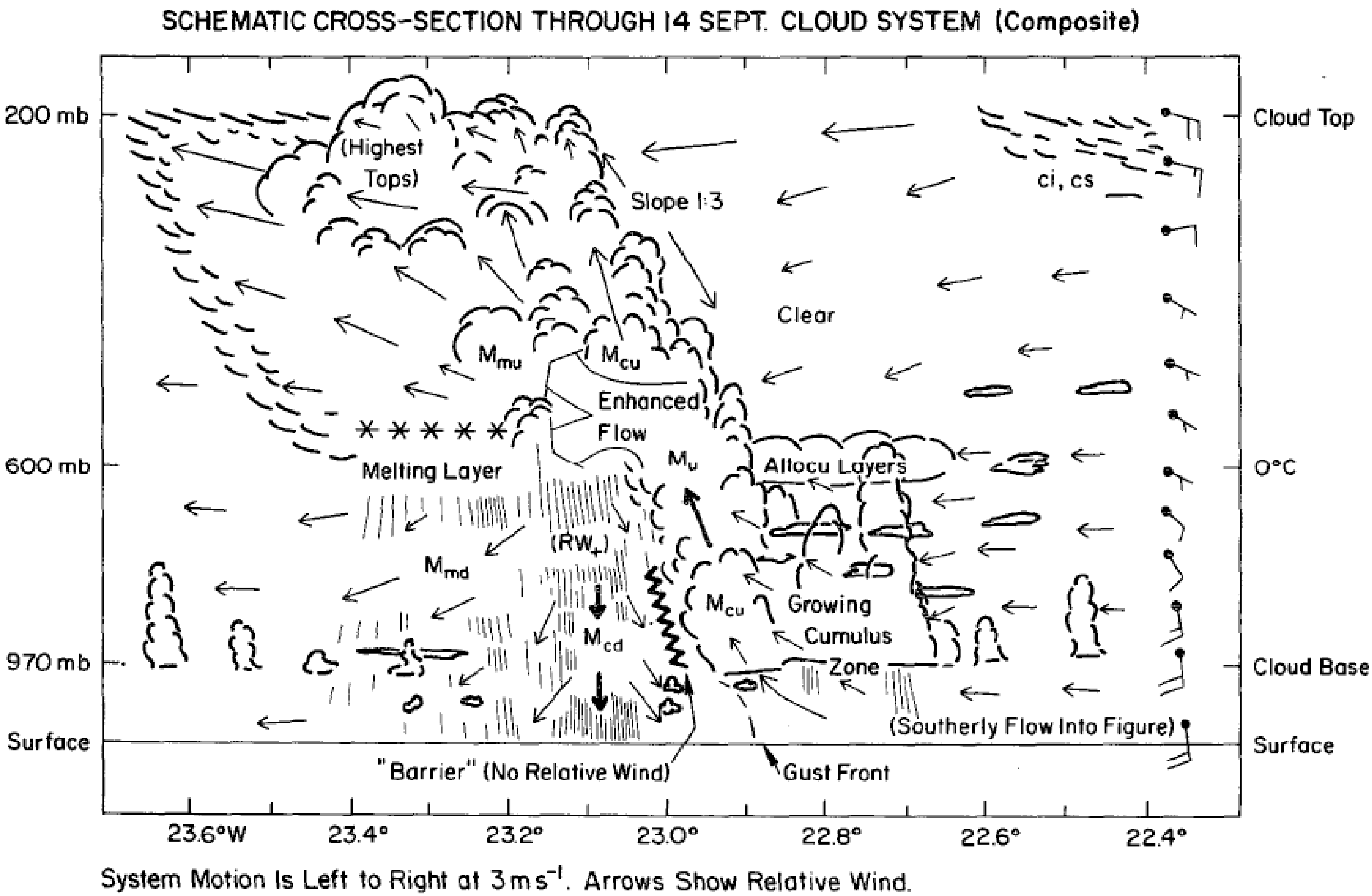

Two day wave cloud morphology (from Takayabu et al. 1996)

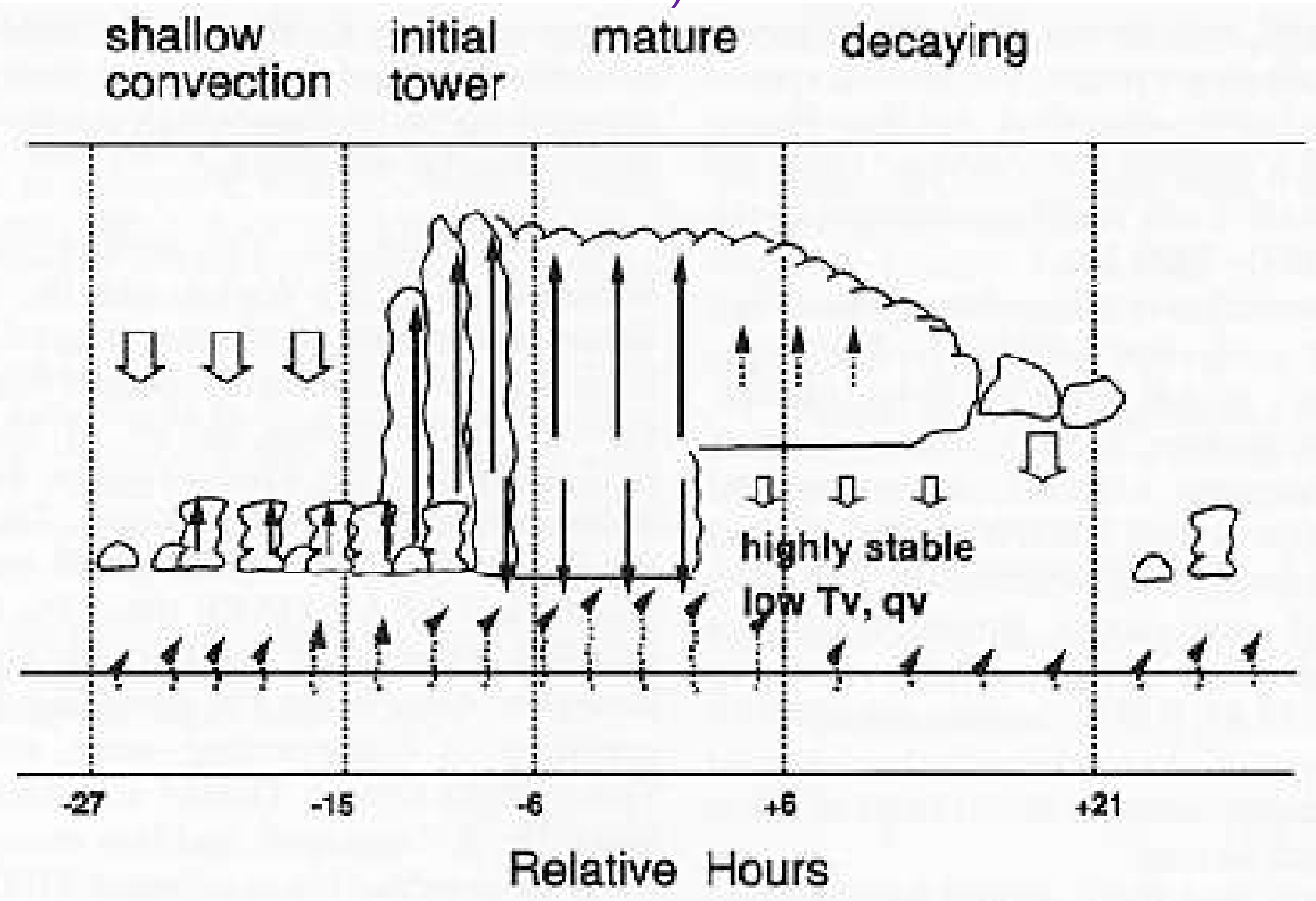

Observed Kelvin wave morphology (from Straub and Kiladis 2003)

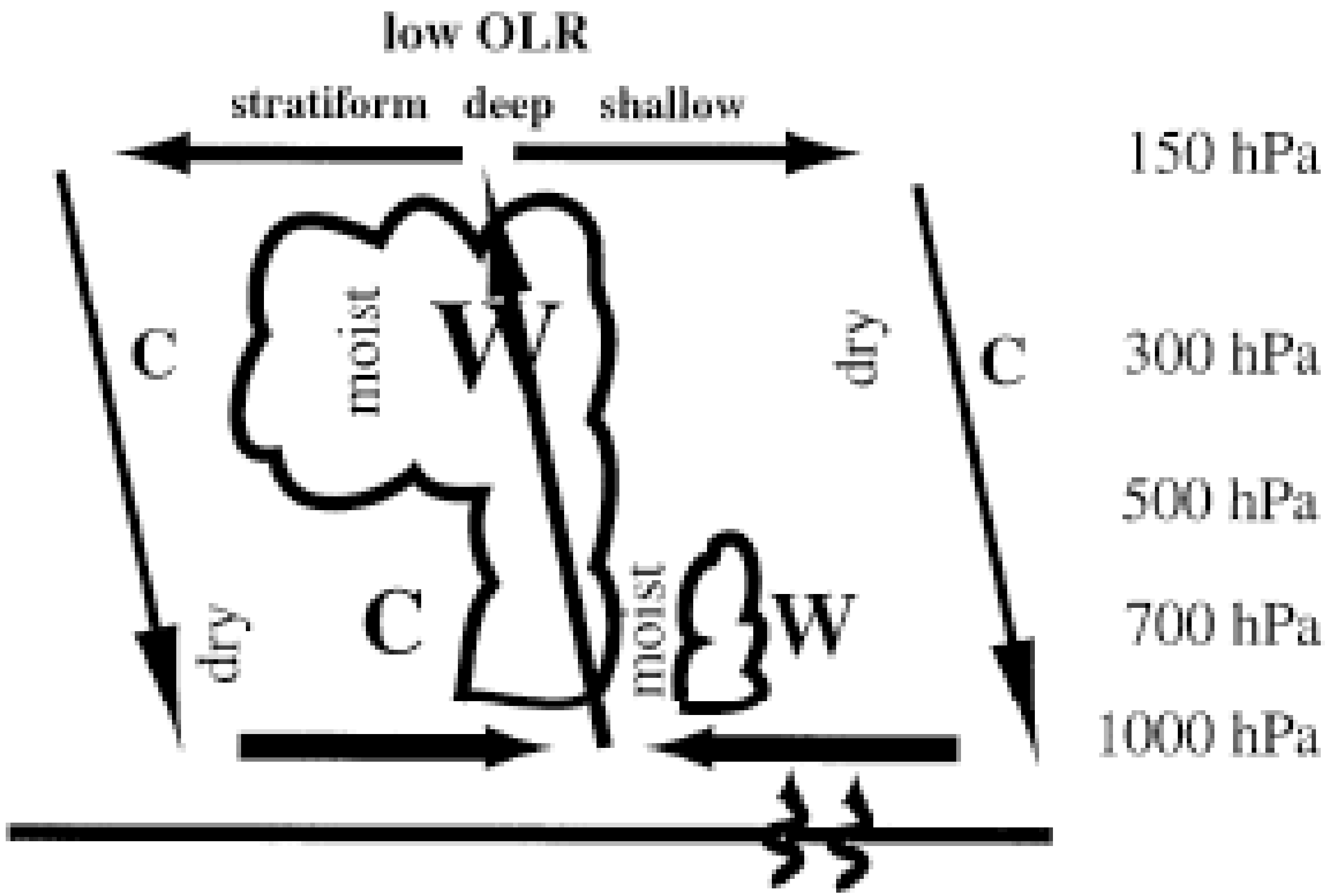

Morphology of MJO (from Wang 2005)

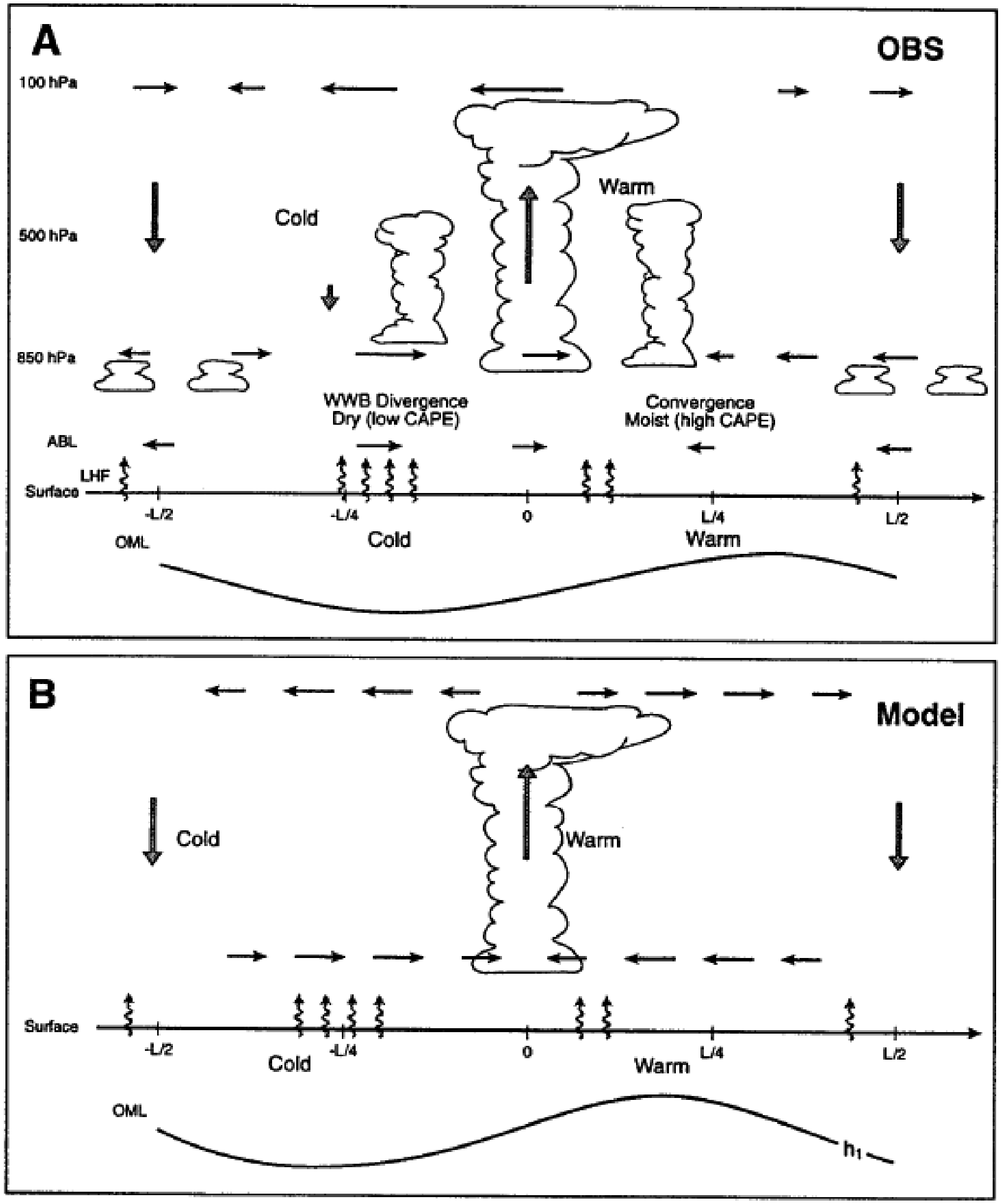

Equatorial Wave Structure

Consistent with a progression of shallow to deep convection, followed by stratiform precipitation for the Kelvin, Westward Inertio-gravity (2-day) Waves, and Easterly Waves

This was also observed during COARE for the MJO (e.g. Lin and Johnson 1996; Johnson et al. 1999; Lin et al. 2004)

This evolution is similar to that occurring on the Mesoscale Convective Complex scale

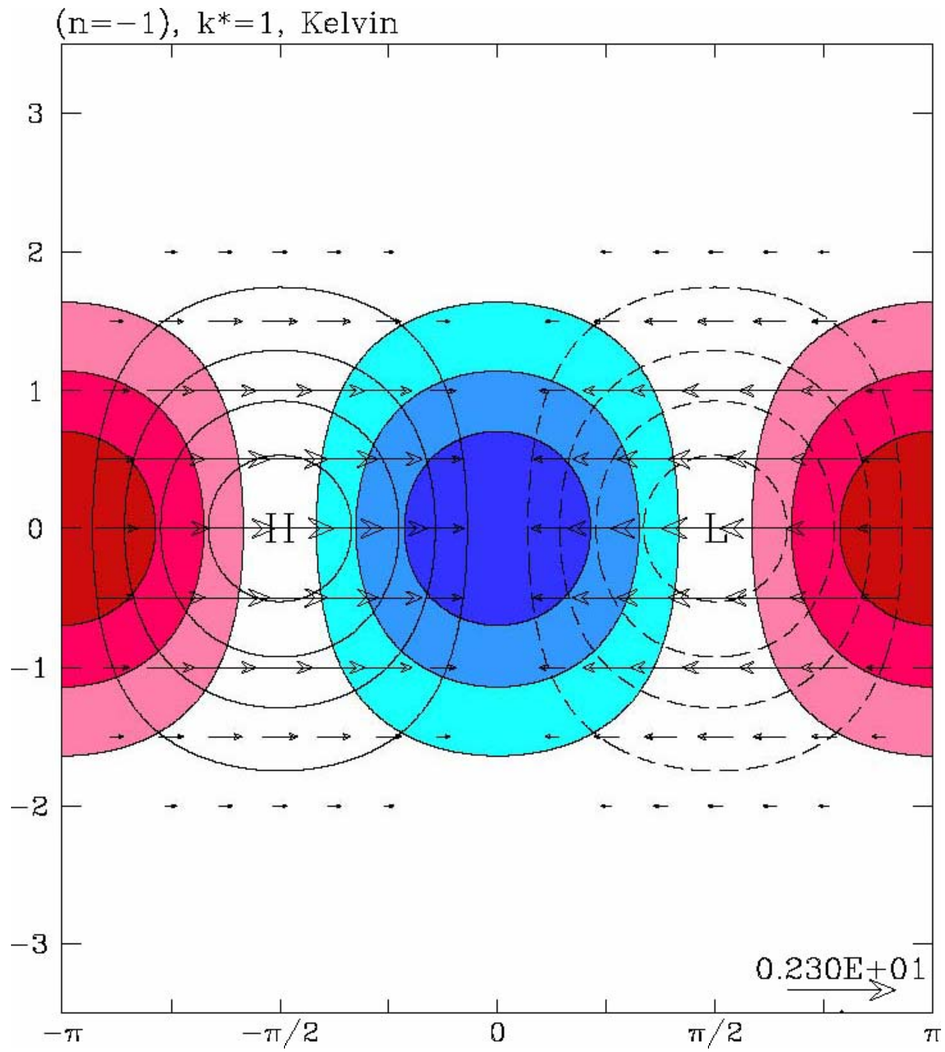

(n=−1), k*=1, Kelvin
3
2
1
0
−1
−2
−3
H
L
0.230E+01
−π
−π/2
0
π/2
π

ECMWF reanalysis regression

OLR (shading), 1000-hPa Z (contours), 1000-hPa winds (vectors)

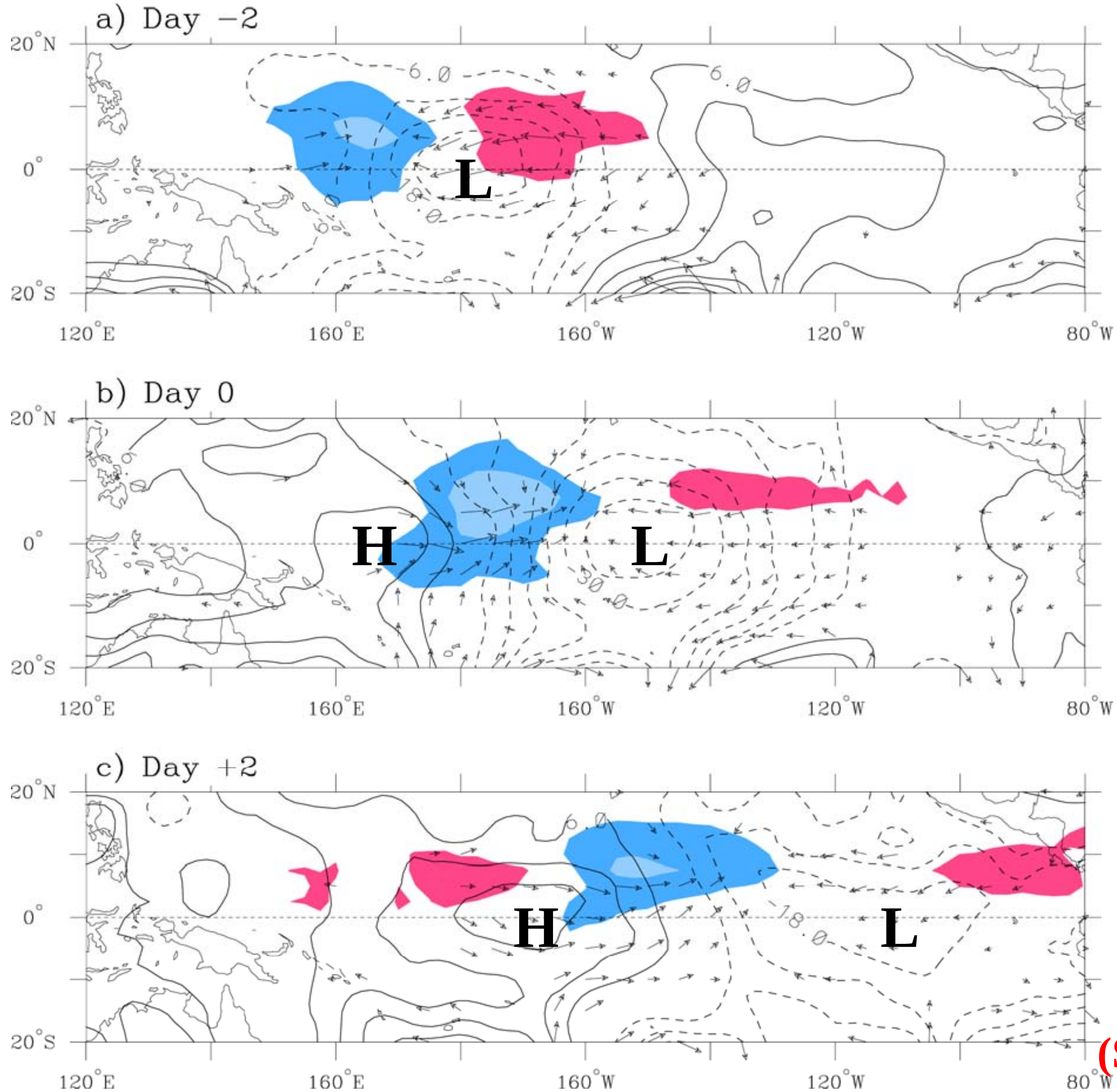

Dynamical fields are symmetric with respect to the equator; convection is centered in NH along ITCZ

(Straub and Kiladis, 2002)

Kelvin wave in Majuro radiosonde data: 1979-1999 (Straub and Kiladis, 2003)

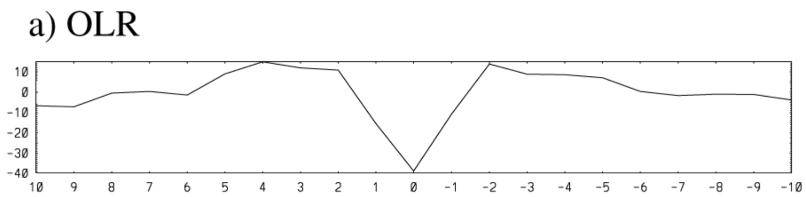

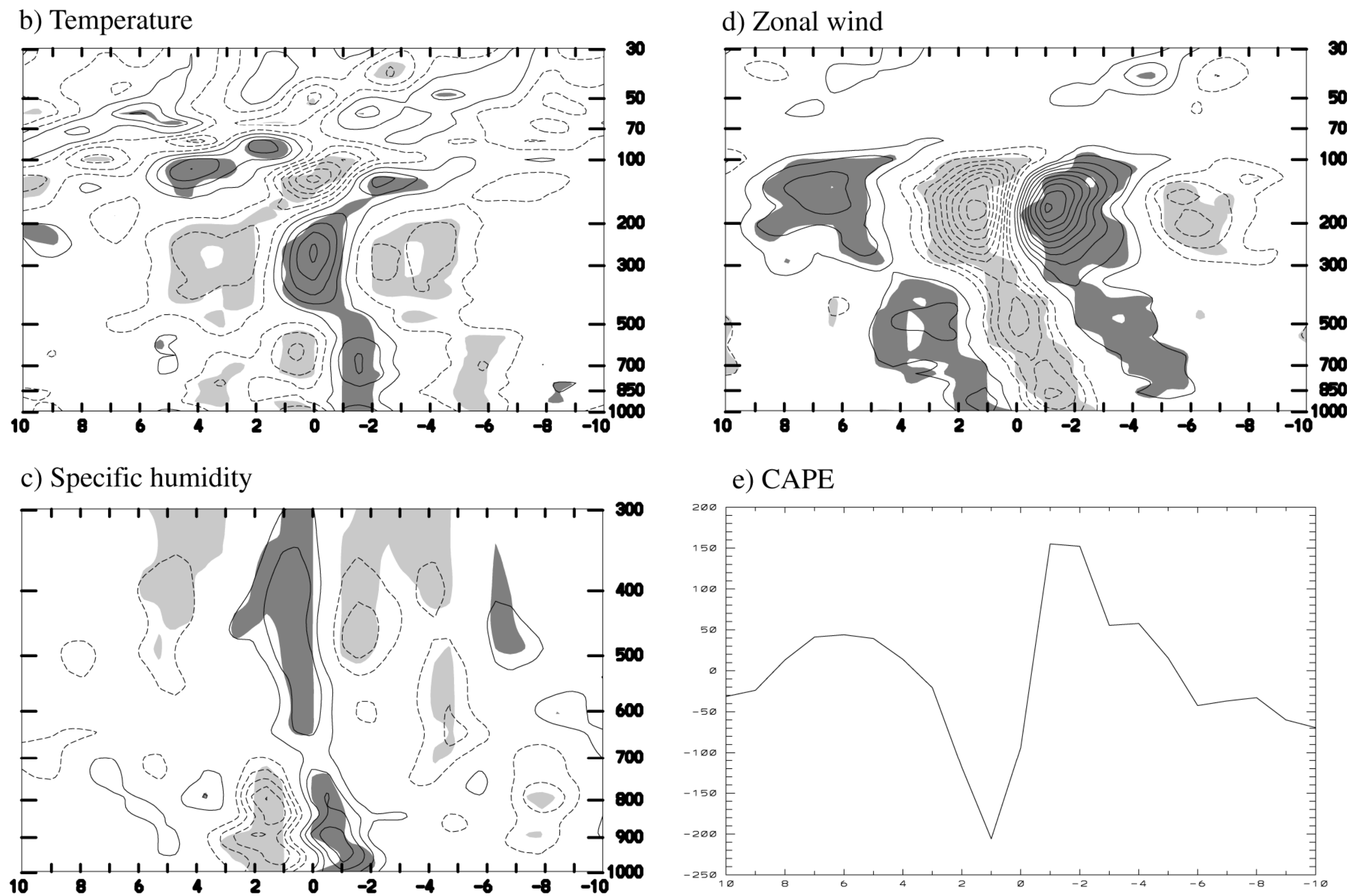

Zonal Wind Anomaly over the IFA

Two day waves during COARE,
from Haertel and Kiladis, 2004

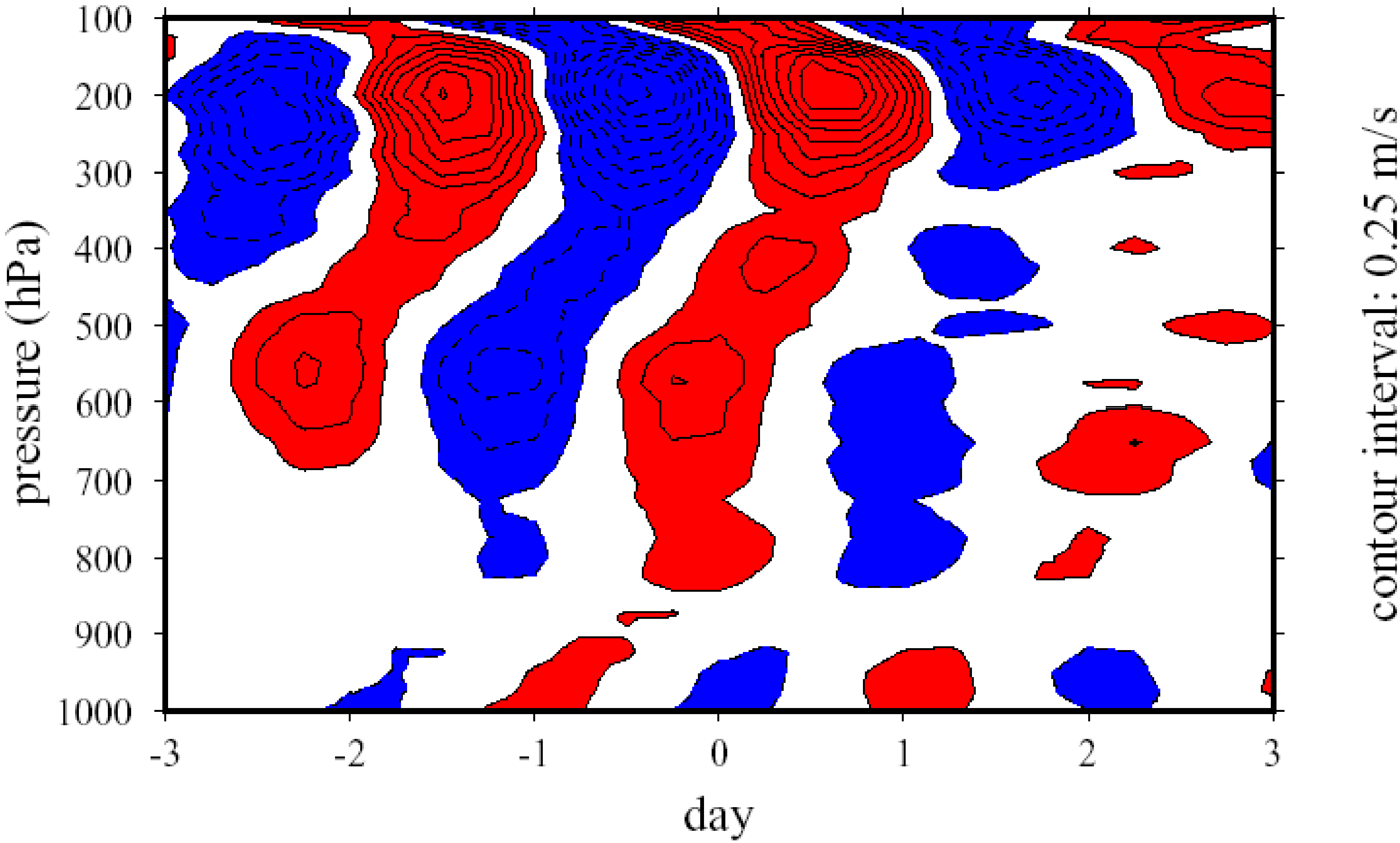

Temperature Anomaly over the IFA

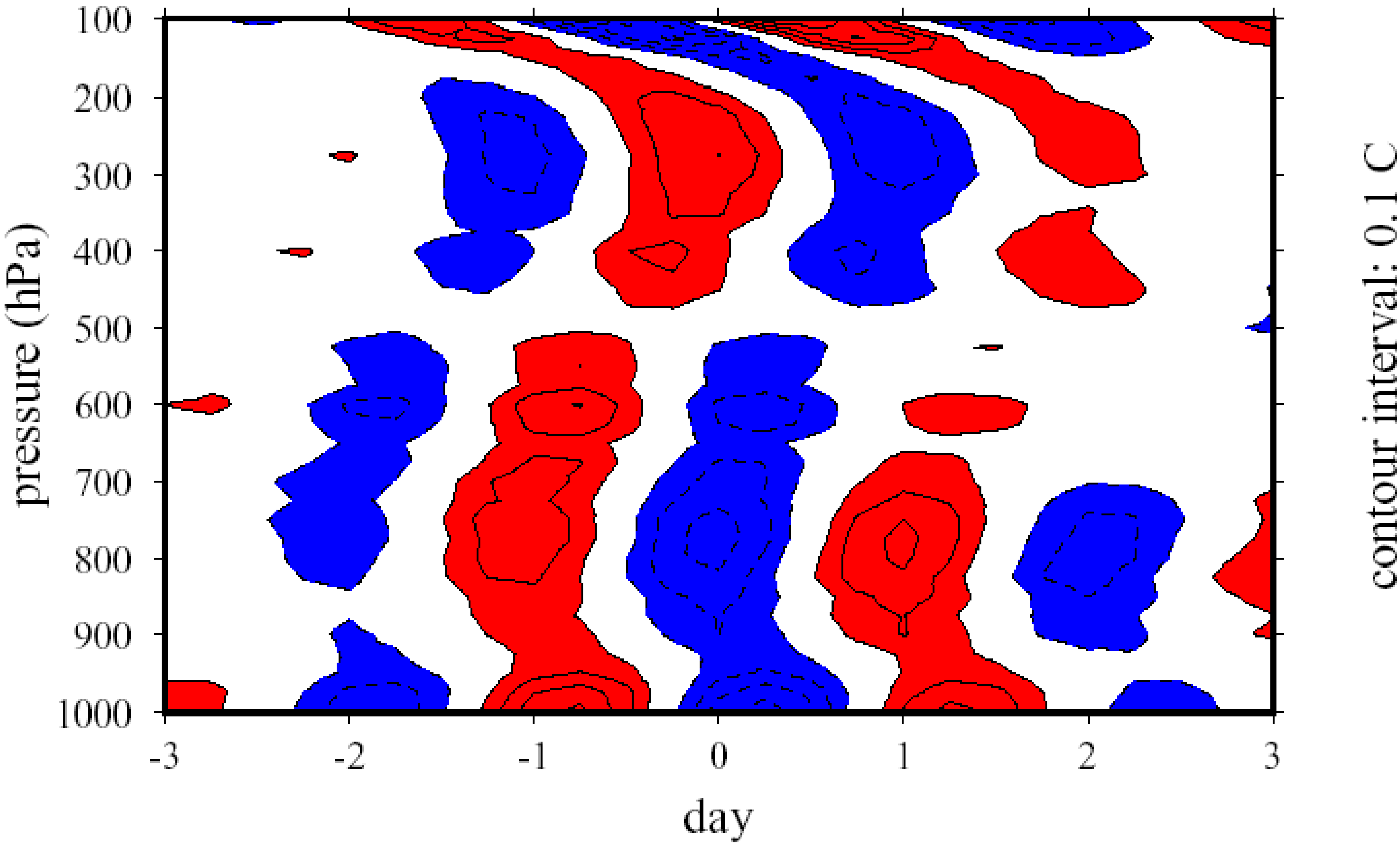

Moisture Anomaly over the IFA

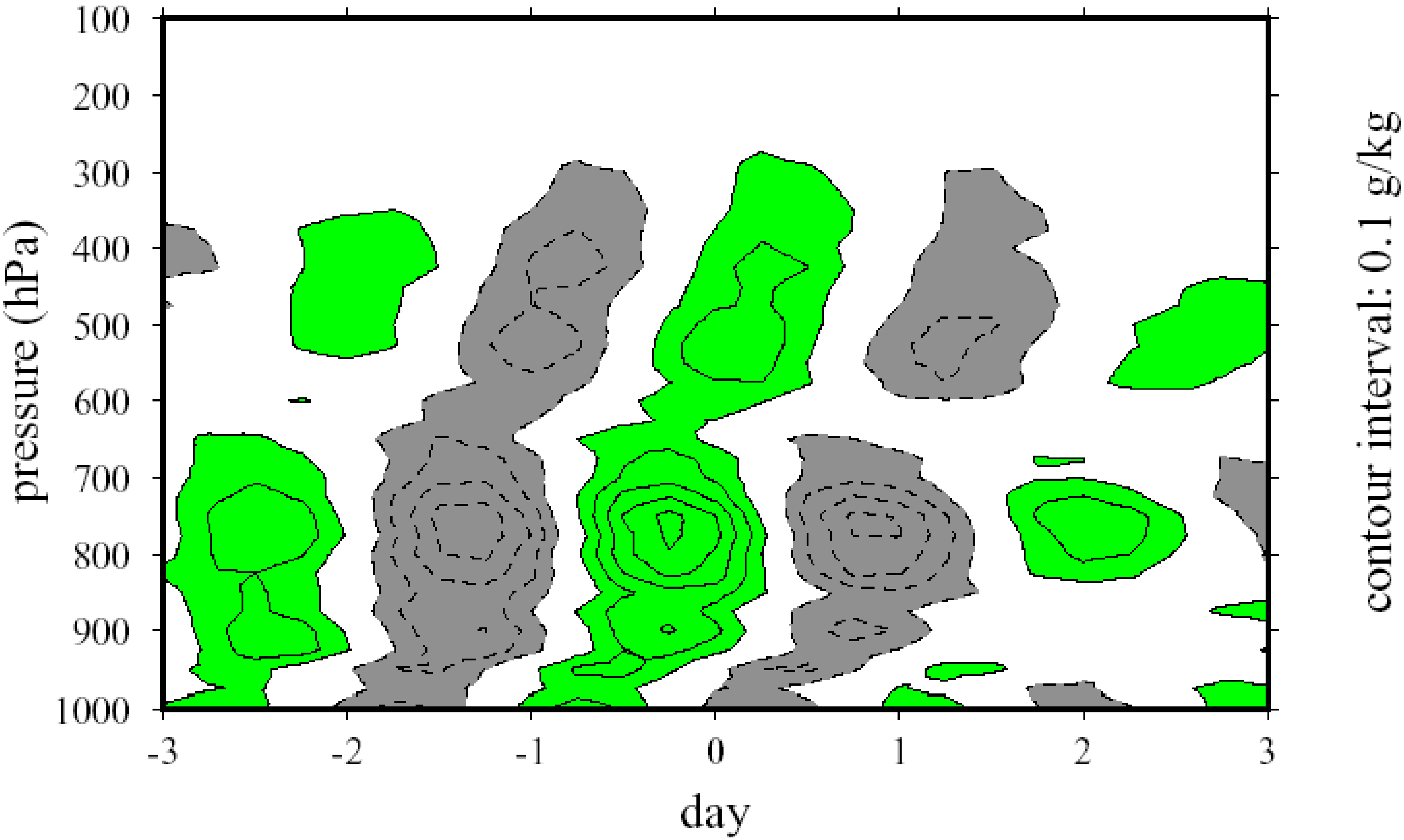

Heating Anomaly over the IFA

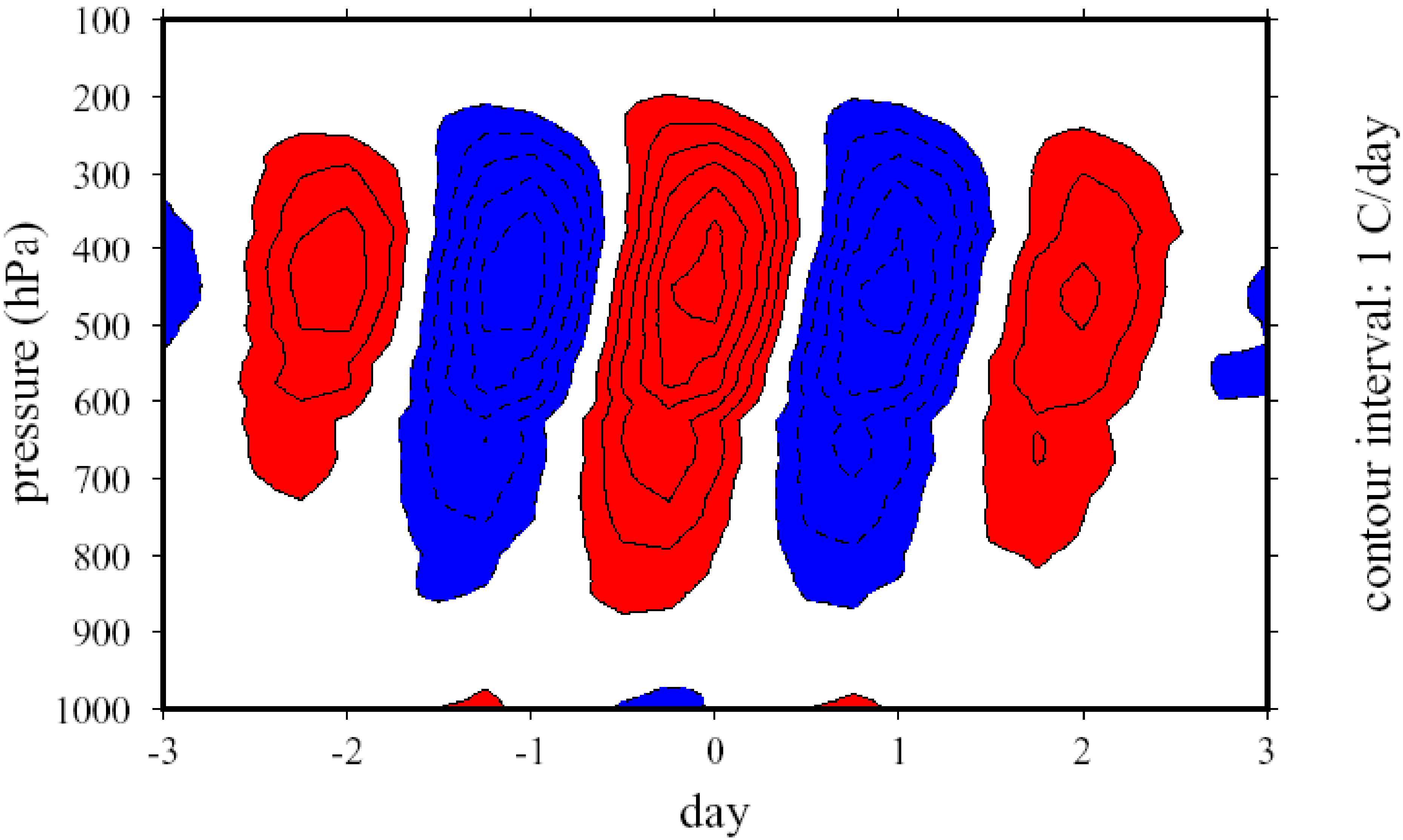

Zonal Wind at Honiara (10°S, 160°E) Regressed against MJO-filtered OLR (scaled -40 W m^2) for 1979-1999

OLR

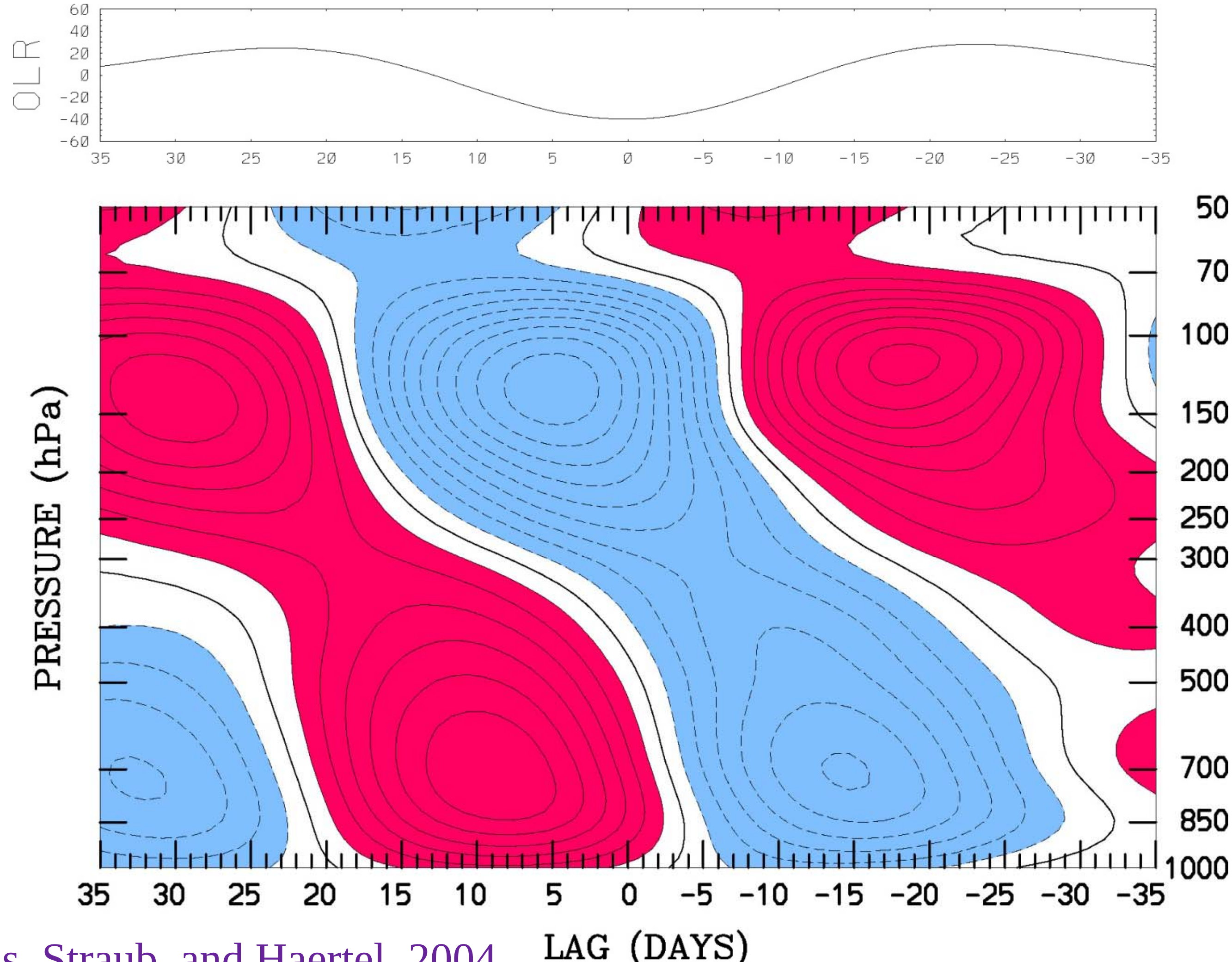

Pressure (hPa)

from Kiladis, Straub, and Haertel, 2004

OLR (top, Wm^{-2})

U Wind (contours, .5 m s^{-1}), red positive

Zonal Wind at Seychelles (5°S, 55°E) Regressed against MJO-filtered OLR (scaled -40 W m2) for 1979-1999

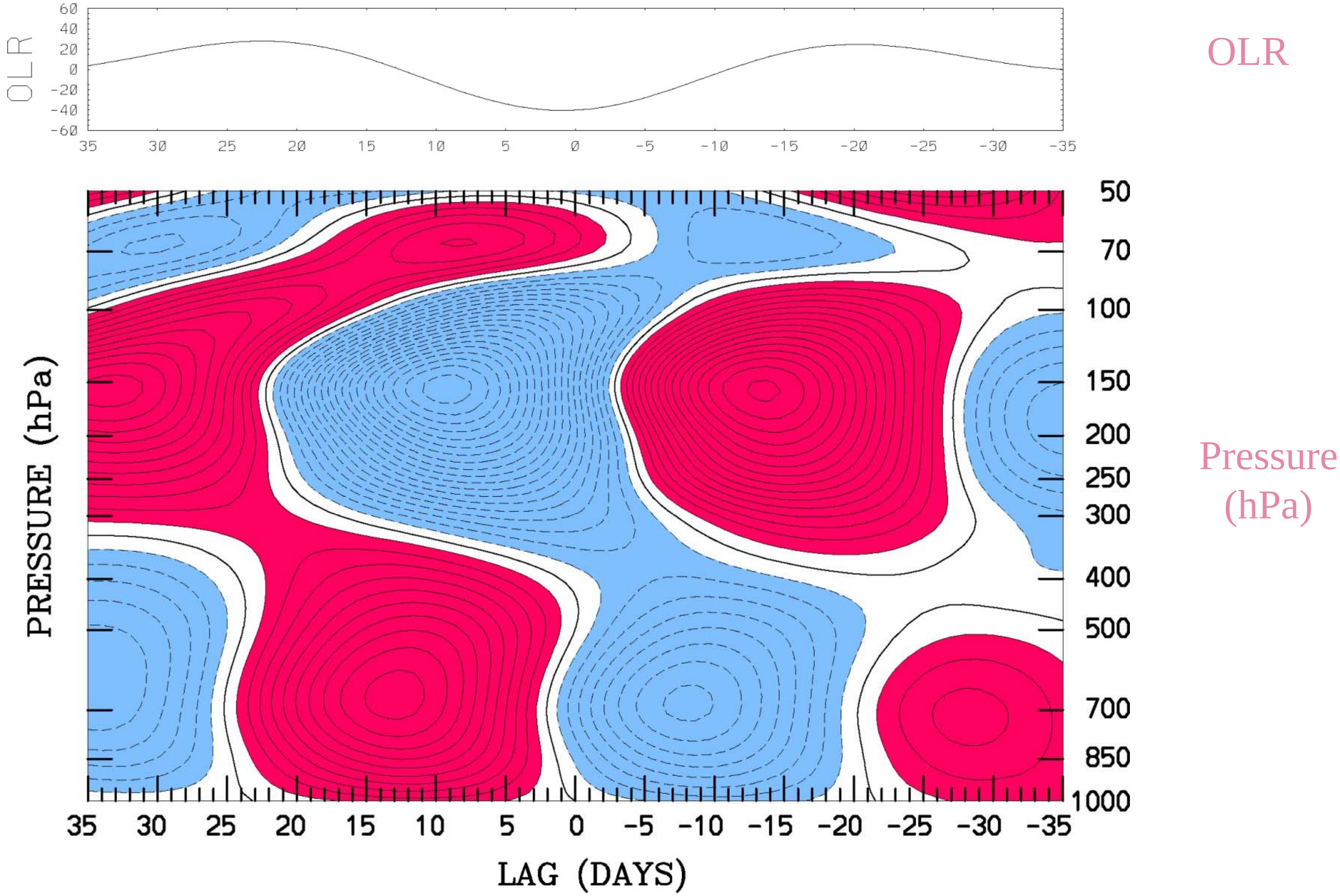

OLR (top, Wm^{-2})
U Wind (contours, .5 m s^{-1}), red positive

Zonal Wind at Diego Garcia (7.5°S, 72°E) Regressed against MJO-filtered OLR (scaled -40 W m^2) for 1979-1999

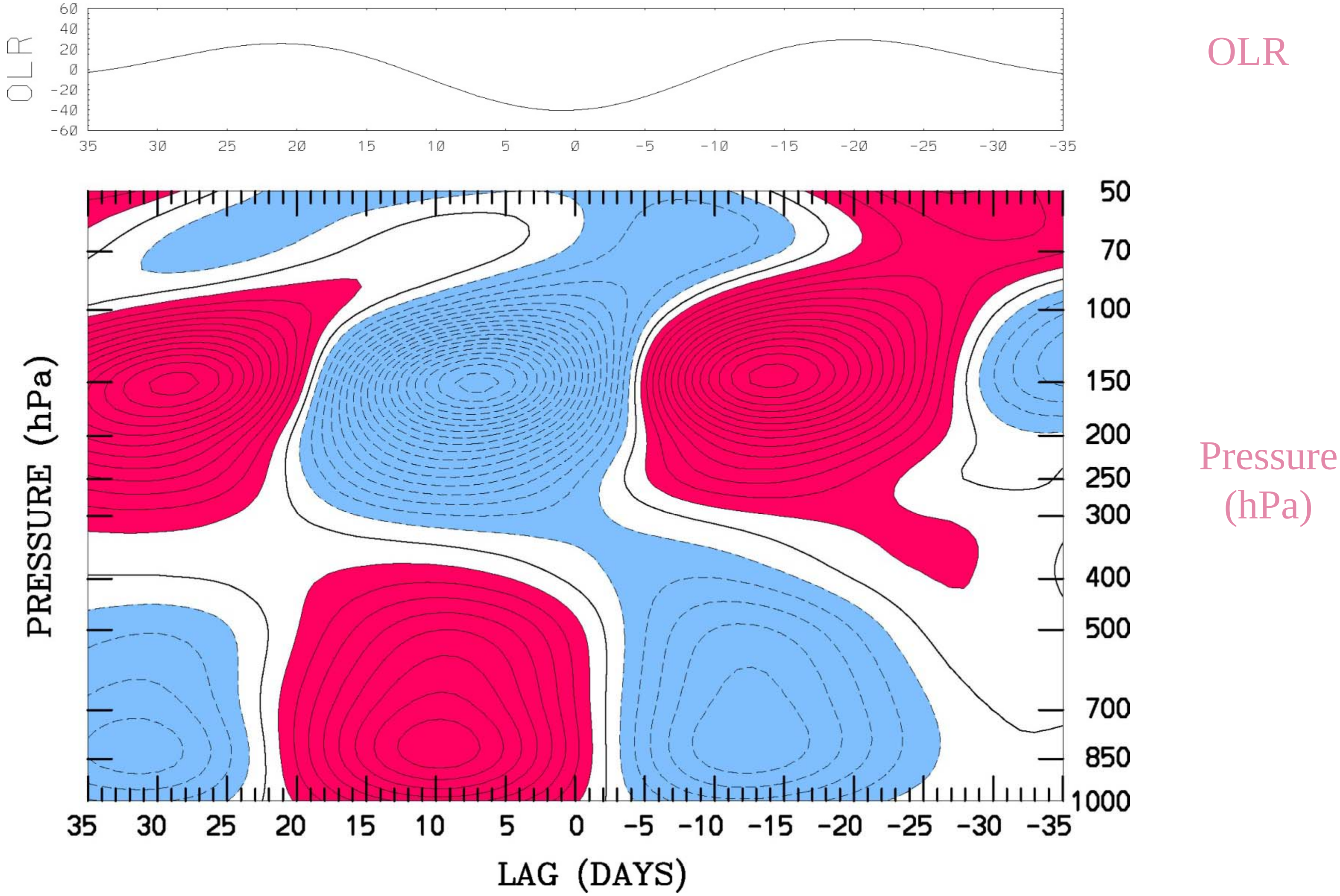

OLR (top, Wm^{-2})

U Wind (contours, .5 m s^{-1}), red positive

Temperature at Tarawa (Eq, 172.5°E) Regressed against MJO-filtered OLR (scaled -40 W m^2) for 1979-1999

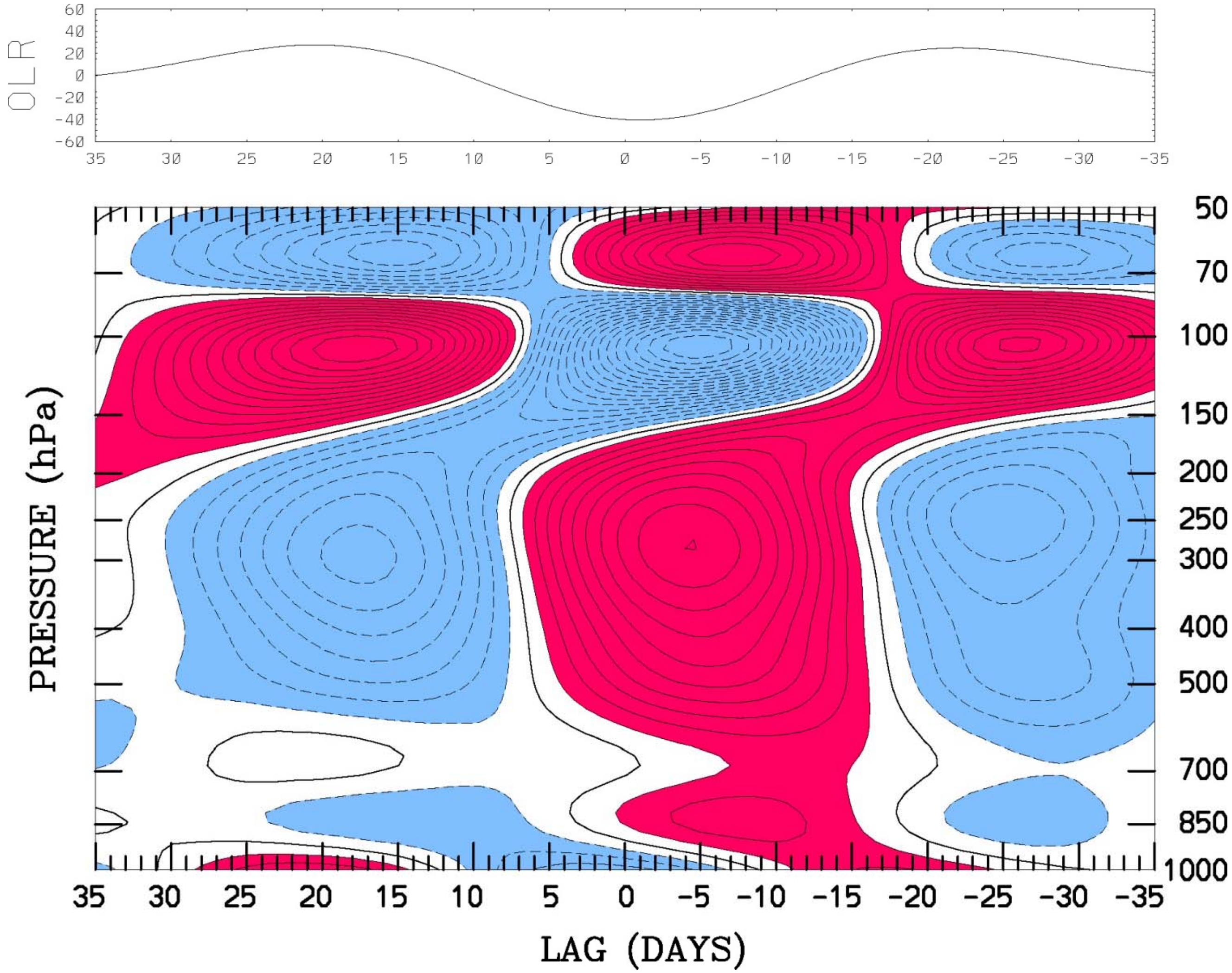

OLR (top, Wm^{-2})

Temperature (contours, .1 °C), red positive

Temperature at Honiara (10°S, 160.0°E) Regressed against MJO-filtered OLR (scaled -40 W m2) for 1979-1999

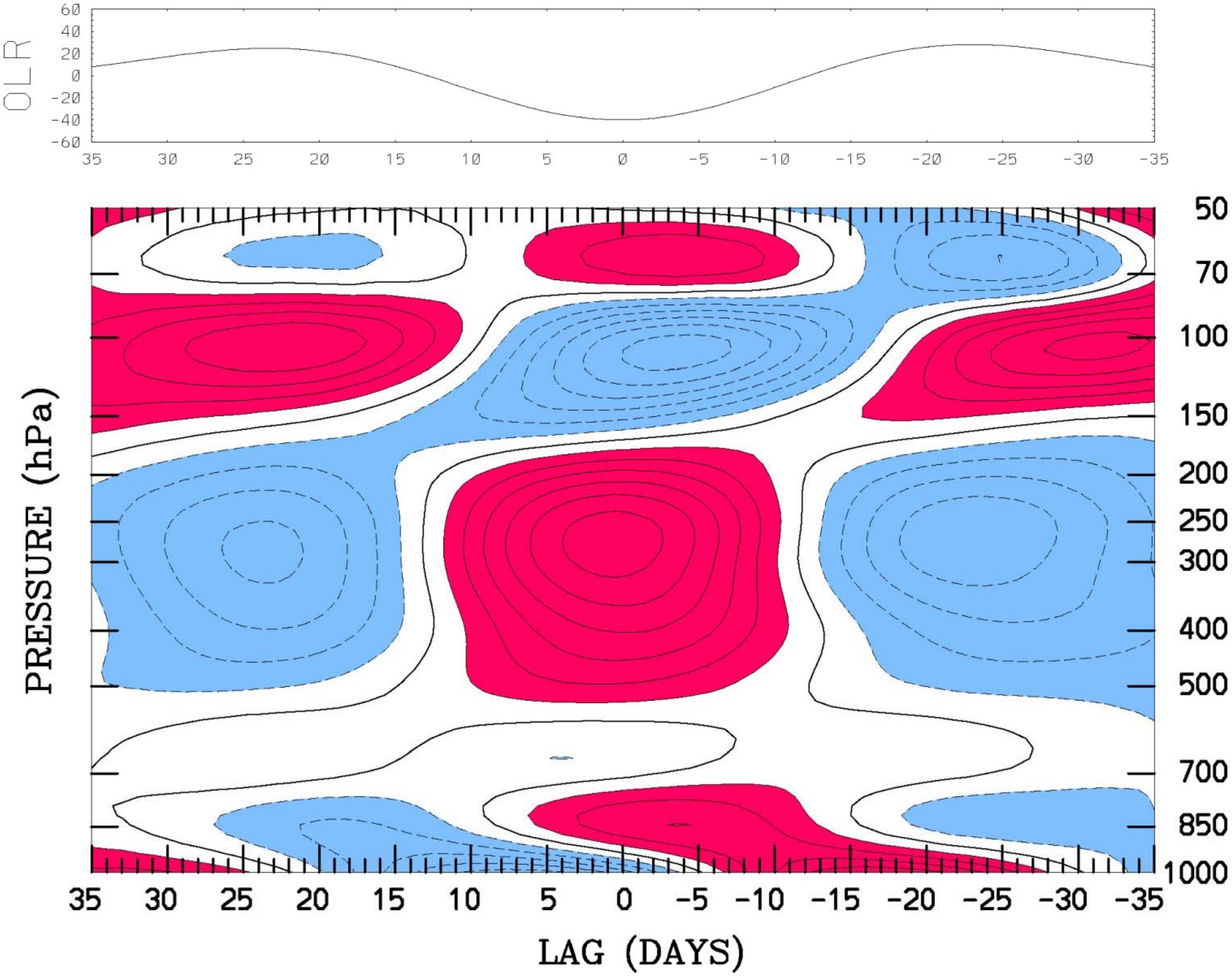

OLR

Pressure (hPa)

OLR (top, Wm^{-2})

Temperature (contours, .1 °C), red positive

Temperature at Diego Garcia (7.5°S, 72°E) Regressed against MJO-filtered OLR (scaled -40 W m^2) for 1979-1999

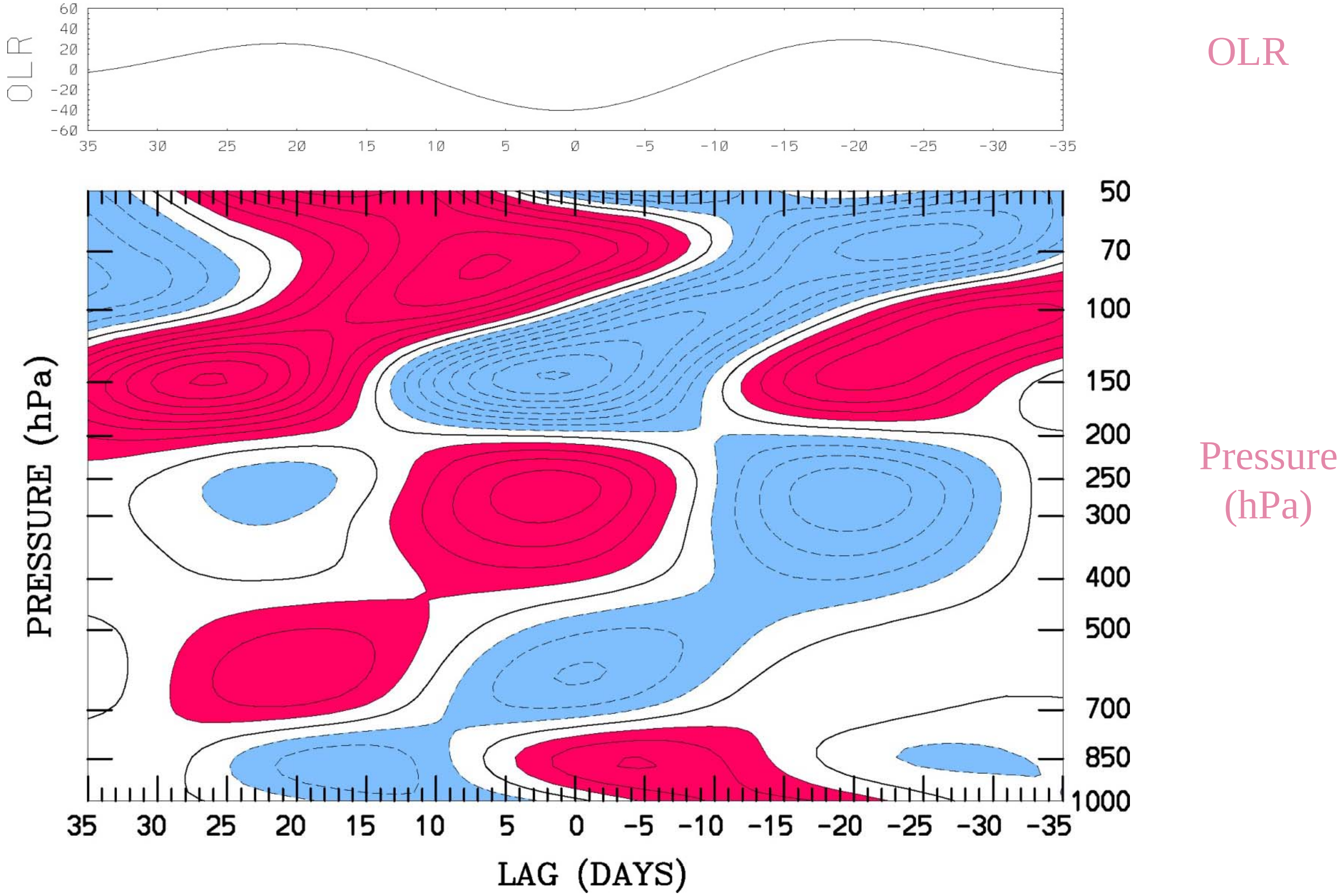

OLR (top, Wm^{-2})
Temperature (contours, .1 °C), red positive

Temperature at Seychelles (5°S, 55°E) Regressed against MJO-filtered OLR (scaled -40 W m^2) for 1979-1999

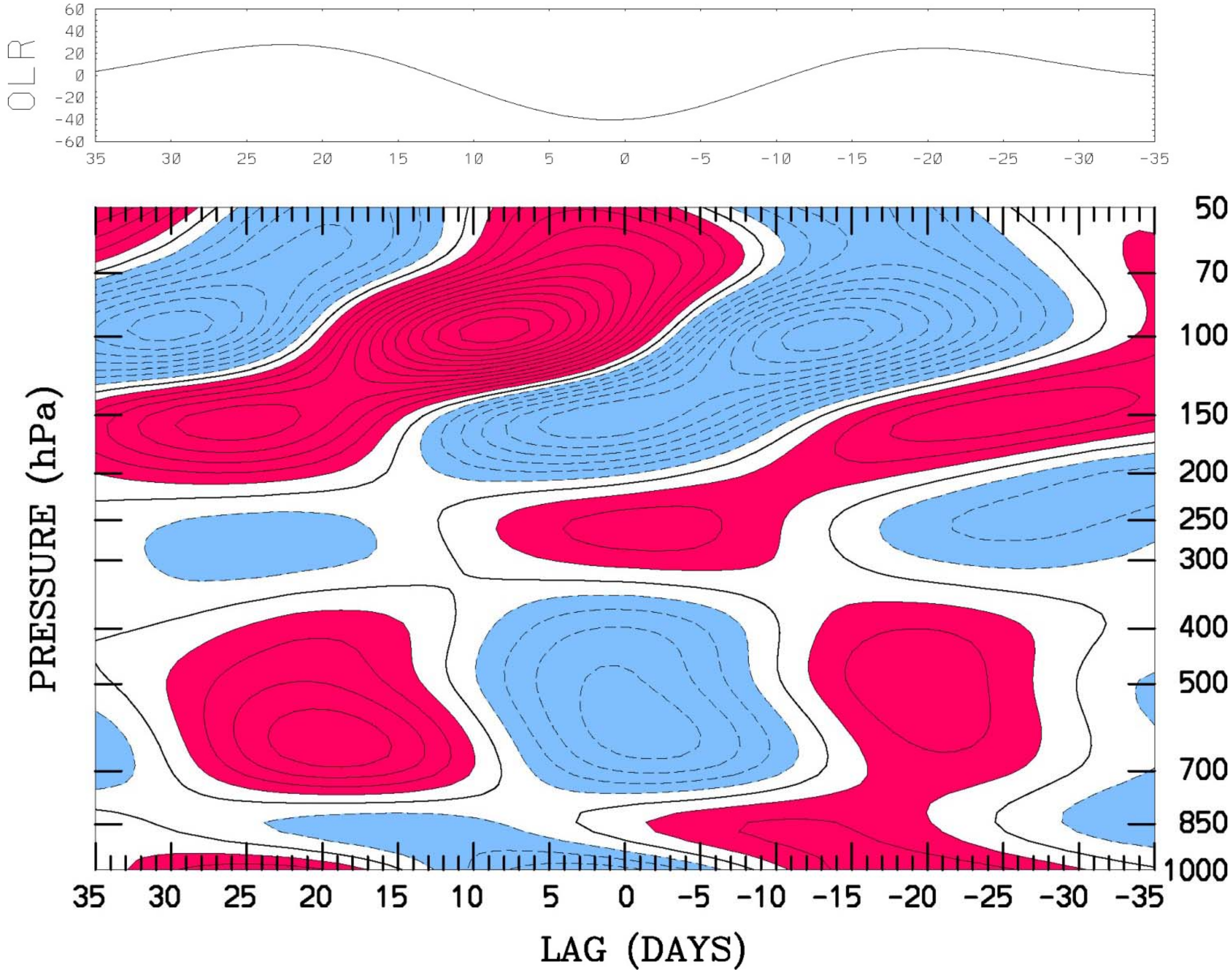

OLR

Pressure (hPa)

OLR (top, Wm^{-2})

Temperature (contours, .1 °C), red positive

Specific Humidity at Diego Garcia (7.5°S, 72°E) Regressed against MJO-filtered OLR (scaled -40 W m^2) for 1979-1999

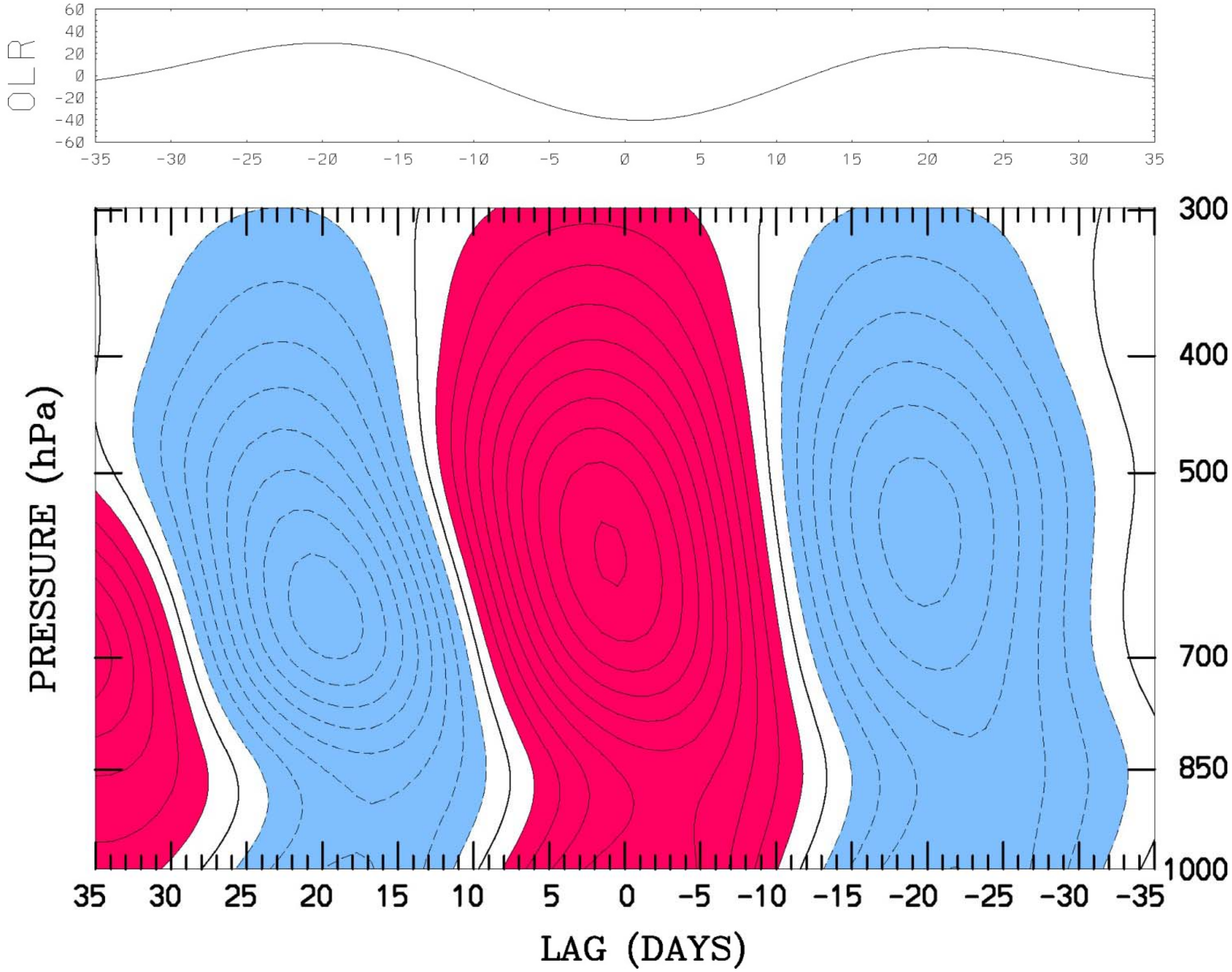

OLR

Pressure (hPa)

OLR (top, Wm^{-2})

Specific Humidity (contours, 1 X 10^{-1} g kg^{-1}), red positive

Specific Humidity at Medan (2.5°N, 97.5°E) Regressed against MJO-filtered OLR (scaled -40 W m^2) for 1979-1999

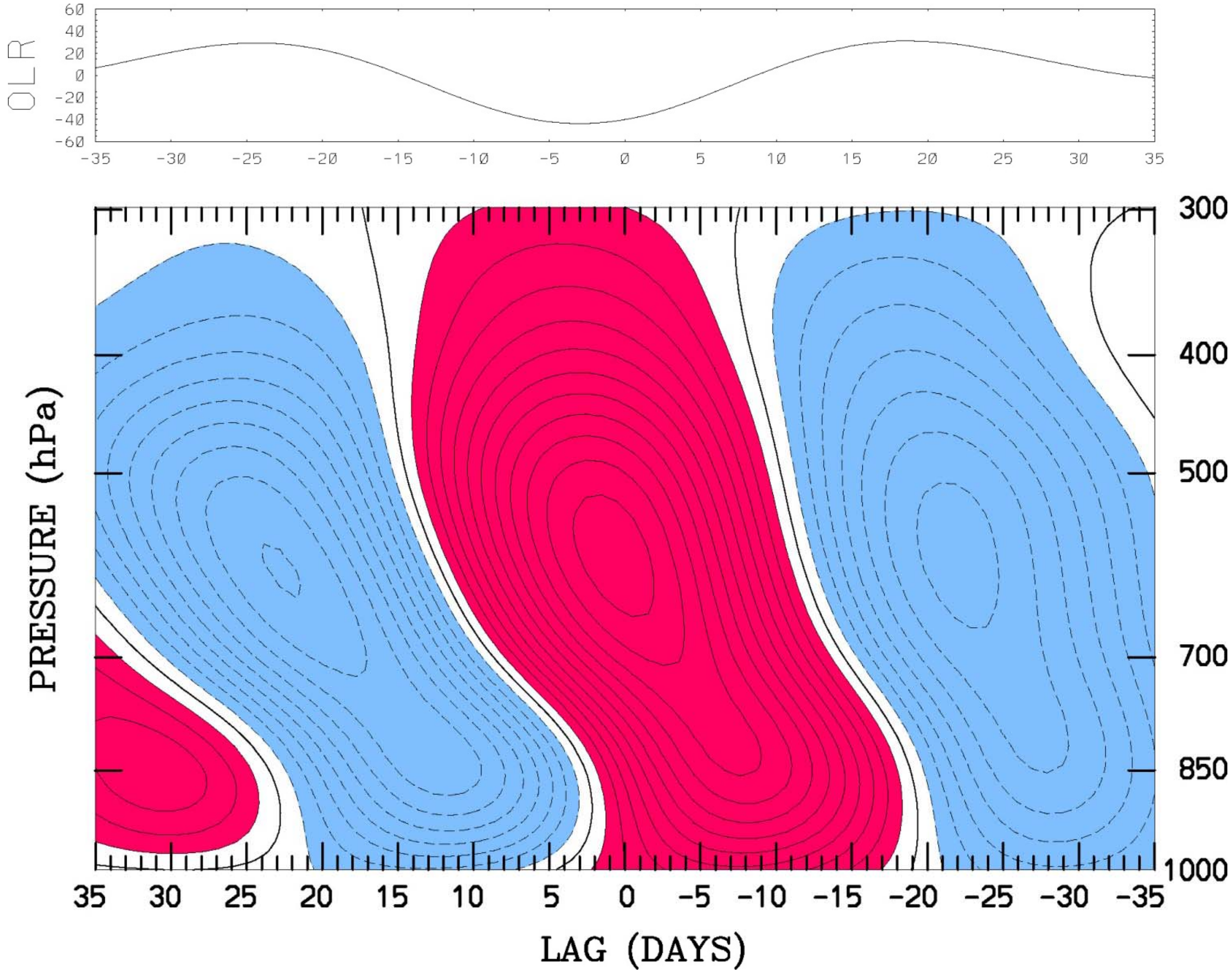

OLR (top, Wm^{-2})

Specific Humidity (contours, 1 X 10^{-1} g kg^{-1}), red positive

Specific Humidity at Tarawa (Eq, 172.5°E) Regressed against MJO-filtered OLR (scaled -40 W m²) for 1979-1999

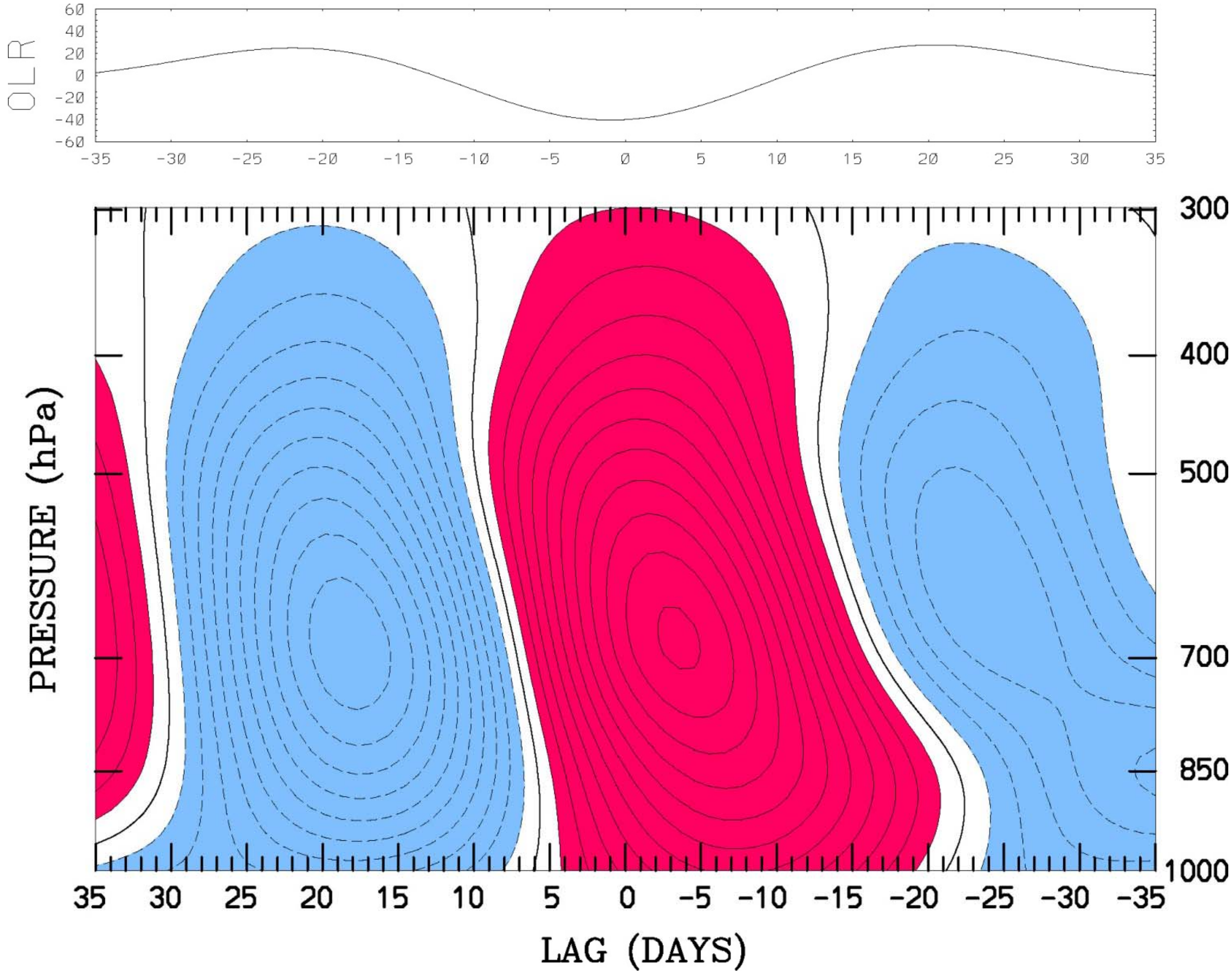

OLR

Pressure (hPa)

OLR (top, Wm^{-2})

Specific Humidity (contours, 1 X 10^{-1} g kg^{-1}), red positive

Specific Humidity at Truk (7.5°N, 152.5°E) Regressed against MJO-filtered OLR (scaled -40 W m^2) for 1979-1999

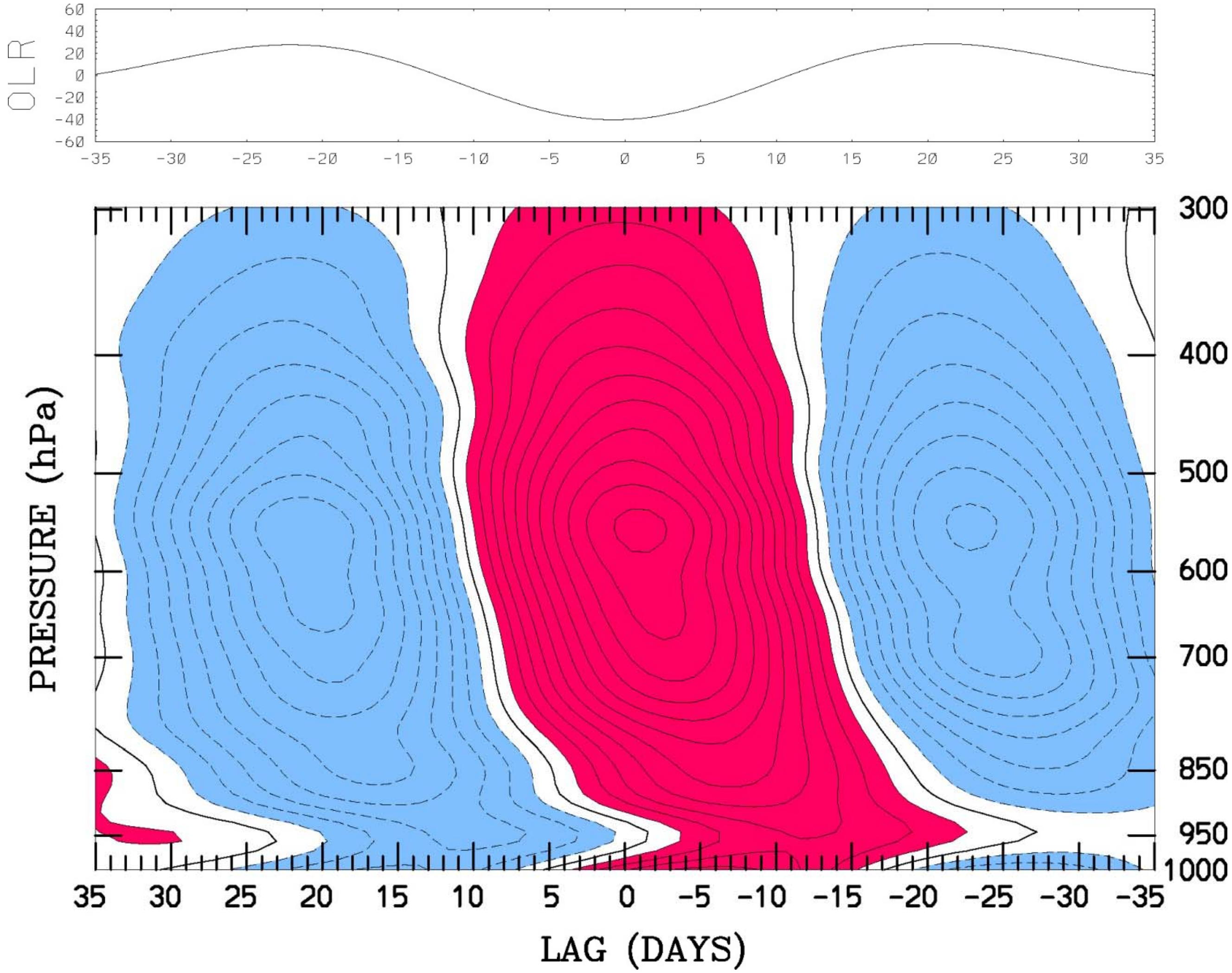

OLR

Pressure (hPa)

OLR (top, Wm^{-2})
Specific Humidity (contours, 1 X 10^{-1} g kg^{-1}), red positive

Q1 Regressed against MJO-filtered OLR over the IFA during COARE

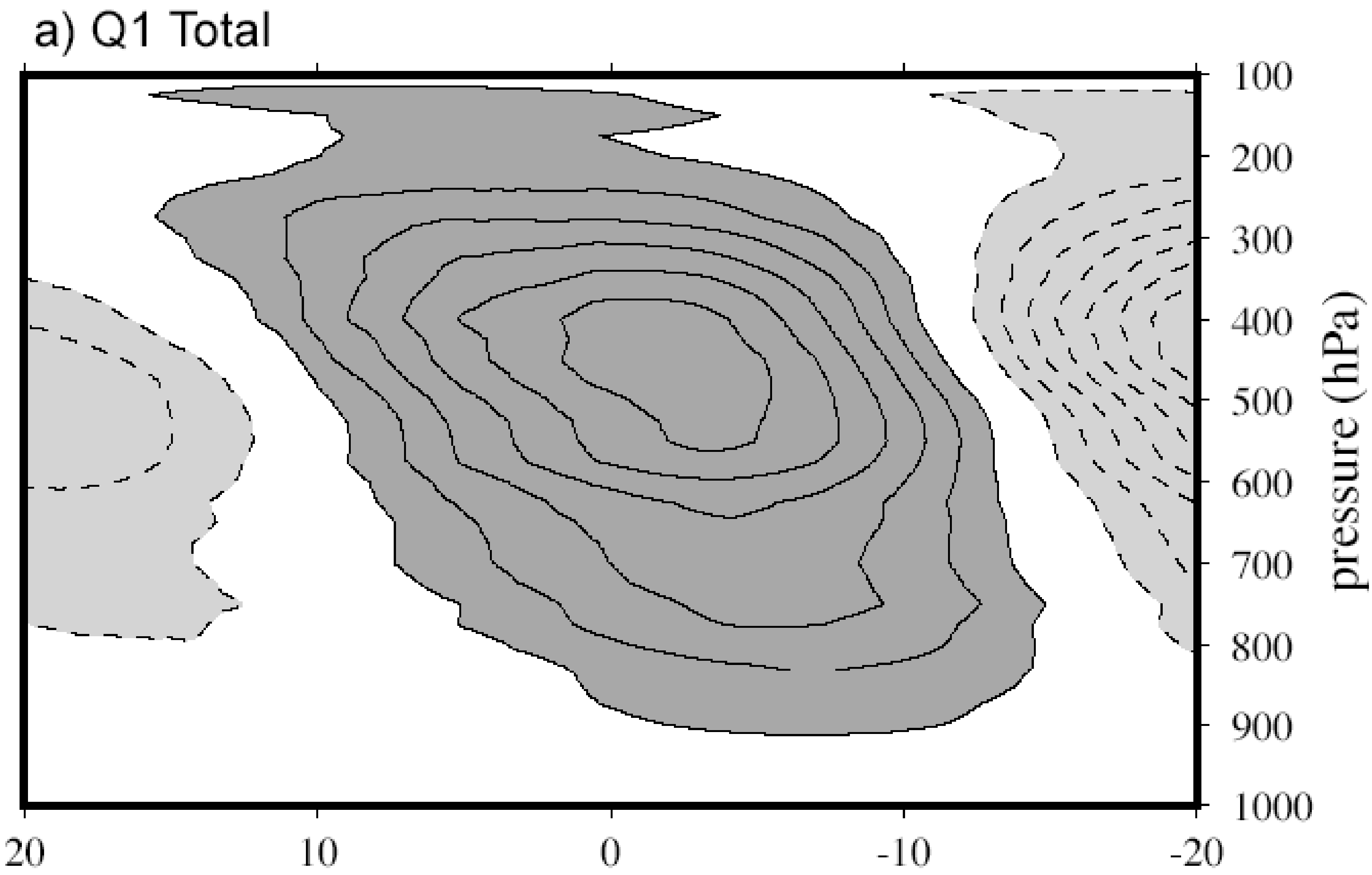

Q1 Regressed against MJO-filtered OLR over the IFA during COARE

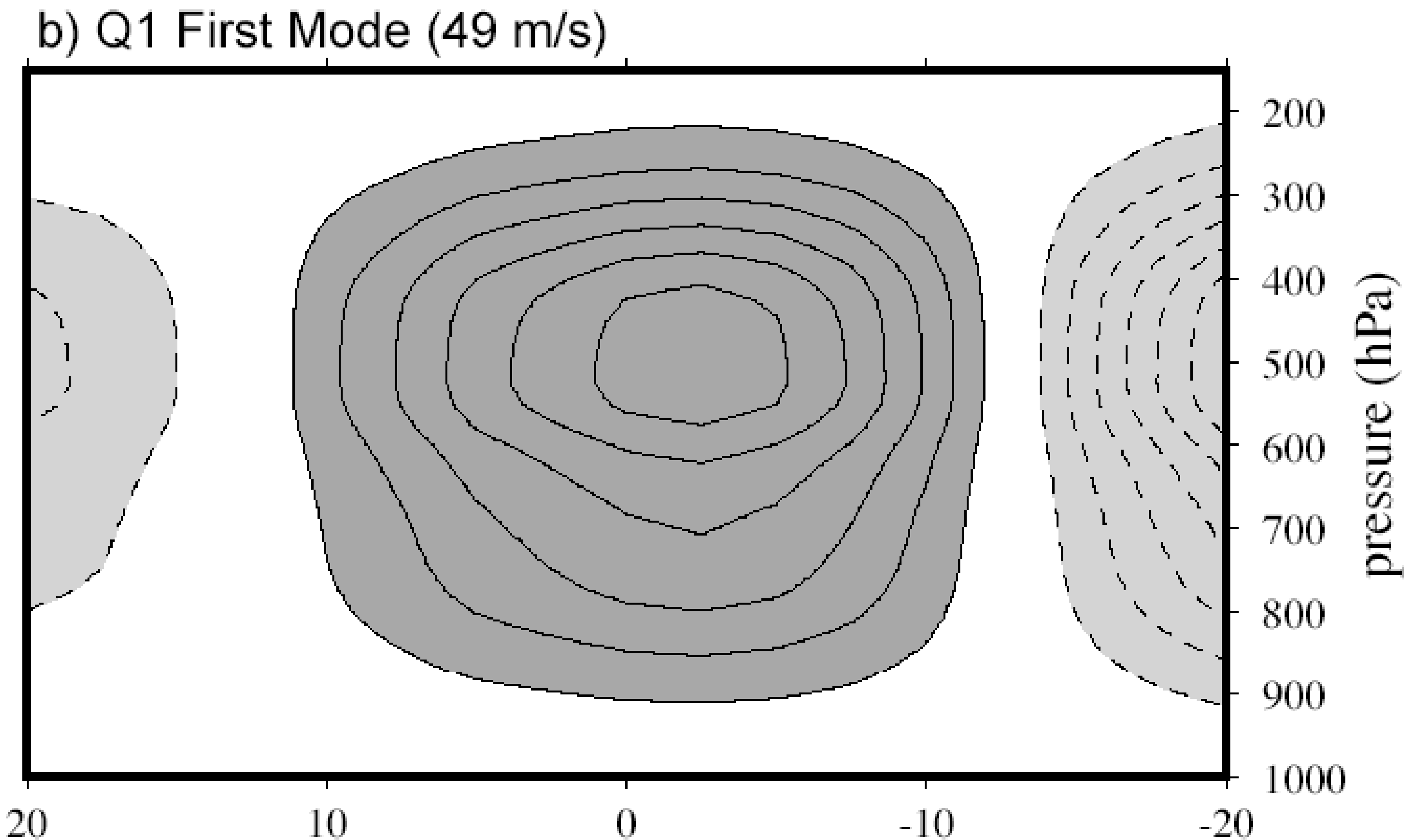

Q1 Regressed against MJO-filtered OLR over the IFA during COARE

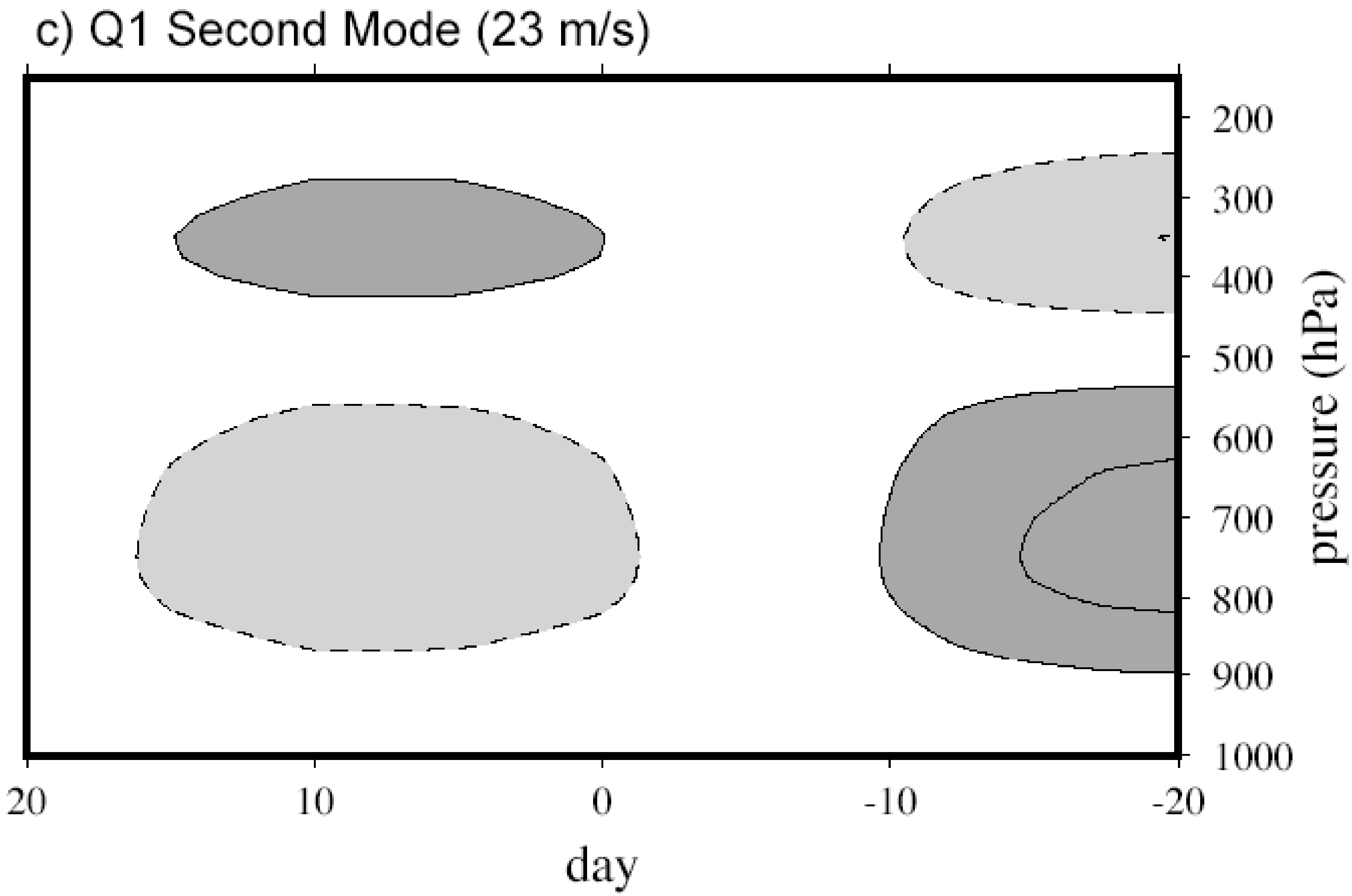

Dynamical Structures

All equatorial waves studied have tilted vertical structures, with:

Easterlies ahead of and westerlies following the convective region

Warm lower tropospheric temperatures ahead of the wave, with cooling behind. The mid-troposphere is warm within the convective region, indicating that latent heating more than compensates for vertical motion.

Waves are moist ahead (high CAPE) and dry following the deep convection

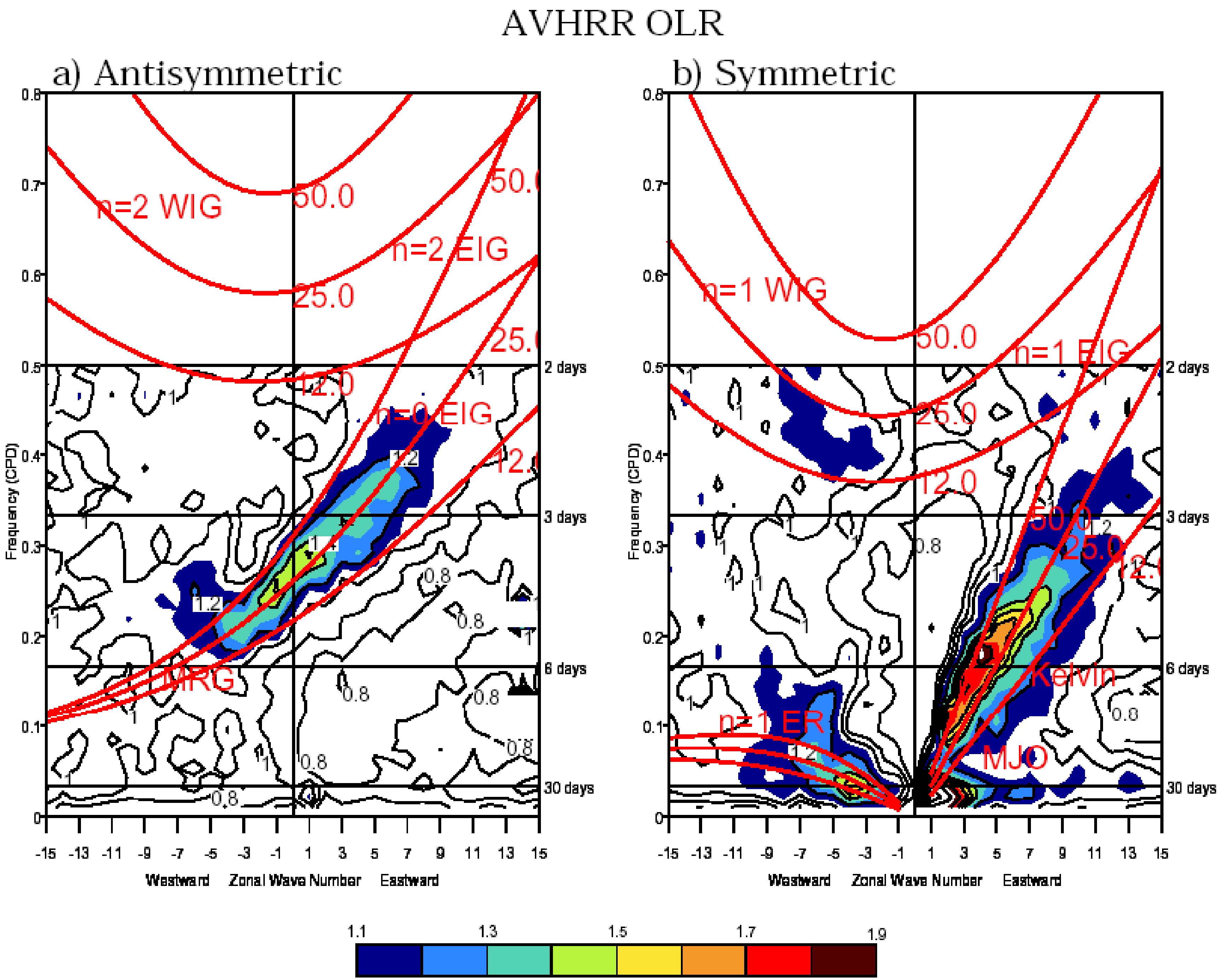
AVHRR OLR
a) Antisymmetric
b) Symmetric
n=2 WIG
n=2 EIG
n=0 EIG
MRG
n=1 WIG
n=1 EIG
n=1 ER
Kelvin
MJO
50.0
25.0
12.0
2 days
3 days
6 days
30 days
Frequency (CPD)
Westward
Zonal Wave Number
Eastward
1.1
1.2
1.3
1.4
1.5
1.6
1.7
1.8
1.9

CSIRO_Mk2 OLR

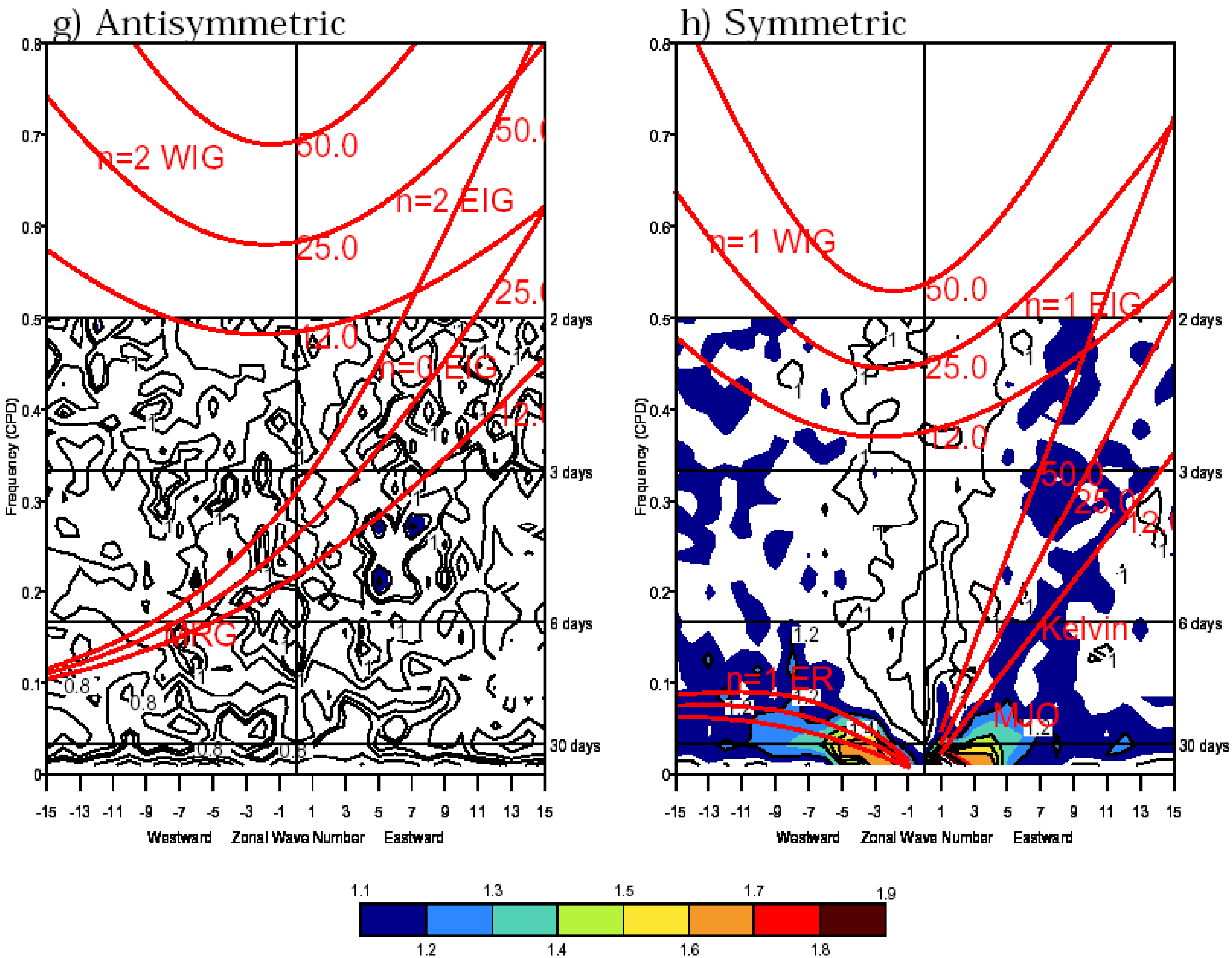

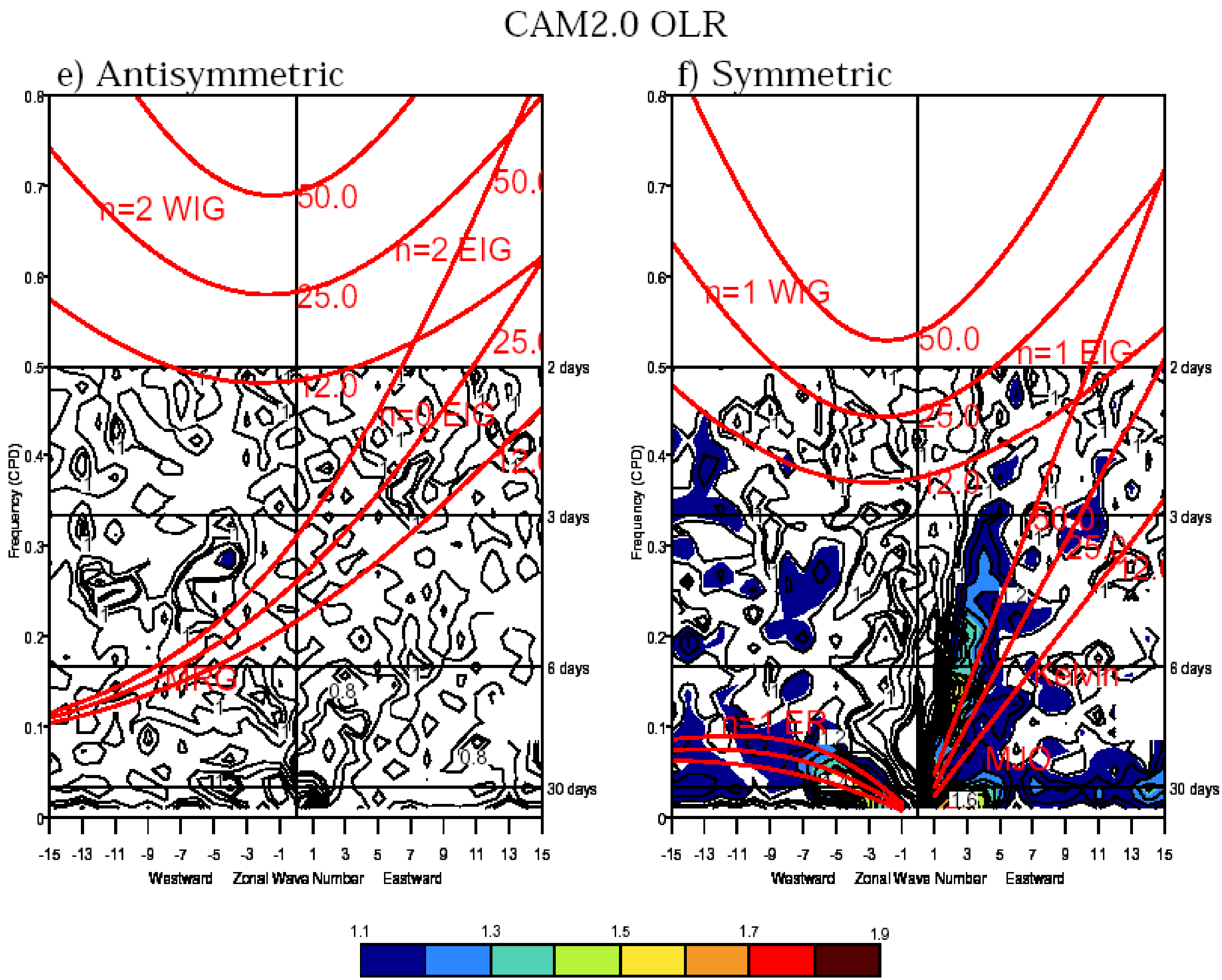
CAM2.0 OLR
e) Antisymmetric
f) Symmetric
n=2 WIG
n=2 EIG
n=0 EIG
MRG
n=1 WIG
n=1 EIG
n=1 ER
Kelvin
MJO
50.0
25.0
12.0
2 days
3 days
6 days
30 days
Frequency (CPD)
Westward
Zonal Wave Number
Eastward
1.1
1.2
1.3
1.4
1.5
1.6
1.7
1.8
1.9

ECHAM4_OPYC3 OLR

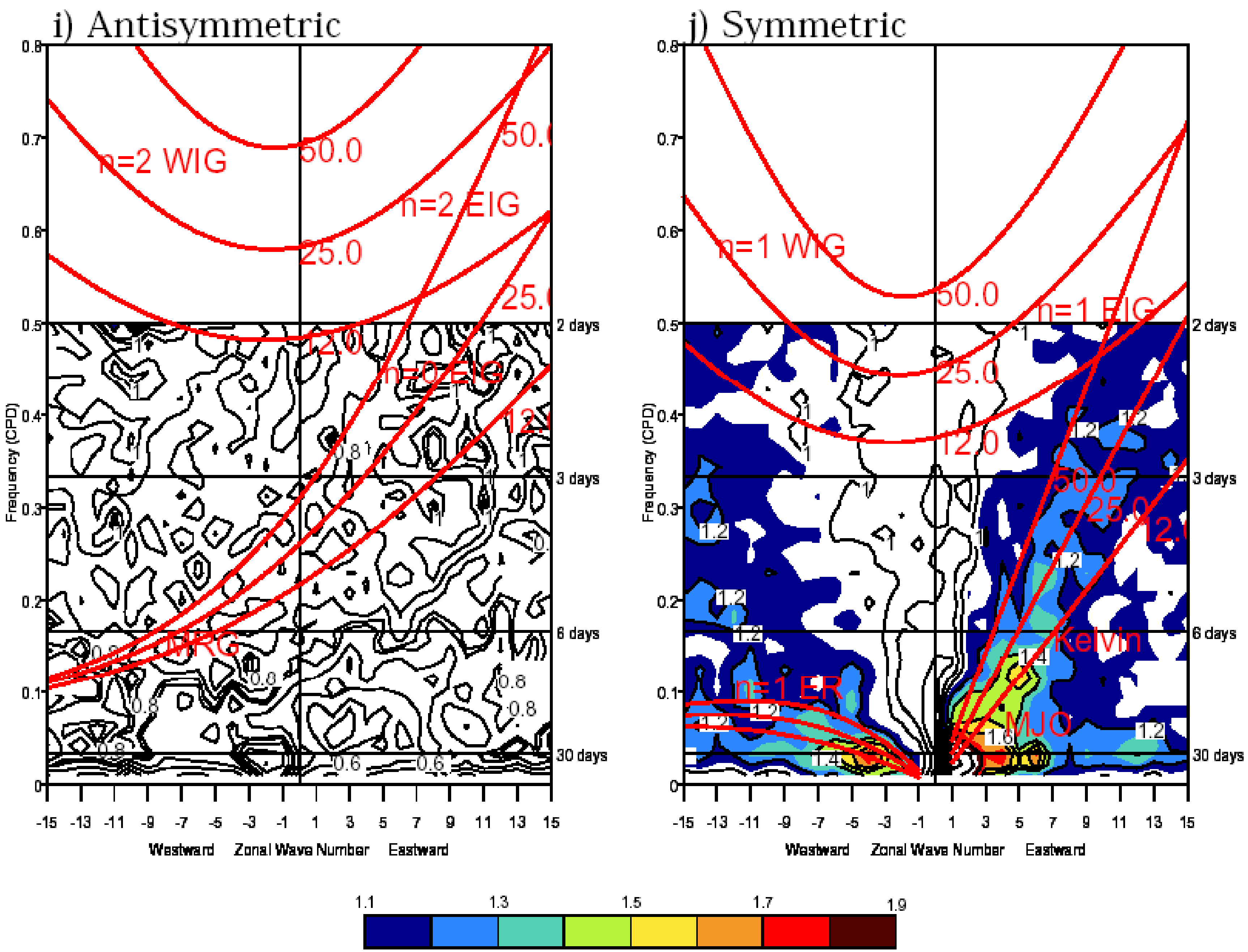

ECHO-G OLR

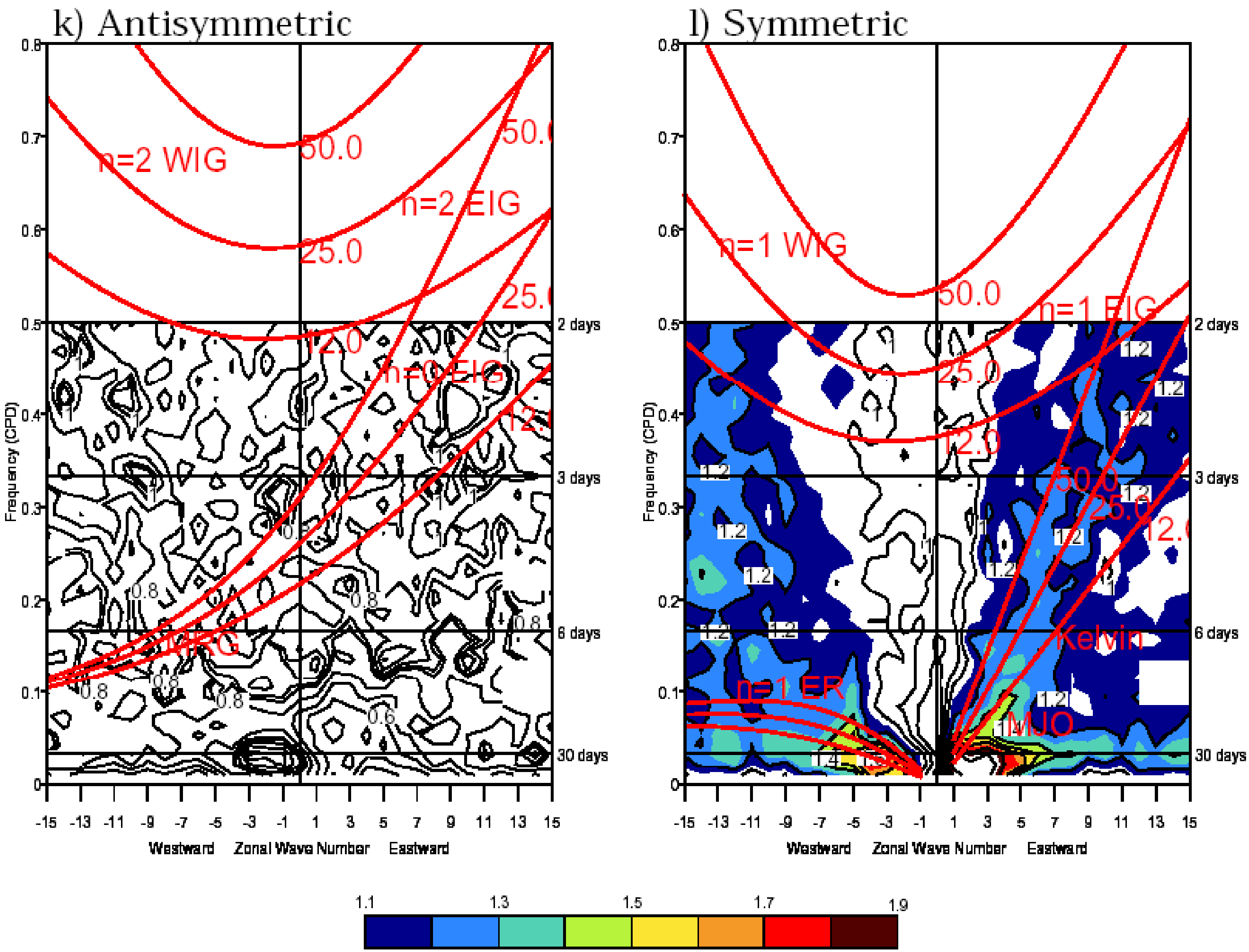

k) Antisymmetric
l) Symmetric
Frequency (CPD)
n=2 WIG
n=2 EIG
n=0 EIG
MRG
n=1 WIG
n=1 EIG
n=1 ER
Kelvin
MJO
2 days
3 days
6 days
30 days
Westward
Zonal Wave Number
Eastward

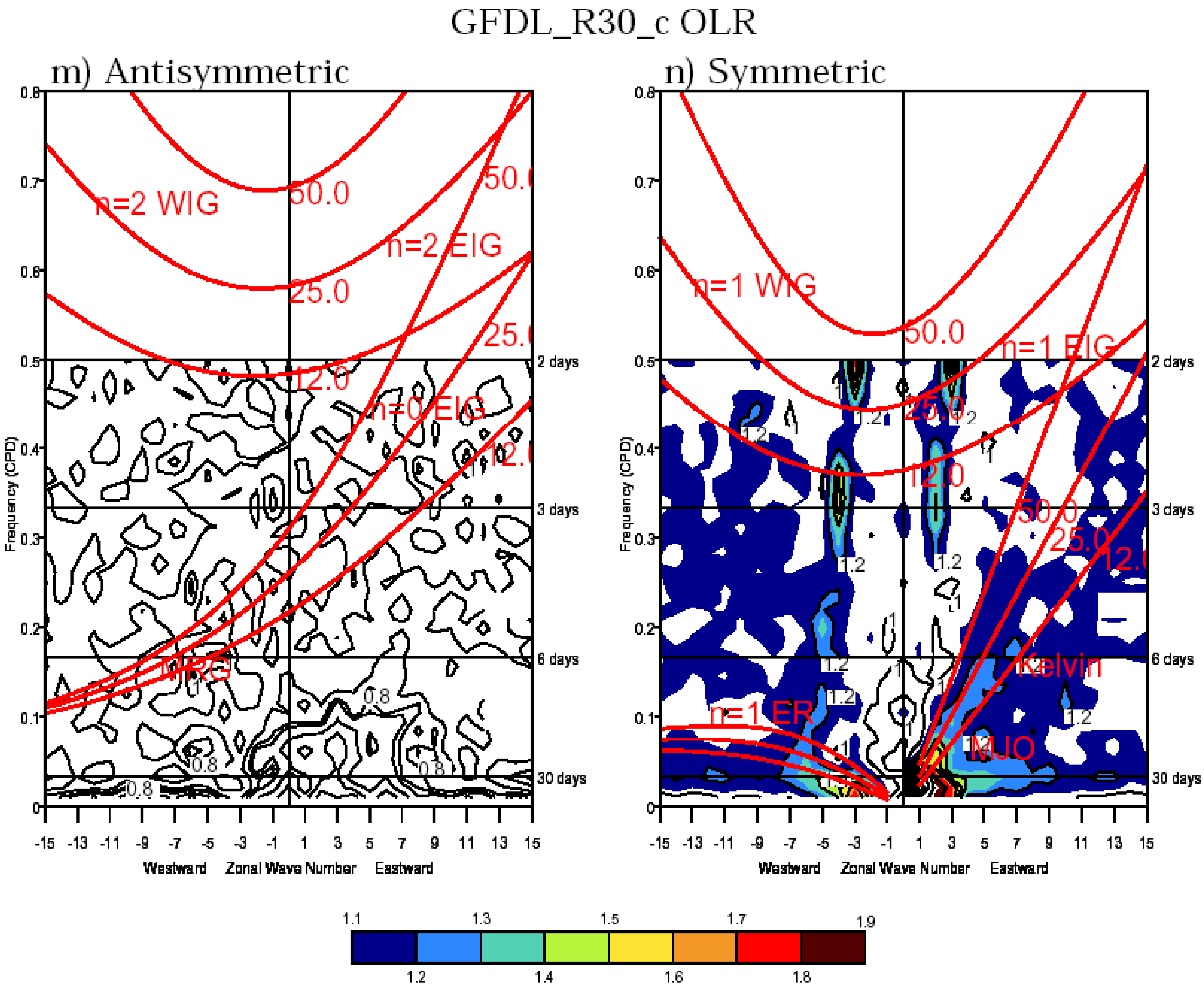
GFDL_R30_c OLR
m) Antisymmetric
n) Symmetric
n=2 WIG
n=2 EIG
n=0 EIG
MRG
n=1 WIG
n=1 EIG
n=1 ER
Kelvin
MJO
2 days
3 days
6 days
30 days
Frequency (CPD)
Westward Zonal Wave Number Eastward

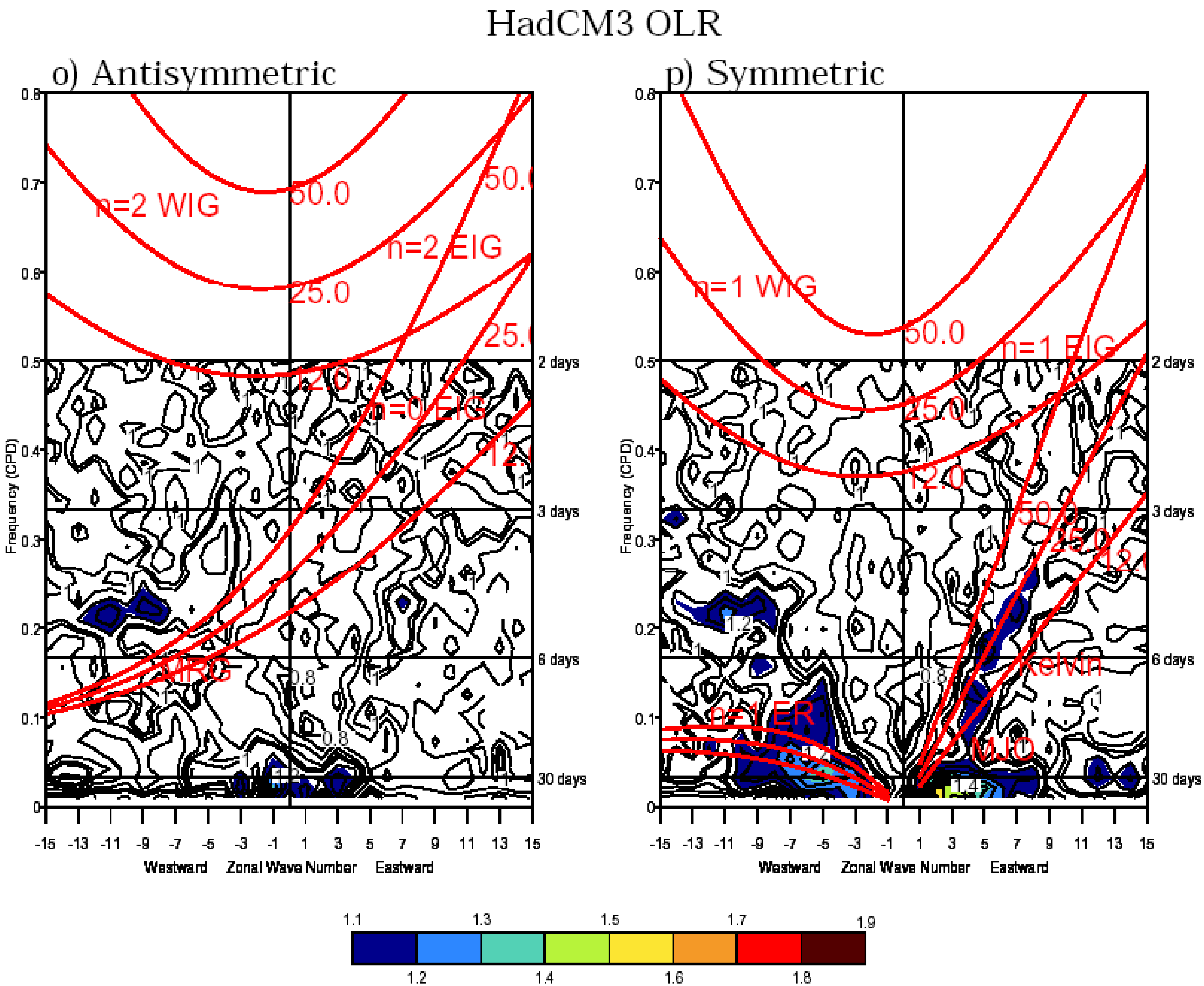
HadCM3 OLR
o) Antisymmetric
p) Symmetric
Frequency (CPD)
Westward Zonal Wave Number Eastward
2 days
3 days
6 days
30 days
n=2 WIG
n=2 EIG
n=0 EIG
MRG
n=1 WIG
n=1 EIG
n=1 ER
Kelvin
MJO
50.0
25.0
12.0
1.1
1.2
1.3
1.4
1.5
1.6
1.7
1.8
1.9

PCM OLR

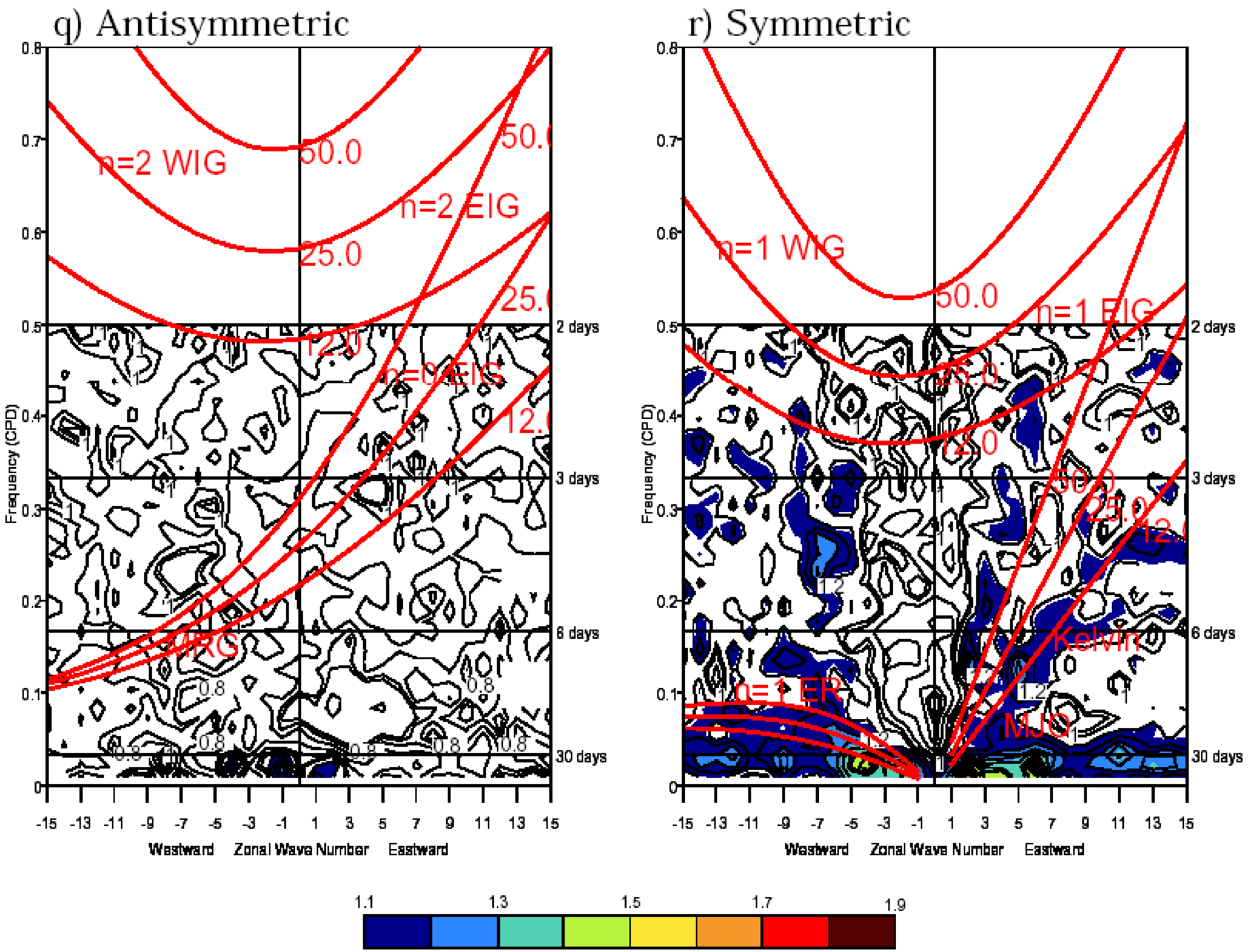

q) Antisymmetric
r) Symmetric
Frequency (CPD)
Westward Zonal Wave Number Eastward
n=2 WIG
n=2 EIG
n=0 EIG
MRG
n=1 WIG
n=1 EIG
n=1 ER
Kelvin
MJO
50.0
25.0
12.0
2 days
3 days
6 days
30 days
1.1
1.2
1.3
1.4
1.5
1.6
1.7
1.8
1.9

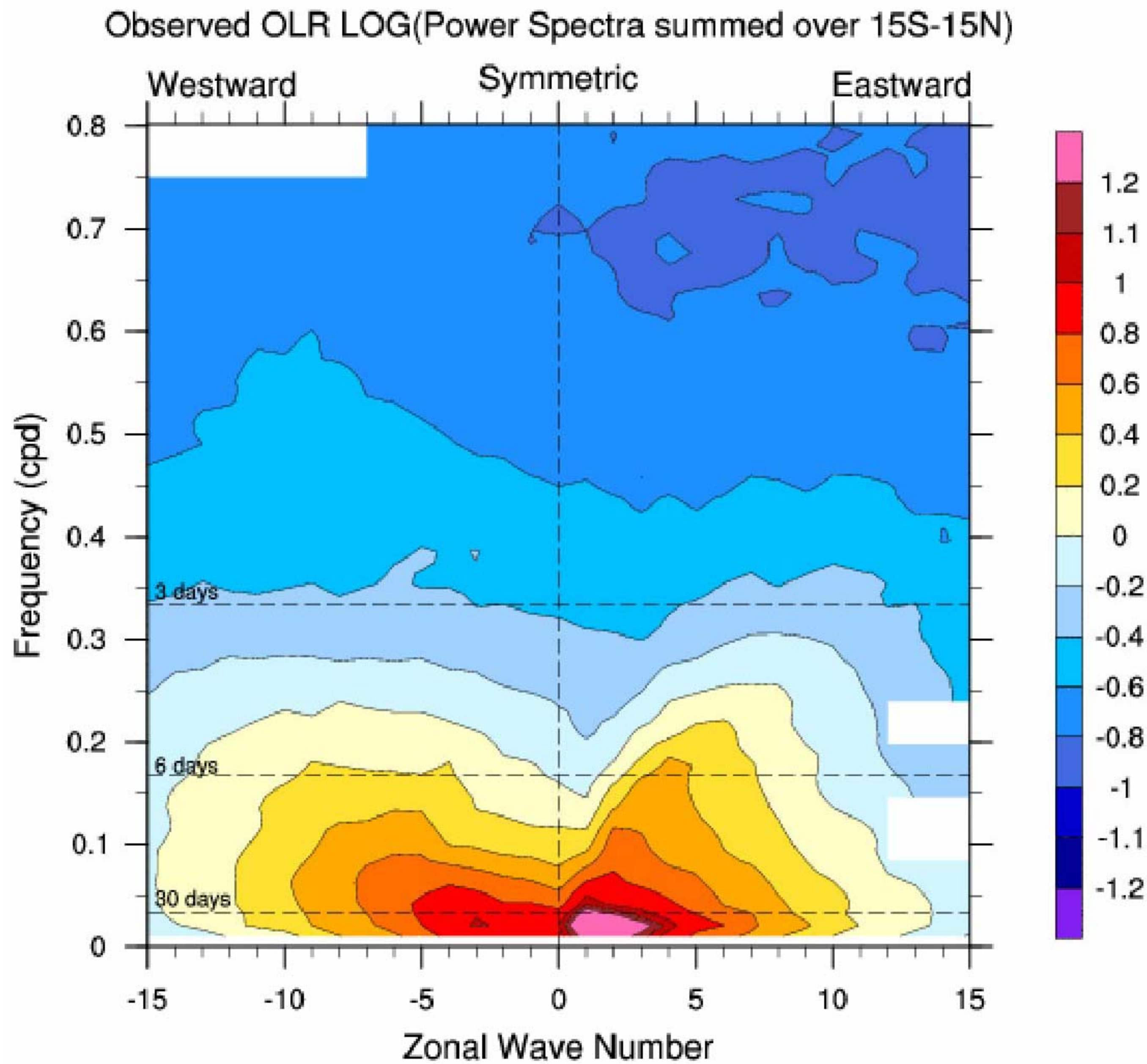

Observed OLR LOG(Power Spectra summed over 15S-15N)
Westward
Symmetric
Eastward
Frequency (cpd)
0.8
0.7
0.6
0.5
0.4
0.3
0.2
0.1
0
3 days
6 days
30 days
-15
-10
-5
0
5
10
15
Zonal Wave Number
1.2
1.1
1
0.8
0.6
0.4
0.2
0
-0.2
-0.4
-0.6
-0.8
-1
-1.1
-1.2

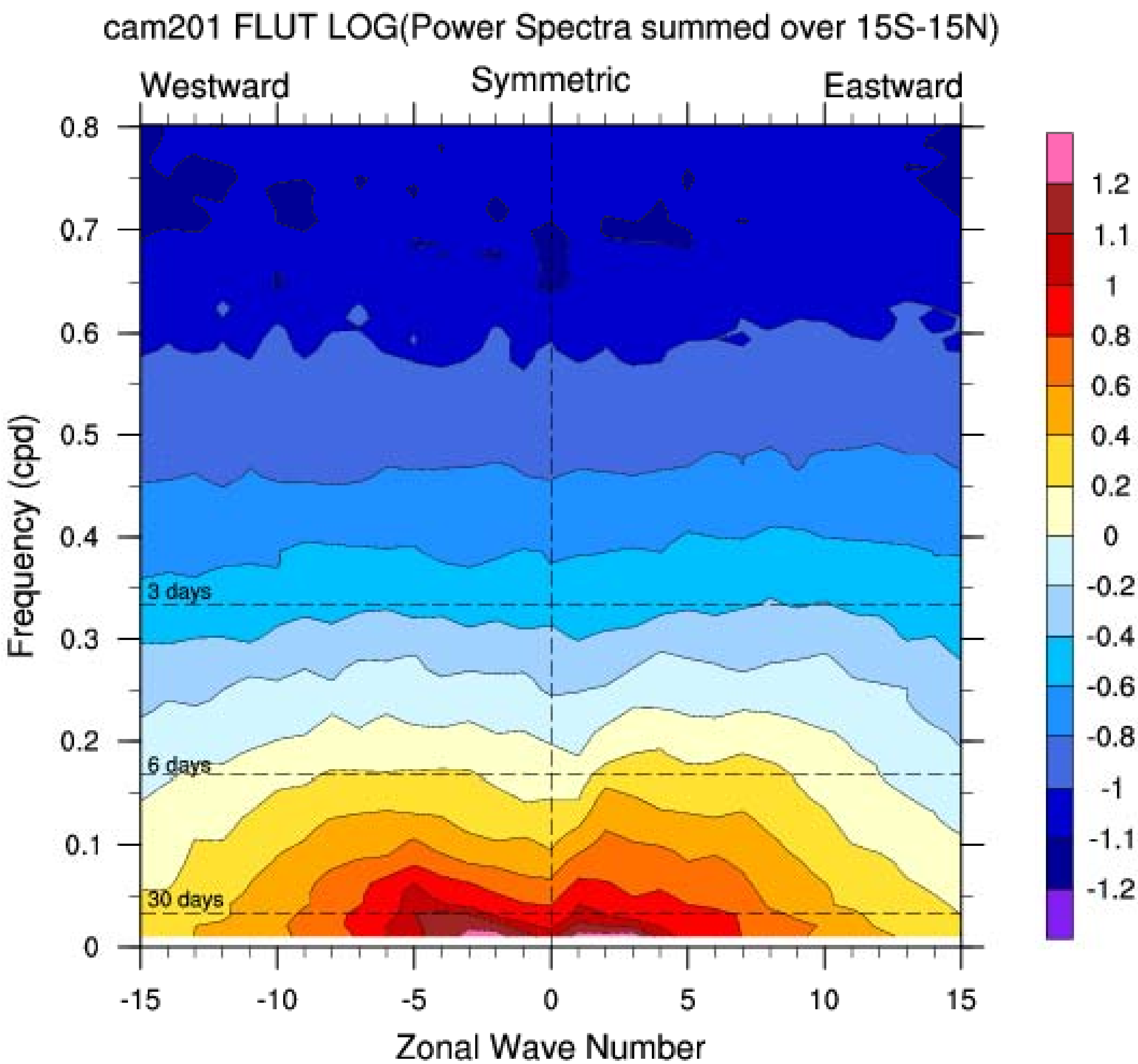

cam201 FLUT LOG(Power Spectra summed over 15S-15N)
Westward
Symmetric
Eastward
0.8
0.7
0.6
0.5
0.4
0.3
0.2
0.1
0
Frequency (cpd)
3 days
6 days
30 days
-15
-10
-5
0
5
10
15
Zonal Wave Number
1.2
1.1
1
0.8
0.6
0.4
0.2
0
-0.2
-0.4
-0.6
-0.8
-1
-1.1
-1.2

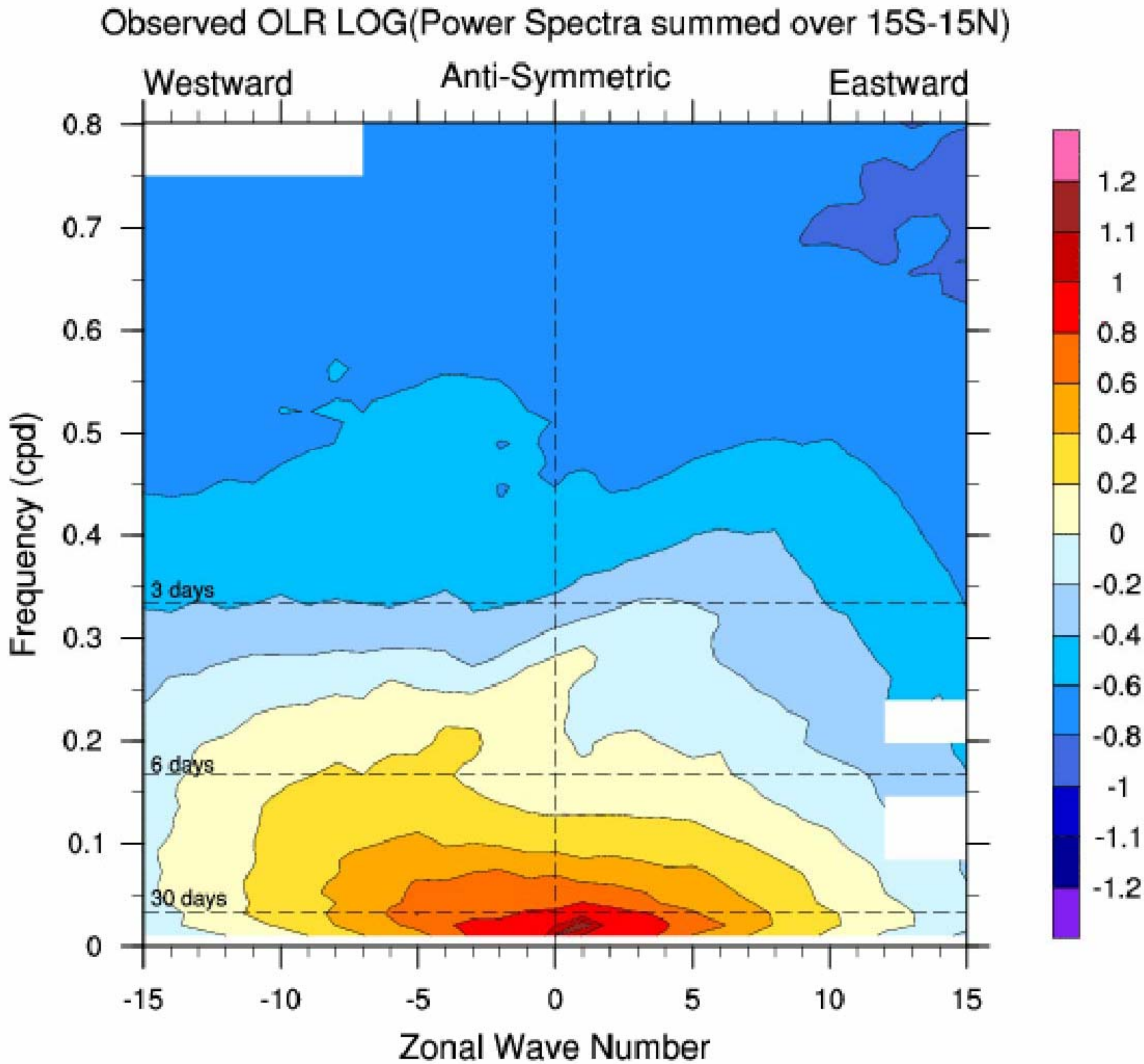
Observed OLR LOG(Power Spectra summed over 15S-15N)
Westward
Anti-Symmetric
Eastward
Frequency (cpd)
0.8
0.7
0.6
0.5
0.4
0.3
0.2
0.1
0
3 days
6 days
30 days
-15
-10
-5
0
5
10
15
Zonal Wave Number
1.2
1.1
1
0.8
0.6
0.4
0.2
0
-0.2
-0.4
-0.6
-0.8
-1
-1.1
-1.2

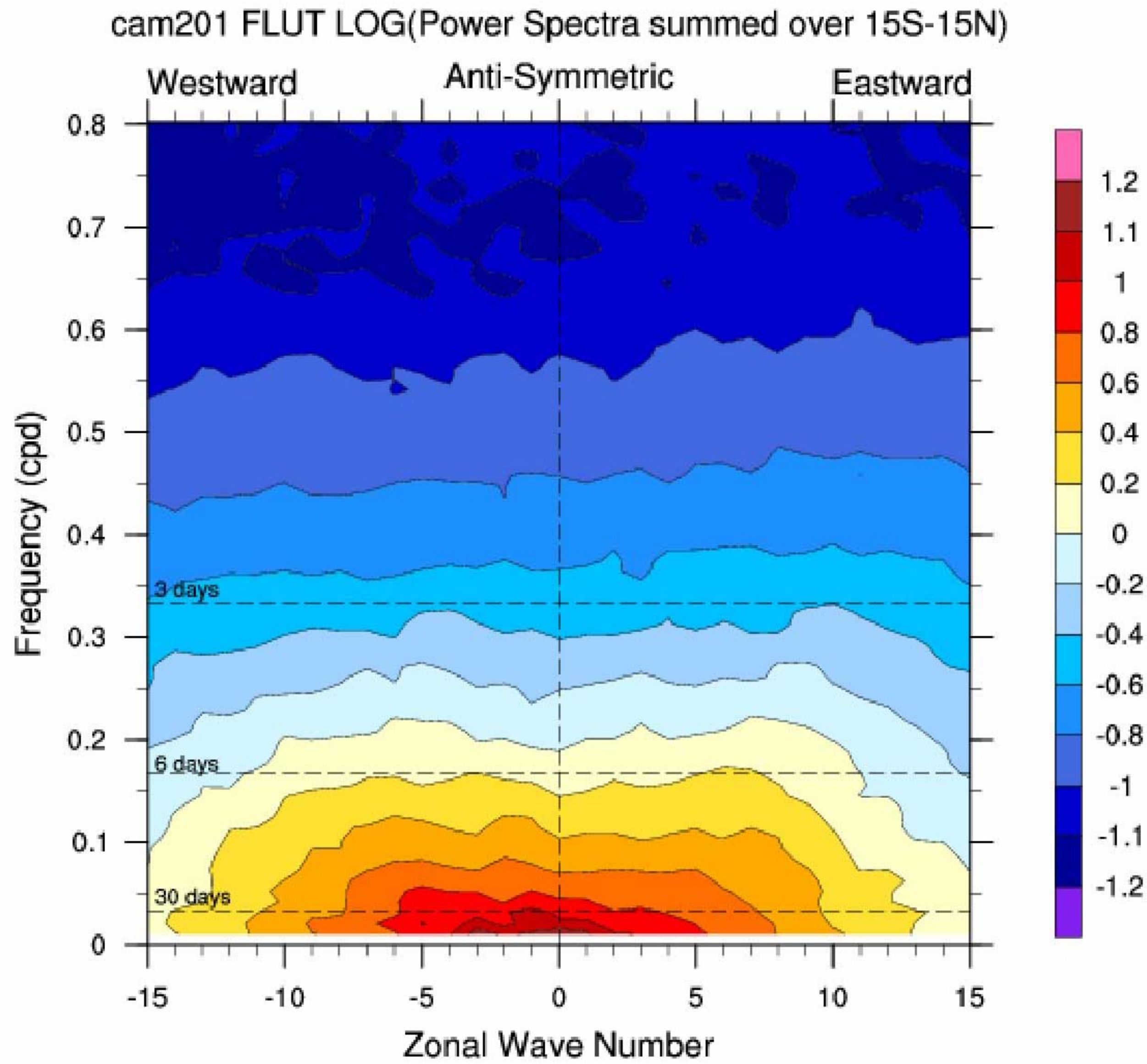
cam201 FLUT LOG(Power Spectra summed over 15S-15N)
Westward
Anti-Symmetric
Eastward
Frequency (cpd)
Zonal Wave Number
3 days
6 days
30 days
0.8
0.7
0.6
0.5
0.4
0.3
0.2
0.1
0
-15
-10
-5
0
5
10
15
1.2
1.1
1
0.8
0.6
0.4
0.2
0
-0.2
-0.4
-0.6
-0.8
-1
-1.1
-1.2

Conclusions

Although the MJO is comprised of a variety of higher frequency, smaller scale disturbances, the dynamical structures of all of these waves resemble each other in many important aspects, all consistent with shallow cumulus leading to deep convection followed by stratiform precipitation

There is a high degree of self-similar behavior seen in equatorial waves across a wide variety of scales

General Circulation Models do not represent such scale interactions, and most do not adequately represent the MJO or other equatorial modes sufficiently well.

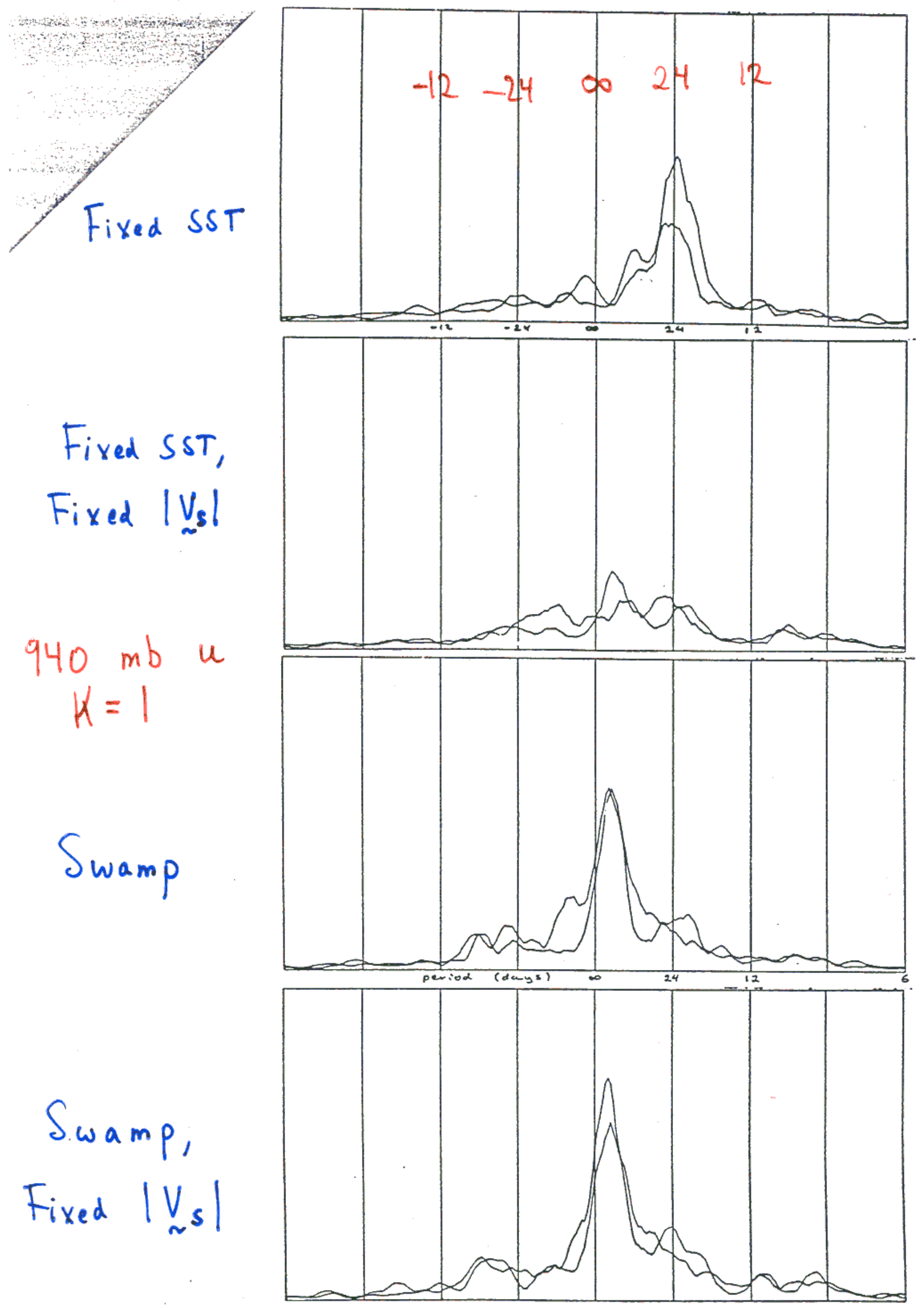

Figure 3. As for Figure 1, but for u at 940 mb, wavenumber 1. The vertical scale is one quarter that of Figure 1.

Neelin et al., JAS, 1987

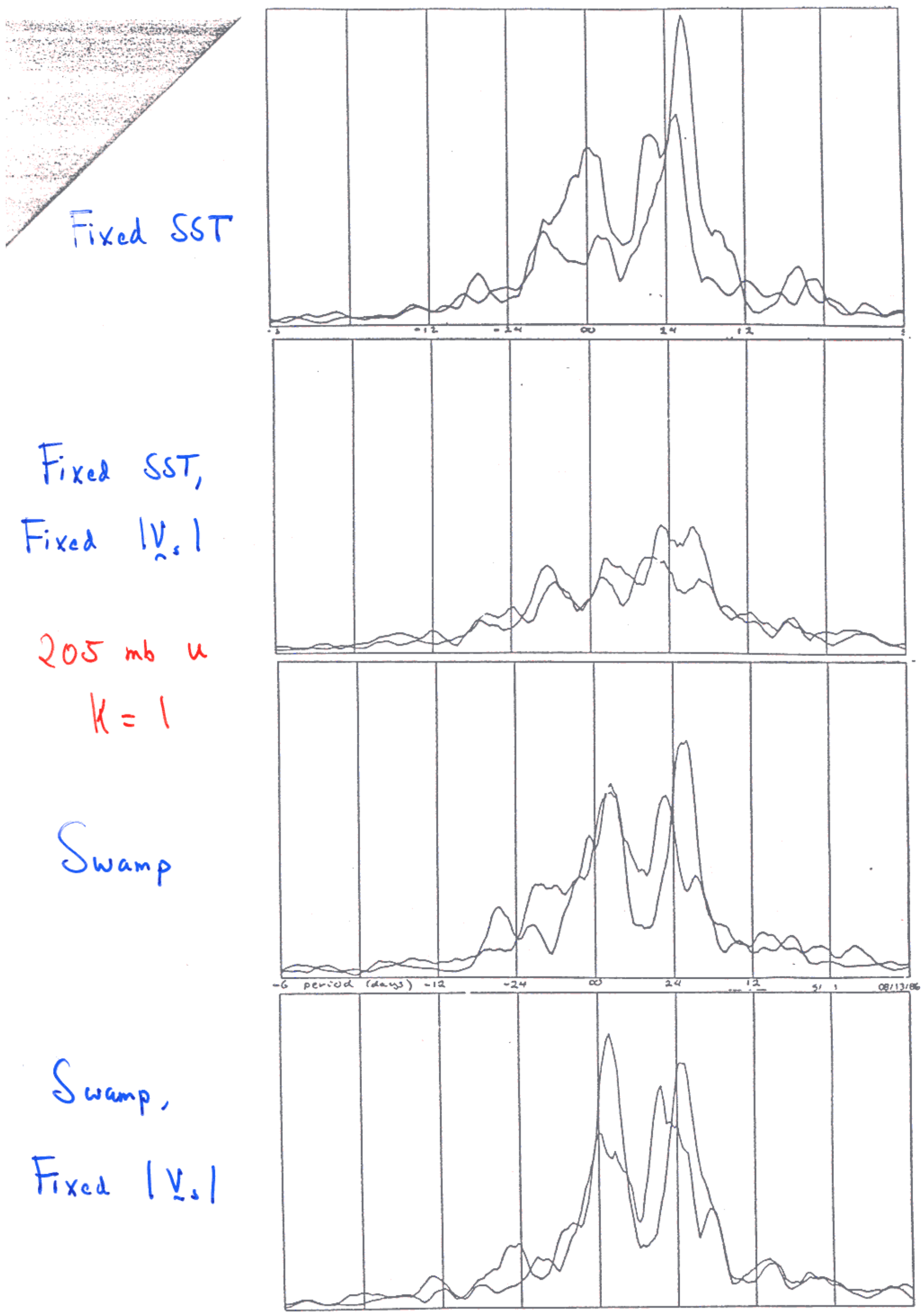
Fixed SST
Fixed SST,
Fixed |V_s|
205 mb u
K = 1
Swamp
Swamp,
Fixed |V_s|
period (days)
-12
-24
∞
24
12

Tropical cyclone activity and the MJO

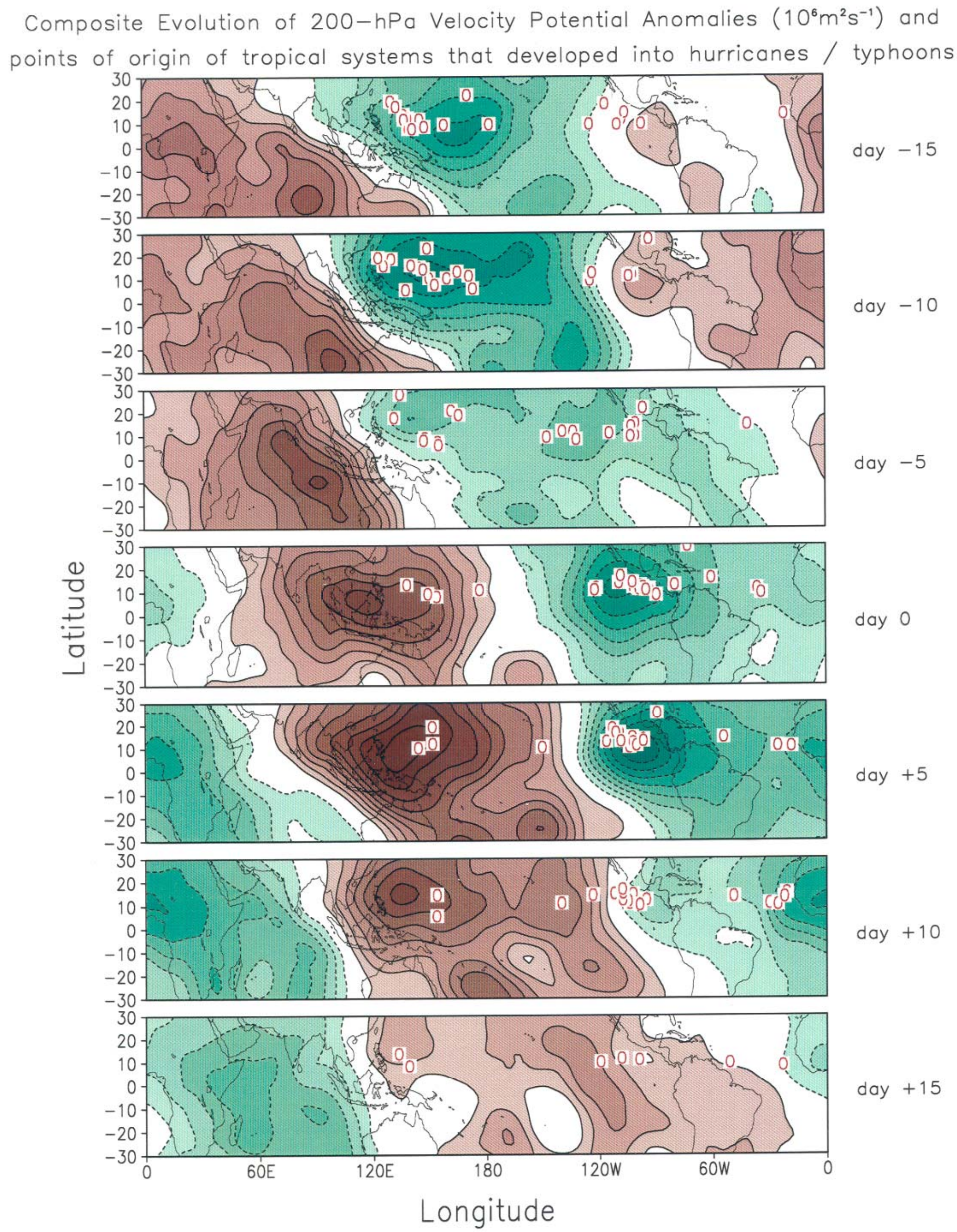

12.811 Tropical Meteorology
Spring 2011